Aus dem

Institut für Experimentelle und Klinische Pharmakologie und Pharmakogenomik der Universität Tübingen
Abteilung Pharmakologie, Experimentelle Therapie und Toxikologie

Vascular calcification: the role of Orai and store-operated Ca^{2+} entry

Inaugural-Dissertation
zur Erlangung des Doktorgrades
der Medizin

der Medizinischen Fakultät
der Eberhard Karls Universität
zu Tübingen

vorgelegt von

Ma, Ke

2023

Dekan:	Professor Dr. B. Pichler
1. Berichterstatter:	Professor Dr. Dr. B. Nürnberg
2. Berichterstatter:	Professor Dr. T. Wieder

Tag der Disputation: 25.01.2023

Table of contents

Table of contents I
List of figures IV
List of tables VI
List of abbreviations VII
1. Introduction 1
1.1 Vascular calcification 1
1.1.1 Background 1
1.1.2 Dysregulation of bone mineral metabolism in individuals with CKD 2
1.1.3 Mechanisms of calcification in individuals with CKD 4
1.1.4 Osteo/chondrocytic differentiation of VSMCs 5
1.2 Ca^{2+} signaling 8
1.2.1 Ca^{2+} homeostasis in resting cells 8
1.2.2 Core of the Ca^{2+} signaling network 9
1.2.3 Store-operated Ca^{2+} entry; the mechanism of Ca^{2+} release-activated Ca^{2+} channel 9
1.2.4 SERCA inhibitors and SOCE in VSMCs 12
1.3 Phosphate-dependent osteoinductive signaling in VSMCs 14
1.4 Study aim 17
2. Materials and Methods 18
2.1 Materials 18
2.1.1 Cells, medium, and inhibitors 18
2.1.2 Chemicals and reagents 18
2.1.3 Primers and antibodies 21
2.1.4 Solutions and buffers 22
2.1.5 Consumables and instruments 23
2.1.6 Software 24

2.2 Methods 25
2.2.1 Cell culture 25
2.2.2 Drug preparation and *in vitro* treatment 25
2.2.3 Quantitative PCR 25
2.2.4 Silencing of ORAI1 27
2.2.5 Protein extraction and western blotting 28
2.2.6 Ca^{2+} measurements 30
2.2.7 TNSALP activity assay 30
2.2.8 Alizarin red S staining 31
2.2.9 Calcium content assay 31
2.2.10 Statistical analysis 31
3. Results 32
3.1 β-glycerophosphate sensitivity of osteogenic markers in HAoSMCs 32
3.2 Phosphate stimulated ORAI1 and STIM1 mRNA and protein expression in HAoSMCs 33
3.3 Phosphate stimulated SOCE in HAoSMCs 35
3.4 ORAI1 antagonists inhibited phosphate-stimulated SOCE 39
3.5 The SGK1 antagonist GSK650394 inhibited phosphate-stimulated *ORAI1* and *STIM1* gene expression in HAoSMCs 45
3.6 The SGK1 antagonist GSK650394 inhibited phosphate-stimulated SOCE in HAoSMCs 46
3.7 ORAI1 inhibition blocked phosphate-stimulated osteo/chondrogenic signaling and extracellular calcification in HAoSMCs 49
3.8 High K^+ concentrations stimulated osteogenic marker expression in HAoSMCs 59
4. Discussion 61

4.1 Research models for studying medial vascular calcification 62
4.2 Signaling pathways involved in medial vascular calcification 63
4.3 Interference with functional ORAI1 66
4.4 Conclusions 67
5. Summary 69
Zusammenfassung 71
6. References 73
7. Declaration of Contributions 90
8. Publications 91
Acknowledgments 93

List of figures

Figure 1 Simplified terminology for biological calcification 2
Figure 2 A summary of mineral metabolism during normal kidney function and CKD 4
Figure 3 Involvement of multiple factors associated with VSMCs in VCm 7
Figure 4 Predicted mechanism of action of ORAI1 and STIM1 12
Figure 5 Treatment with 2 mM BGP stimulated osteogenic marker expression in HAoSMCs 32
Figure 6 Phosphate stimulated ORAI1 and STIM1 mRNA and protein expression in HAoSMCs 34
Figure 7 Phosphate stimulated SOCE in HAoSMCs 36
Figure 8 Thirty minutes of phosphate treatment did not affect intracellular Ca^{2+} release or SOCE in HAoSMCs 38
Figure 9 Inhibition of SOCE by MRS1845 at different concentrations 40
Figure 10 MRS1845 inhibited phosphate-stimulated SOCE in HAoSMCs 42
Figure 11 2-APB inhibited phosphate-stimulated SOCE in HAoSMCs 44
Figure 12 GSK650394 inhibited phosphate-stimulated *ORAI1* and *STIM1* mRNA expression in HAoSMCs 46
Figure 13 GSK650394 inhibited phosphate-stimulated SOCE 48
Figure 14 MRS1845 inhibited phosphate-stimulated osteo/chondrogenic signaling in HAoSMCs 50
Figure 15 2-APB inhibited phosphate-stimulated osteo/chondrogenic signaling in HAoSMCs 52
Figure 16 MRS1845 and 2-APB inhibited phosphate-stimulated extracellular calcification in HAoSMCs 54
Figure 17 siORAI1 suppressed ORAI1 mRNA and protein expression in HAoSMCs 56
Figure 18 siORAI1 inhibited phosphate-stimulated expression of osteogenic

markers in HAoSMCs 58
Figure 19 High K^+ concentrations stimulated osteogenic marker expression in HAoSMCs 60
Figure 20 Schematic representation of the signaling cascade involved in phosphate-stimulated osteo/chondrogenic transdifferentiation of VSMCs and VCm 61

List of tables

Table 2.1: List of cells used and medium with additives 18
Table 2.2: List of pharmacological inhibitors used 18
Table 2.3: List of chemicals used in the project 18
Table 2.4: List of reagents used in the project 20
Table 2.5 List of primers used for quantitative PCR..... 21
Table 2.6: List of antibodies used in the project..... 21
Table 2.7 List of solutions and buffers used in the study 22
Table 2.8: List of consumables and instruments used 23
Table 2.9: List of software used 24
Table 2.10: Recipes for the resolving and stacking gels 28

List of abbreviations

%	Percent
$[Ca^{2+}]_i$	Cytosolic calcium concentration
°C	Degree celsius
$1,25(OH)_2D_3$	1,25-dihydroxyvitamin D_3
$25(OH)D_3$	25-hydroxyvitamin D_3
2-APB	2-Aminoethoxydiphenyl borate
ALP	Alkaline phosphatase
AM	Acetoxymethyl
ANOVA	Analysis of variance
APS	Ammonium persulfate
ATP	Adenosine triphosphate
BGP	β-glycerophosphate
BMP-2	Bone morphogenetic protein-2
BSA	Bovine serum albumin
Ca^{2+}	Calcium ion
CaCC	Ca^{2+} activated Cl^- channel
CBFA1	Core-binding factor α-1
CC1	Coiled-coil 1
CDI	Ca^{2+}-dependent inactivation
cDNA	Complementary deoxyribonucleic acid
CKD	Chronic kidney disease
cm^2	Square centimeter
CPA	Cyclopiazonic acid
CRAC	Ca^{2+} release activated Ca^{2+} channel
CT	Cycle threshold
DAG	Diacylglycerol
dH_2O	Distilled water
dL	Deciliter
DMSO	Dimethyl sulfoxide
DNA	Deoxyribonucleic acid

DNase	Deoxyribonuclease
D-PBS	Dulbecco’s phosphate-bufferd saline
ECM	Extracellular matrix
EDTA	Ethylenediaminetetraacetic acid
EGTA	Ethylene glycol-bis(β-aminoethyl ether)-N,N,N’,N’-tetraacetic acid
ER	Endoplasmic reticulum
FBS	Fetal bovine serum
FGF-23	Fibroblast growth factor 23
GAPDH	Glyceraldehyde 3-phosphate dehydrogenase
GPCR	G protein-coupled receptor
HAoSMC	Human aortic smooth muscle cell
HEK293	Human embryonic kidney 293
HEPES	4-(2-Hydroxyethyl)-piperazine-1-ethanesulfonic acid
HL-60	Human leukemia 60
HRP	Horseradish peroxidase
IC_{50}	Half-maximal inhibitory concentration
IKKα	IκB kinase α
IKKβ	IκB kinase β
IP_3	Inositol 1,4,5-triphosphate
IP_3R	Inositol 1,4,5-triphosphate receptor
K^+	Potassium ion
M	Molar
MagNuM	Magnesium-nucleotide-regulated metal cation current
mg	Milligram
Mg	Magnesium
MGP	Matrix Gla protein
mM	Millimolar
MSX2	Msh homeobox 2
mTOR	Mammalian target of rapamycin
Na^+	Sodium ion
NCKX	Na^+/Ca^{2+}-K^+ exchanger

NCX	Na^+/Ca^{2+} exchanger
Nedd	Neural precursor cell-expressed developmentally downregulated
NF-κB	Nuclear factor κ light chain enhancer of activated B cells
nM	Nanomolar
OCN	Osteocalcin
OPN	Osteopontin
ORAI	Calcium release-activated calcium modulator
P	Phosphorus
PAGE	Polyacrylamide gel electrophoresis
PCR	Polymerase chain reaction
PDK1	3-Phosphoinositide-dependent kinase 1
PFA	Paraformaldehyde
Pi	Inorganic phosphate
PI3K	Phosphoinositide 3-kinase
PIP_2	Phosphatidylinositol 4,5-bisphospate
PLC	Phospholipase C
PMCA	Plasma membrane Ca^{2+} ATPase
PMSF	Phenylmethylsulfonyl fluoride
pNP	p-Nitrophenol
pNPP	p-nitrophenyl phosphate
PPi	Inorganic pyrophosphate
PTH	Parathyroid hormone
PVDF	Polyvinylidene fluoride
RIPA	Radioimmunoprecipitation assay
RNA	Ribonucleic acid
RNase	Ribonuclease
ROCC	Receptor-operated Ca^{2+} channel
RTK	Receptor tyrosine kinase
RUNX2	Runt-related transcription factor 2
RyR	Ryanodine receptor
SAM	Sterile α motif

SD	Standard deviation
SDS	Sodium dodecyl sulfate
SERCA	Sarco/endoplasmic reticulum Ca^{2+} ATPase
SGK1	Serum and glucocorticoid-inducible kinase 1 or Serine/threonine-protein kinase 1
siRNA	Small interfering ribonucleic acid
SM22-α	Smooth muscle protein 22-α
SOAR	STIM1–ORAI-activating region
SOCE	Store-operated Ca^{2+} entry
SOX9	SRY-Box transcription factor 9
STIM	Stromal interaction molecule
TBS	Tris-buffered saline
TBST	Tris-buffered saline containing 1% Tween 20
TEMED	N,N,N',N'-Tetramethylethylendiamid
TG	Thapsigargin
TNSALP	Tissue-nonspecific alkaline phosphatase
TRP	Transient receptor potential
TRPC	Canonical transient receptor potential
U	Unit
VC	Vascular calcification
VCi	Intimal vascular calcification
VCm	Medial vascular calcification
VOCC	Voltage-operated Ca^{2+} channel
VOCE	Voltage-operated Ca^{2+} entry
VSMC	Vascular smooth muscle cell
w/v	Weight/volume
αSMA	α-Smooth muscle actin
µg	Microgram
µM	Micromolar

1. Introduction

1.1 Vascular calcification (VC)

1.1.1 Background

VC is the ectopic deposition of hydroxyapatite crystals in the vascular system (Schlieper et al., 2016). VC is divided into two main types according to the location of calcium deposits in the vascular wall: medial vascular calcification (VCm) and intimal vascular calcification (VCi) (Figure 1). VCi is often associated with atherosclerotic plaques, which are strongly correlated with an elevated risk of ischemic coronary syndromes (Fuster et al., 1990). VCm was formerly referred to as Mönckeberg's medial sclerosis but is currently defined as several pathological conditions with disparate origins but a similar result (medial calcification), particularly without luminal narrowing (Goldsmith et al., 2004). Although both types of VC exist in the population with chronic kidney disease (CKD), VCm is a more specialized vascular pathology prevalent in this population (Amann, 2008, Shroff et al., 2008). It induces arterial stiffness, which results in decreased cardiac perfusion, systolic hypertension, and heart failure (London et al., 2005, London, 2011), thus increasing CKD mortality. VCm develops quickly, particularly in patients on dialysis (Bellasi et al., 2009), and is linked to a further decline in cardiovascular function, culminating in cardiovascular mortality in young adults comparable to that in the average very elderly population (Foley and Parfrey, 1998, Goodman et al., 2000, Mitsnefes, 2012). Thus, in patients with CKD, VCm is a powerful predictor of both cardiovascular and all-cause death (Block et al., 2004, Go et al., 2004, Young et al., 2005, Demer and Tintut, 2008, Guerin et al., 2008, Mizobuchi et al., 2009).

VCm was initially presumed to result from passive hydroxyapatite deposition caused by supersaturation of serum calcium and phosphate concentrations, a noncellularly regulated degenerative process. However, our understanding of VCm has been considerably improved by research conducted over the past two

decades. It is a bone-like ossification process intimately linked to vascular smooth muscle cells (VSMCs) and mediated via multiple signaling pathways (Iyemere et al., 2006, Moe and Chen, 2008, Leopold, 2015, Voelkl et al., 2019)

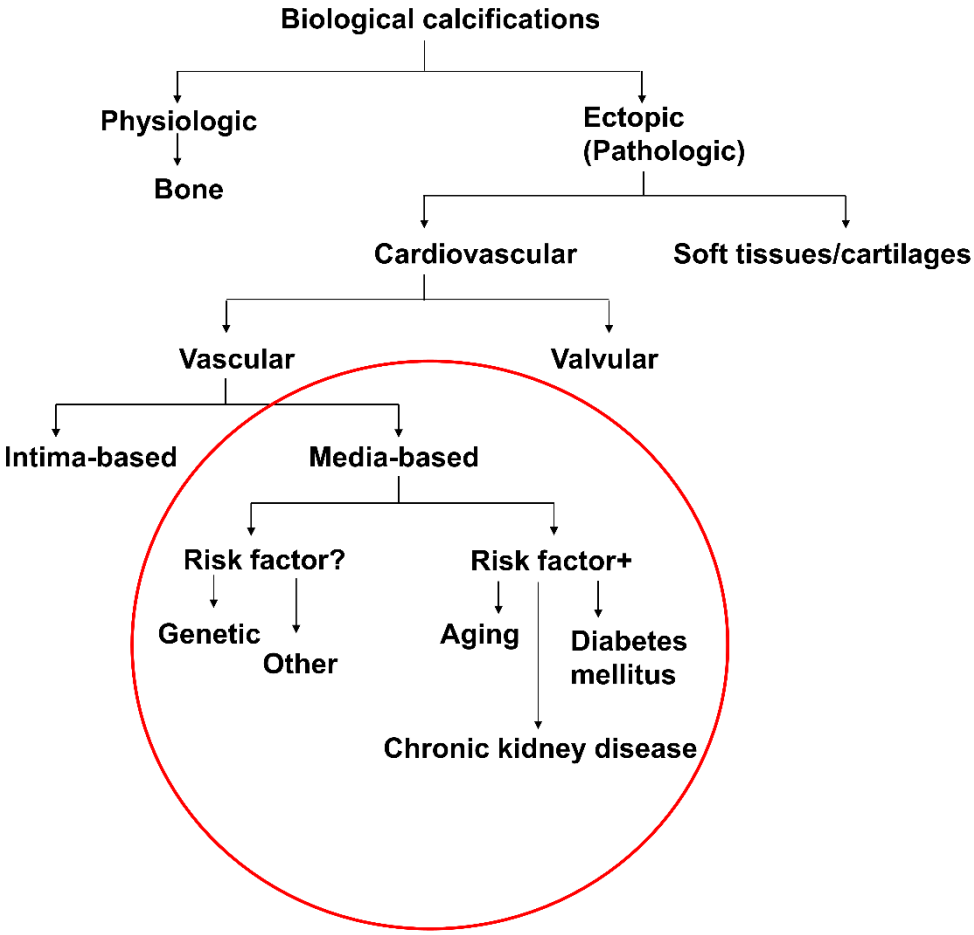

Figure 1 Simplified terminology for biological calcification.
The nomenclature is proposed depending on the presence or lack of recognized risk factors. Mönckeberg's medial sclerosis is the most prevalent variant of VCm and is commonly associated with CKD, diabetes mellitus, and aging. [Modified from (Lanzer et al., 2014)]

1.1.2 Dysregulation of bone mineral metabolism in individuals with CKD

Increased serum phosphate levels are an independent risk factor for

cardiovascular events and mortality, particularly in populations with CKD (Young et al., 2005, Kendrick and Chonchol, 2008, Adeney et al., 2009). Serum phosphate concentrations higher than 1.77 mM, which are common in patients with end-stage renal disease, are strongly correlated with cardiovascular events and sudden death (Block et al., 2004, Noordzij et al., 2006, Tentori et al., 2008). Additionally, in the average population with normal renal function or in patients with early-stage CKD, a relatively modest increase in serum phosphate levels within the normal–high range (1.1-1.45 mM) is associated with increases in cardiovascular and all-cause mortality (Tonelli et al., 2005, Foley, 2009, Kestenbaum et al., 2009, Tonelli et al., 2009, Eddington et al., 2010).

The regulation of phosphate excretion by the kidney is critical for maintaining the phosphate balance under normal physiological conditions. Kidney damage impairs the capacity of mammals to maintain phosphate homeostasis. The serum phosphate concentration is normally maintained in a range from 0.8 mM to 1.45 mM under physiological conditions (Burtis et al., 2012). In the early stages of CKD, renal insufficiency results in impaired phosphate excretion and lower α-klotho levels, while serum phosphate levels are not elevated, potentially due to decreased renal tubular absorption of phosphate via upregulation of parathyroid hormone (PTH) and fibroblast growth factor 23 (FGF-23) in bone (Koh et al., 2001, Levin et al., 2007, Isakova et al., 2011). However, as renal function deteriorates, phosphate excretion further decreases, leading to hyperphosphatemia (CKD stage 4-5) (Slatopolsky et al., 1968, Craver et al., 2007). Furthermore, elevated serum FGF-23 levels reduce $1,25(OH)_2D_3$ synthesis by inhibiting 1α-hydroxylase activity and stimulating 24-hydroxylase activity in the proximal tubules of the kidney, in which 1α-hydroxylase converts $25(OH)D_3$ to $1,25(OH)_2D_3$ and 24-hydroxylase converts $1,25(OH)_2D_3$ to inactive metabolites (Shimada et al., 2004, Perwad et al., 2007). FGF-23, together with decreased 1α-hydroxylase activity due to renal damage during CKD, leads to low $1,25(OH)_2D_3$ levels and

subsequent hypocalcemia. When both hyperphosphatemia and hypocalcemia are present, additional PTH secretion is strongly stimulated, subsequently resulting in secondary hyperparathyroidism (sHPT) and bone mineralization disorders. These normal compensatory mechanisms eventually fail, and dysregulated phosphate metabolism, combined with calcium dysregulation, promotes VCm in individuals with CKD (Figure 2).

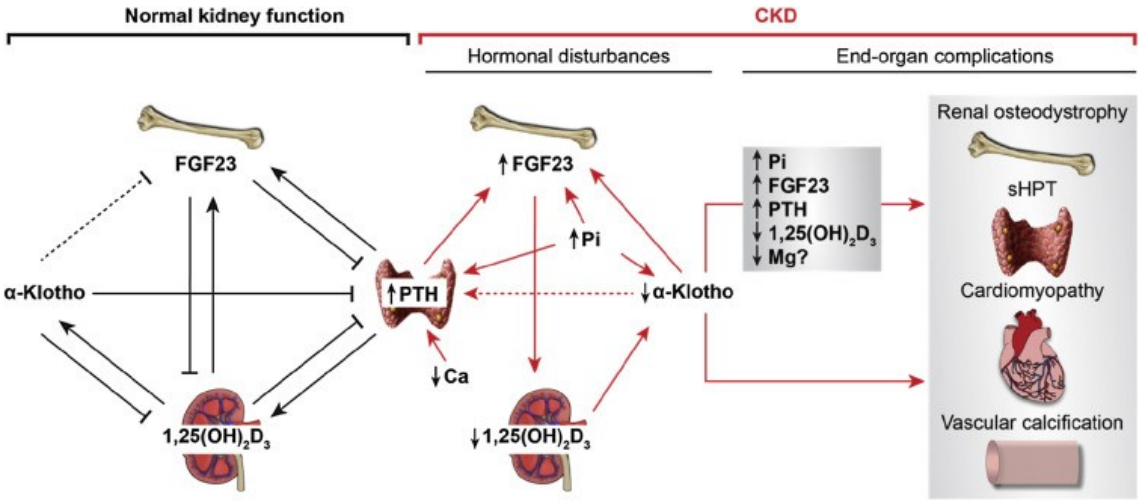

Figure 2 A summary of mineral metabolism during normal kidney function and CKD.

Ca: calcium; Pi: inorganic phosphate; Mg: magnesium. [from (Ferrè et al., 2020), copyright license number 5137900278266, provided by Elsevier and Copyright Clearance Center]

1.1.3 Mechanisms of calcification in individuals with CKD

With the establishment of VCm models *in vivo* and *in vitro*, the main mechanisms of VCm currently being considered are (1) inhibitor loss, (2) osteo/chondrocytic differentiation, (3) cell apoptosis, (4) dysregulated mineral homeostasis, (5) nidus formation, and (6) matrix degradation or modification (Moe and Chen, 2008, Sage et al., 2010, Shanahan et al., 2011, Leopold, 2015, Voelkl et al., 2019).

Under physiological conditions, active cellular defense mechanisms

efficiently prevent the formation of ectopic calcification, and calcification is highly likely to develop when these defense mechanisms are overwhelmed. In individuals with CKD, the uremic environment places VSMCs under severe calcification stress. Hyperphosphatemia and occasional hypercalcemia may overwhelm inhibitory systems. Additionally, various toxins in the uremic environment, such as inflammatory factors and lipid oxidation products, contribute to oxidative stress and DNA damage in VSMCs (Vaziri, 2004, Yamada et al., 2012). Over time, damaged VSMCs gradually lose the ability to produce sufficient amounts of inhibitors and undergo phenotypic switching, eventually losing their contractile characteristics and converting to synthetic cells. As long as unfavorable stimuli persist, these synthetic VSMCs continue to maladaptively transdifferentiate into osteo/chondrocytes and release matrix vesicles. These matrix vesicles have alkaline phosphatase activity, forming a microenvironment that is prone to the formation of alkaline calcium and phosphate deposits that contain hydroxyapatite crystals, which are released in a high-phosphate or/and hypercalcemic environment (Iyemere et al., 2006, Shanahan, 2007). Moreover, VSMCs may undergo apoptosis or necrosis, which increases the local calcium concentration, providing an additional nidus for calcification and further depleting the ability of VSMCs to produce inhibitors (Shroff et al., 2008).

1.1.4 Osteo/chondrocytic differentiation of VSMCs

As previously stated, when VSMCs are exposed to procalcific conditions, particularly hyperphosphatemia, they undergo a phenotypic transition characterized by increased expression of bone-related genes and loss of contractile markers. The osteoinductive transcription factors include core-binding factor α-1 (*CBFA1*), also known as runt-related transcription factor 2 (*RUNX2*), osterix, msh homeobox 2 (*MSX2*), sry (sex determining region Y)-box 9 (*SOX9*), and alkaline phosphatase (*ALPL*, encodes the tissue-nonspecific isozyme ALP in humans) (Jono et al., 2000a, Steitz et al., 2001, Chen et al., 2002, Tyson et al.,

2003, Iyemere et al., 2006, Mathew et al., 2008, Speer et al., 2010). Smooth muscle protein 22-α (SM22-α) and α-smooth muscle actin (αSMA) are contractile markers (Steitz et al., 2001).

CBFA1 is critical in mediating VSMC phenotypic switching by activating bone-related genes and inhibiting lineage-specific gene expression, and *CBFA1* silencing suppresses VSMC osteo/chondrogenic differentiation and VCm (Tanaka et al., 2008, Speer et al., 2010, Sun et al., 2012). *MSX2* functions as an upstream regulator of *CBFA1* during osteoblast differentiation, promoting *CBFA1* and osterix expression in VSMCs (Satokata et al., 2000, Lee et al., 2010). *CBFA1* promotes the expression and activation of osterix (Nishio et al., 2006). *SOX9* and *CBFA1* are essential for osteochondral progenitor cells to differentiate into chondrocytes or osteoblasts (Komori et al., 1997, Bi et al., 1999, Yamashiro et al., 2004). *SOX9* deficiency abolishes cartilage and bone differentiation, whereas *CBFA1* deficiency affects only chondrocyte hypertrophy and bone formation (Zhou et al., 2006). *ALPL* is required for accurate calcium and phosphate mineralization in bones and teeth (Fedde et al., 1999).

Furthermore, osteoinductive transcription factors promote the synthesis and secretion of proteins involved in bone formation and mineralization, including osteocalcin (OCN), bone morphogenetic protein-2 (BMP-2), type I collagen, and tissue-nonspecific alkaline phosphatase (TNSALP), in VSMCs (Shanahan et al., 1999, Shanahan et al., 2011, Lanzer et al., 2014).

BMP-2 is a potent osteogenic protein that is closely related to VCm. Noggin, a BMP-2 inhibitor, was previously shown to block calcification induced by high phosphate concentrations while also preventing increased expression of osterix in VSMCs (Mathew et al., 2007). Compared with the average population, serum BMP-2 levels are considerably higher in patients with end-stage CKD. The serum of patients with CKD promotes *CBFA1* expression in bovine VSMCs, which is subsequently inhibited substantially by noggin (Chen et al., 2006). BMP-2 also

increases phosphate uptake in VSMCs, leading to VCm (Li et al., 2008).

The enzyme TNSALP is critical for promoting normal bone and tooth formation. *ALPL* mutation results in the production of an inadequate amount of TNSALP, allowing compounds such as pyrophosphate (PPi) to accumulate and impede proper mineralization (Fedde et al., 1999). TNSALP also regulates vascular matrix mineralization by inactivating PPi and osteopontin (OPN) to relieve their inhibitory effects on mineralization while providing phosphate or free phosphorus for hydroxyapatite deposition (Jono et al., 2000b, Lomashvili et al., 2004, Shanahan et al., 2011). Elevated TNSALP activity is thus a key event in the development of VCm (Johnson et al., 2006, Demer and Tintut, 2008).

Osteo/chondrogenically transdifferentiated VSMCs may facilitate calcification by inducing an initial nidus of calcification and the growth of hydroxyapatite crystals, therefore promoting VCm. A variety of mechanisms centered on VSMCs are described below (Figure 3).

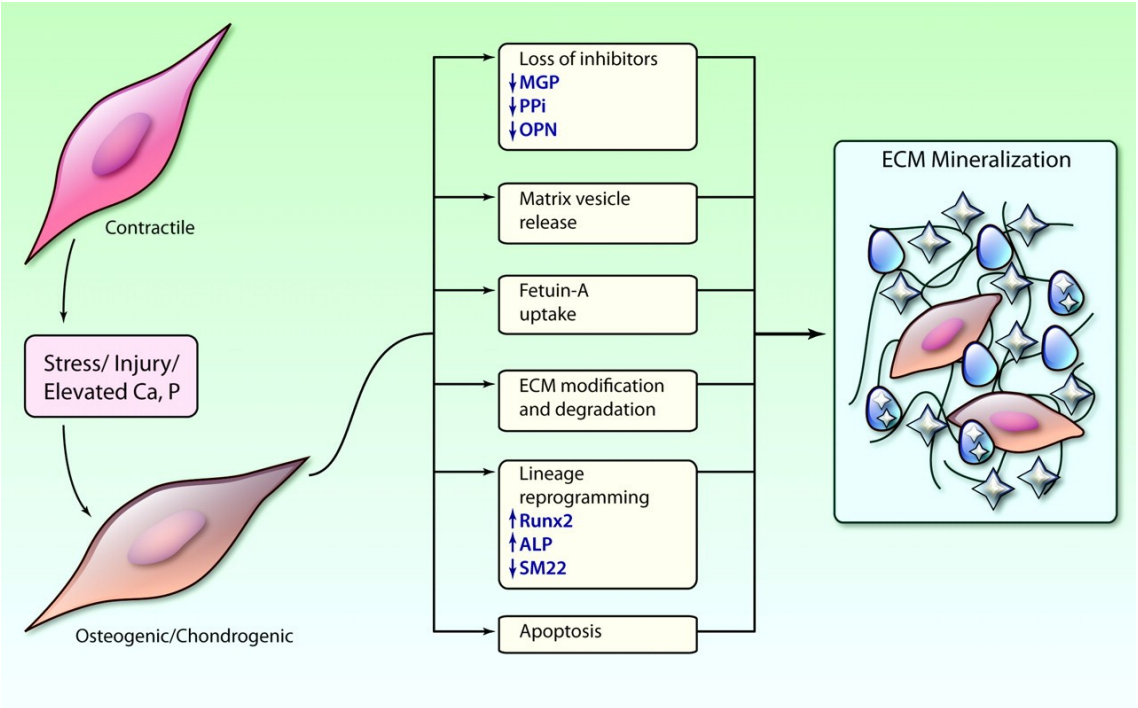

Figure 3 Involvement of multiple factors associated with VSMCs in VCm.
Elevated phosphorus (P) or calcium (Ca) levels, stress, and vascular injury all contribute

to the osteo/chondrogenic differentiation of VSMCs. Inhibitor loss, calcified matrix vesicle release, and extracellular matrix degradation contribute to this process. P- or Ca-induced apoptosis of VSMCs facilitates the formation of the initial calcification nidus.
MGP: matrix Gla protein; PPi: pyrophosphate; OPN: osteopontin. (Illustration Credit: Cosmocyte/Ben Smith). [from (Shanahan et al., 2011), copyright license number: 5138920120094, provided by Wolters Kluwer Health, Inc.]

1.2 Ca^{2+} signaling

As a ubiquitous second messenger, Ca^{2+} plays a vital role in regulating a wide variety of physiological processes, including fertilization, heart activity, information processing in the brain, memory storage, cell apoptosis, gene transcription and translation, and protein modification (Hebert and Brown, 1996, Carafoli, 2002, Berridge, 2012). In resting cells, the cytoplasmic Ca^{2+} concentration $[Ca^{2+}]_i$ is low (approximately 100 nM), while the extracellular $[Ca^{2+}]$ ranges from 1-3 mM (Brini and Carafoli, 2009). Ca^{2+} signaling is characterized by a sudden increase in $[Ca^{2+}]_i$ that drives intracellular processes. Since $[Ca^{2+}]_i$ is at least 10,000 times lower than the extracellular $[Ca^{2+}]$, precise regulation of $[Ca^{2+}]_i$ is critical. Typically, this $[Ca^{2+}]_i$ dynamic is regulated by Ca^{2+}-dependent pumps or channels and through binding to Ca^{2+}-binding proteins and transcription factors (Clapham, 2007).

1.2.1 Ca^{2+} homeostasis in resting cells

A low $[Ca^{2+}]_i$ is maintained through sarco/endoplasmic reticulum Ca^{2+} ATPases (SERCAs), which pump Ca^{2+} into the endoplasmic reticulum (ER), or through plasma membrane Ca^{2+} ATPases (PMCAs), which pump Ca^{2+} out of the cell. Both of these physiological activities consume ATP (Berridge et al., 2003, Kosk-Kosicka, 2005). A second mechanism of cytosolic Ca^{2+} regulation consists of Na^+/Ca^{2+} exchangers (NCXs) or Na^+/Ca^{2+}-K^+ exchangers (NCKXs). NCXs exchange one Ca^{2+} for three Na^+, whereas NCKXs exchange one K^+ and one Ca^{2+} for four Na^+. In the resting state, Ca^{2+}/K^+ extrusion with Na^+ entry generally occurs, and Ca^{2+}/K^+ entry/Na^+ extrusion can occur when the ion concentration

inside and outside the cell changes (Khananshvili, 2014). PMCAs and NCXs/NCKXs are mutually beneficial. PMCAs maintain a relatively low $[Ca^{2+}]_i$ for an extended period, while NCKs/NCKXs perform the necessary fast changes during cardiac action potential generation (Hilgemann et al., 2006).

1.2.2 Core of the Ca^{2+} signaling network

Ca^{2+} channel opening at the plasma membrane is triggered by voltage changes or the binding of intra/extracellular ligands. The initial increase in $[Ca^{2+}]_i$ triggers the release of more Ca^{2+}, mostly from the ER, via Ca^{2+}-sensitive ryanodine receptors (RyRs). Activation of phospholipase C (PLC) by G protein-coupled receptors (GPCRs) or receptor tyrosine kinases (RTKs) results in the hydrolysis of membrane-bound phosphatidylinositol 4,5-bisphosphate (PIP_2) to generate inositol 1,4,5-triphosphate (IP_3) and diacylglycerol (DAG) (Clapham, 1995, Berridge, 1997). IP_3 then binds to its receptor (IP_3R) on the ER and mediates Ca^{2+} release (Clapham, 1995).

1.2.3 Store-operated Ca^{2+} entry; the mechanism of Ca^{2+} release-activated Ca^{2+} channel

Ca^{2+} constantly leaks from the ER, while the ER continuously takes up Ca^{2+} from the cytoplasm via SERCAs. If these pumps fail, Ca^{2+} levels in the ER decrease. Additionally, if cells are cultured in medium with a low $[Ca^{2+}]$, PMCAs pump leaked Ca^{2+} out through the cell membrane, depleting Ca^{2+} in the ER. Ca^{2+} depletion results from IP_3R-mediated Ca^{2+} release from the ER in response to receptor activation, since PMCAs pump Ca^{2+} out through the cell membrane faster than it is replaced in the ER. The ER serves as the primary intracellular Ca^{2+} store; when ER $[Ca^{2+}]$ is depleted, Ca^{2+} entry from the extracellular space, referred to as store-operated Ca^{2+} entry (SOCE), is activated (Putney, 1986, Putney, 1990, Putney, 1999, Putney and McKay, 1999, Parekh and Putney, 2005).

Subsequent research validated this hypothesis by detecting a store-operated current, which was highly selective for Ca^{2+}, inwardly rectifying and not voltage

dependent, namely, the Ca^{2+} release-activated Ca^{2+} channel (CRAC) current (I_{CRAC}). (Hoth and Penner, 1992). Notably, I_{CRAC} is triggered in response to a reduction in ER [Ca^{2+}], not an increase in $[Ca^{2+}]_i$.

However, the molecular mechanism of SOCE remains unclear. The transient receptor potential (TRP) protein is hypothesized to be closely related to SOCE based on research on light transmission in *Drosophila*. TRP was identified in 1969, and its gene encodes a Ca^{2+}-permeable channel component. TRP channels are a superfamily of cation channels comprising seven subfamilies. TRPC1-TRPC7 are seven members of the canonical transient receptor potential (TRPC) gene family (Minke, 2006). Studies employing small interfering RNA (siRNA) and overexpression techniques have shown that TRPC1 contributes to the molecular mechanism of SOCE in VSMCs (Kunichika et al., 2004, Minke, 2006). On the other hand, the relationship between pool depletion and SOCE activation remains unclear. No significant progress in elucidating the molecular mechanism of SOCE was achieved until the identification of two distinct specific components, stromal interaction molecule (STIM) (Roos et al., 2005, Zhang et al., 2005b) and calcium release-activated calcium modulator (ORAI), which was discovered a year later (Feske et al., 2006, Vig et al., 2006).

The STIM protein mainly includes three parts: 1. an EF-hand motif, located at the N-terminus; 2. one transmembrane domain; and 3. a cytoplasmic region required for ORAI protein activation at the C-terminus (Figure 4). The N-terminal Ca^{2+}-binding EF-hand motif of STIM senses the [Ca^{2+}] in the ER lumen, while its sterile α motif (SAM) may promote multimerization (Lewis, 2007, Stathopulos et al., 2009). Similarly, the C-terminus of STIM interacts with ORAI, linking ER Ca^{2+} pool depletion to SOCE activation (Wang et al., 2014). STIM has two homologs, STIM1 and STIM2, with approximately 61% homology and different expression levels in the body; both proteins function as Ca^{2+} sensors in the ER (Williams et al., 2001, Cahalan, 2009, Collins and Meyer, 2011). STIM1 forms homomultimers

or heteromultimers with STIM2. But STIM2 has a lower affinity for Ca^{2+} than STIM1, it senses slight changes in the depletion of the ER Ca^{2+} pool, thus possibly serving as a feedback regulator that maintains the fundamental Ca^{2+} homeostasis between the cytoplasm and ER lumen (Brandman et al., 2007).

The ORAI1 protein contains four transmembrane regions and intracellular N- and C-termini (Feske et al., 2006). Two of the four transmembrane regions of ORAI1 contain highly conserved glutamic acid residues, which function as Ca^{2+} binding sites. Studies using whole-cell patch clamp techniques revealed that the glutamic acid residues of ORAI1 are required for the ion conductance and Ca^{2+} selectivity of CRACs (Prakriya et al., 2006, Vig et al., 2006, Yeromin et al., 2006). ORAI1 is structurally related to two other protein homologs, ORAI2 and ORAI3. ORAI2 and ORAI3 have not been extensively studied in CRACs, and previous research has not drawn clear conclusions. ORAI2 and ORAI3 function similarly to ORAI1 in CRACs (Mercer et al., 2006, Lis et al., 2007). ORAI2 slows the ability of ORAI1 to guide Ca^{2+}, thus decreasing Ca^{2+} entry (Vaeth et al., 2017). ORAI3 responds completely differently to putative CRAC inhibitors than ORAI1 and ORAI2 (Zhang et al., 2020). Therefore, ORAI1 is now accepted to play a predominant role in mediating CRAC activity (Gwack et al., 2007).

A potential mechanism of SOCE in most nonexcitable cells is described below (Stathopulos et al., 2008, Wang et al., 2008, Schindl et al., 2009, Varnai et al., 2009, Roberts-Thomson et al., 2010). In resting cells, ER [Ca^{2+}] interacts with the EF-hand motif of STIM to form the EF-hand–SAM domain. When ER [Ca^{2+}] is depleted, Ca^{2+} dissociates from the EF-hand motif, allowing the EF-hand–SAM domain to unfold and become extremely unstable, thus activating the STIM1 protein and inducing its oligomerization. After oligomerization, the STIM1 protein translocates from the ER and gradually approaches the ORAI1 protein located on the cytoplasmic membrane for interaction. The ORAI1 protein self-assembles into a tetramer that forms a channel, activating the CRAC and subsequently

allowing extracellular Ca^{2+} to enter the cell (Figure 4).

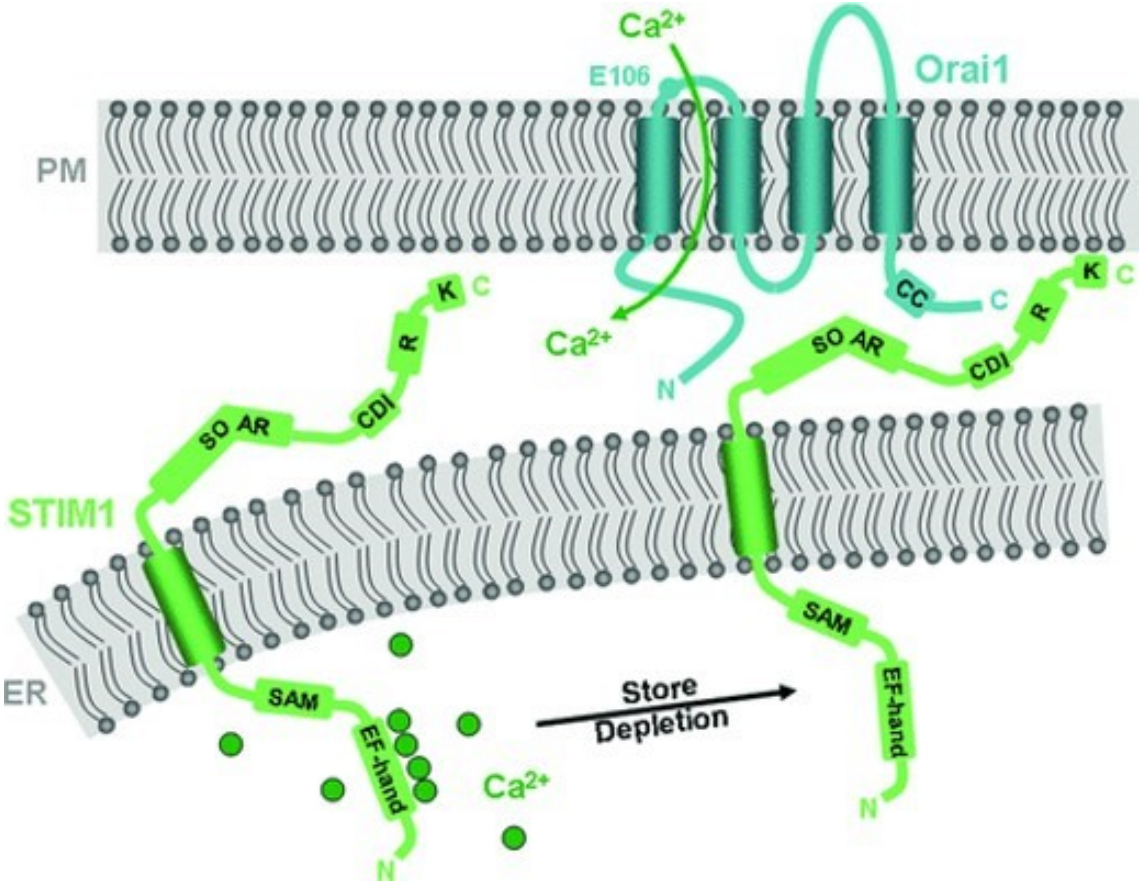

Figure 4 Predicted mechanism of action of ORAI1 and STIM1
ER lumen-localized STIM1 contains a Ca^{2+}-sensing EF-hand domain and a SAM, and cytoplasmic STIM1 contains a SOAR, a CDI domain, a regulatory domain (R) and a polylysine (K) domain. When the Ca^{2+} store is depleted, STIM1 rearranges within the ER membrane, interacts with the ORAI1 channel protein in the plasma membrane, and activates the channel. The ORAI1 protein has a four-transmembrane structure with cytoplasmic N- and C-termini. The C-terminus contains a putative coiled-coil structure essential for the functional STIM1 interaction. Glutamic acid 106 (E106) is selective for Ca^{2+} and functions as the selectivity filter of CRACs.
SOAR: STIM1–ORAI-activating region; CDI: Ca^{2+}-dependent inactivation; R: regulatory domain; K: polylysine domain. [from (Smyth et al., 2010), copyright license number: 5143891429415, provided by John Wiley and Sons]

1.2.4 SERCA inhibitors and SOCE in VSMCs

The function of SOCE has been investigated using drugs such as cyclopiazonic acid (CPA) and thapsigargin (TG). Both permanently block

SERCAs, depleting Ca^{2+} in the ER and therefore initiating SOCE. These drugs deplete the ER Ca^{2+} store without activating G proteins and are used to distinguish between Ca^{2+} entering through CRACs and Ca^{2+} entering through receptor-operated Ca^{2+} channels (ROCCs). The elevation of $[Ca^{2+}]_i$ and cellular responses induced by SERCA inhibitors might be interpreted as indications of the involvement of SOCE in signaling pathways.

VSMCs possess contractile activity, which is required for normal vascular tone and blood pressure regulation. Extracellular Ca^{2+} influx or ER $[Ca^{2+}]$ release leads to an increase in $[Ca^{2+}]_i$ in VSMCs, and increased Ca^{2+} binding to calmodulin results in the binding and activation of myosin light-chain kinase, activating myosin ATPase and triggering contraction. SERCA inhibitors also increase $[Ca^{2+}]_i$ in VSMCs, which may affect vascular tone. Therefore, numerous studies have used CPA or TG to assess the function of SOCE in VSMCs and the associated calcium channels involved in vasoconstriction. Unlike nonexcitable cells, voltage-operated calcium channels (VOCCs) are present in the cell membrane of VSMCs, among which L-type VOCCs are the dominant type. However, no clear conclusions on whether VOCCs are involved in the function of SOCE in VSMCs can be drawn from previous studies.

An *in vitro* study reported that TG-induced ER depletion activates SOCE in VSMCs and that this Ca^{2+} influx is independent of IP_3 production and L-type VOCCs (Xuan et al., 1992). However, additional *ex vivo* investigations have reached inconsistent conclusions. SERCA inhibitor-induced contractions in rat retinal, renal and pulmonary arteries are resistant to nifedipine, an L-type VOCC inhibitor, while the contractions in the aorta of mice are nifedipine-sensitive (Leung et al., 2008). Moreover, the contractions in the femoral and carotid arteries of rats and the fundus of mice, cats, and guinea pigs exhibit different sensitivities to nifedipine (Leung et al., 2008). Additionally, elevated $[Ca^{2+}]_i$ in VSMCs does not even necessarily cause contractions (Snetkov et al., 2003, Leung et al., 2008).

Until recently, some studies indicated a distinct role for SOCE. CPA-induced ER [Ca^{2+}] depletion resulted in a prolonged increase in $[Ca^{2+}]_i$ in rabbit cerebral arteries in the presence of a VOCC blocker without inducing contractions (Flemming et al., 2003), while contraction occurred in the absence of a VOCC blocker when the cell membrane was depolarized with a high-K^+ solution. (Flemming et al., 2003). We may speculate from those two findings that the depletion of Ca^{2+} stores causes SOCE activation, a process that is dominated by CRACs and results in a long-lasting increase in $[Ca^{2+}]_i$, which has a limited association with vasoconstriction. In contrast, VOCCs are involved in rapid and transient increases in $[Ca^{2+}]_i$, which are more relevant to vasoconstriction. Therefore, depletion of Ca^{2+} store-induced SOCE is possibly activated in a spatially distinct cellular compartment that is separated from contractile proteins. Additional cellular compartments, such as mitochondria and lysosomes, may regulate local Ca^{2+} levels.

1.3 Phosphate-dependent osteoinductive signaling in VSMCs

Multiple signaling pathways are involved in osteo/chondrocytic transdifferentiation of VSMCs stimulated by phosphate. According to recent research, increased $[Ca^{2+}]_i$ plays a role in this mechanism. In a CKD rat model, the resting $[Ca^{2+}]_i$ was increased in freshly isolated VSMCs; mechanistically, this increase was attributed to enhanced SOCE and suppressed Ca^{2+} efflux (Rodenbeck et al., 2017). An increased $[Ca^{2+}]_i$ is required for osteogenic differentiation and calcification (Nguyen et al., 2020). As in other cells, the $[Ca^{2+}]_i$ in resting VSMCs is closely controlled by PMCAs, SERCAs, and NCXs/NCKXs, which are Ca^{2+} pumps or exchangers. When VSMCs undergo phenotypic switching from the contractile to the proliferative-synthetic phenotype, the levels of Ca^{2+}-regulating proteins such as RYRs are reduced, and the levels of IP_3Rs and TRPC channels are increased (Berra-Romani et al., 2008, House et al., 2008).

The osteoinductive signaling cascade was recently shown to be mediated by serum- and glucocorticoid-inducible kinase (SGK1) (Tuffaha et al., 2018, Voelkl et al., 2018a). Phosphate increases the expression and activity of SGK1 in VSMCs, and SGK1 plays a critical role in phosphate-induced VCm (Voelkl et al., 2018a). Inhibition of SGK1 attenuates phosphate-induced VCm (Voelkl et al., 2018a). The downstream effectors of SGK1-dependent osteoinductive signaling include activating nuclear factor kappa-light-chain-enhancer of activated B cells (NF-κB) (Zhao et al., 2012, Yoshida et al., 2017, Zhang et al., 2017, Voelkl et al., 2018b). As observed in VSMCs and other cells, SGK1 not only phosphorylates IκB kinase α (IKKα), which phosphorylates the inhibitory protein IκB (Tai et al., 2009), but also directly degrades IκBα, leading to the nuclear translocation and activation of NF-κB (Lang et al., 2003, Voelkl et al., 2018a). Calcium oscillations activate NF-κB, which is accompanied by SOCE (Dolmetsch et al., 1998). NF-κB signaling promotes VCm at least partially by inducing increased expression of the osteogenic markers *CBFA1*, *MSX2*, and *ALPL,* as well as TNSALP activity, in VSMCs. (Lee et al., 2010, Voelkl et al., 2018b). Interfering with the activation of the NF-κB pathway inhibits osteo/chondrocytic transdifferentiation of VSMCs and VCm (Zhao et al., 2012, Voelkl et al., 2018a, Voelkl et al., 2018b).

NF-κB was discovered to upregulate the expression of ORAI1, which is activated by STIM1, resulting in an increase in SOCE in human embryonic kidney 293 (HEK293) cells (Eylenstein et al., 2012). SGK1 increases the protein expression level of the membrane protein ORAI1 and enhances I_{CRAC} and SOCE in HEK293 cells. Consequently, when SGK1 is knocked down, the ORAI1 protein expression level and SOCE decrease substantially (Eylenstein et al., 2011). Additionally, SGK1 upregulates ORAI1 expression in VSMCs via the NF-κB pathway (Walker-Allgaier et al., 2017).

Our findings suggest a signaling network connecting $[Ca^{2+}]_i$, SGK1, ORAI1, STIM1, and SOCE. However, the roles of ORAI, STIM1, and SOCE in

orchestrating osteoinductive signaling in VSMCs and VCm remain unclear. Therefore, we hypothesize that an increased extracellular phosphate concentration induces ORAI1/STIM1 expression in VSMCs, followed by the upregulation of SOCE.

1.4 Study aim

The purpose of this study was to explore whether ORAI1, STIM1, and SOCE are responsive to β-glycerophosphate (BGP), a phosphate donor, in human aortic smooth muscle cells (HAoSMCs) and investigate the role of ORAI1-induced SOCE in the orchestration of osteogenic signals.

Additionally, VSMC phenotypic switching involves alterations in VOCCs (Munoz et al., 2013); membrane depolarization via VOCCs also increases $[Ca^{2+}]_i$. This study investigated whether VOCCs are also involved in this mechanism.

2. Materials and Methods

2.1 Materials

2.1.1 Cells, medium, and inhibitors

Table 2.1: List of cells used and medium with additives.

Name	Supplier
Antibiotic-antimycotic (100x)	Invitrogen, Karlsruhe, Germany
Fetal bovine serum (FBS)	Gibco, Grand Island, USA
HAoSMC	Gibco, Grand Island, USA
Human vascular smooth muscle cell basal medium (Medium 231)	Gibco, Grand Island, USA
Trypsin-ethylenediaminetetraacetic acid (EDTA) (0.25%)	Gibco, Paisley, UK

Table 2.2: List of pharmacological inhibitors used.

Name	Supplier
2-Aminoethoxydiphenyl borate (2-APB)	Tocris, Bristol, United Kingdom
GSK650394	Sigma, Steinheim, Germany
MRS1845	Tocris, Bristol, United Kingdom
TG	Invitrogen, Goettingen, Germany

2.1.2 Chemicals and reagents

Table 2.3: List of chemicals used in the project.

Name	Supplier
30 % acrylamid/bis-acrylamid (29:1)	Carl Roth, Karlsruhe, Germany
4-(2-Hydroxyethyl)-piperazine-1-ethanesulfonic acid (HEPES)	Carl Roth, Karlsruhe, Germany
Alizarin red S	Sigma-Aldrich, St. Louis, USA
Ammonium persulfate (APS)	Carl Roth, Karlsruhe, Germany
Bovine serum albumin (BSA)	Sigma-Aldrich, St. Louis, USA

Calcium chloride ($CaCl_2$)	Sigma-Aldrich, St. Louis, USA
Chloroform	Carl Roth, Karlsruhe, Germany
D-(+)-glucose	Sigma-Aldrich, St. Louis, USA
Developer and Replenisher	Kodak, USA
Dimethyl sulfoxide (DMSO)	Carl Roth, Karlsruhe, Germany
Dulbecco's phosphate-buffered saline (D-PBS)	Sigma-Aldrich, St. Louis, USA
Ethanol 99%	Carl Roth, Karlsruhe, Germany
Ethylene-glycol-bis(β-aminoethyl)-N,N,N',N'-tetraacetic acid (EGTA)	VWR, Leuven, Belgium
Glycine	Carl Roth, Karlsruhe, Germany
Hydrochloric acid 32% (HCl)	Carl Roth, Karlsruhe, Germany
Isopropanol	Carl Roth, Karlsruhe, Germany
Magnesium sulfate ($MgSO_4$)	Sigma-Aldrich, St. Louis, USA
Methanol	Carl Roth, Karlsruhe, Germany
N,N,N′,N′-Tetramethylethylenediamine (TEMED)	Carl Roth, Karlsruhe, Germany
Non-fat milk powder	Carl Roth, Karlsruhe, Germany
Nuclease-free H_2O	Promega, Hilden, Germany
Paraformaldehyde (PFA)	Sigma-Aldrich, St. Louis, USA
Phenylmethylsulfonyl fluoride (PMSF)	Sigma-Aldrich, St. Louis, USA
Polyvinylidene fluoride (PVDF) membrane	Carl Roth, Karlsruhe, Germany
Ponceau S	Carl Roth, Karlsruhe, Germany
Potassium chloride (KCl)	Carl Roth, Karlsruhe, Germany
Roti®-Load 1 (4x)	Carl Roth, Karlsruhe, Germany
Silicone paste	Carl Roth, Karlsruhe, Germany
Sodium chloride (NaCl)	Carl Roth, Karlsruhe, Germany
Sodium dodecyl sulfate (SDS)	Carl Roth, Karlsruhe, Germany
Sodium hydrogen phosphate (Na_2HPO_4)	Carl Roth, Karlsruhe, Germany
Sodium hydroxide (NaOH) solution 1N	Carl Roth, Karlsruhe, Germany

Tris-(hydroxymethyl)-aminomethane (Tris)	Carl Roth, Karlsruhe, Germany
Tween-20	Carl Roth, Karlsruhe, Germany
β-Glycerophosphate (BGP)	Sigma-Aldrich, St. Louis, USA

Table 2.4: List of reagents used in the project.

Name	Supplier
ALP colorimetric assay kit	Abcam, USA
Bio-Rad protein assay dye reagent Concentrate	Bio-Rad Laboratories, München, Germany
DNase I	Thermo Fisher Scientific, USA
Fura-2 AM	Invitrogen, Goettingen, Germany
GoScript™ Reverse Transcriptase	Promega, Hilden, Germany
GoTaq® qPCR Master Mix	Promega, Hilden, Germany
Lipofectamine™ transfection agent	Invitrogen, Karlsruhe, Germany
Negative control siRNA	D-001810-10-05, Dharmacon, UK
Negative control siRNA	sc-37007, Santa Cruz Biotech, USA
Oligo(dT)$_{15}$ primers	Promega, Hilden, Germany
ORAI1 siRNA	L-014998-00-0005, Dharmacon, UK
ORAI1 siRNA	sc-76001, Santa Cruz Biotech, USA
PeqGold TriFast	Peqlab, Erlangen, Germany
Pierce™ enhanced chemiluminescence (ECL) western blotting substrate	Thermo Fisher Scientific, USA
Protein marker	Thermo Fisher Scientific, Danvers, USA
QuantiChrom™ Calcium Assay Kit	BioAssay Systems, Hayward, CA
Radioimmunoprecipitation assay (RIPA) lysis buffer (10x)	Cell Signaling Technology, Danvers, USA

Radom primers	Promega, Hilden, Germany

2.1.3 Primers and antibodies

Table 2.5 List of primers used for quantitative PCR.

Name	Orientation	Sequence	Species
ALPL	forward	5'-GGGACTGGTACTCAGACAACG-3'	Human
	reverse	5'-GTAGGCGATGTCCTTACAGCC-3'	
CBFA1	forward	5'-GCCTTCCACTCTCAGTAAGAAGA-3'	Human
	reverse	5'-GCCTGGGGTCTGAAAAAGGG-3'	
GAPDH	forward	5'-TCAAGGCTGAGAACGGGAAG-3'	Human
	reverse	5'-TGGACTCCACGACGTACTCA-3'	
MSX2	forward	5'-TGCAGAGCGTGCAGAGTTC-3'	Human
	reverse	5'-GGCAGCATAGGTTTTGCAGC-3'	
ORAI1	forward	5'-CACCTGTTTGCGCTCATGAT-3'	Human
	reverse	5'-GGGACTCCTTGACCGAGTTG-3'	
SGK1	forward	5'-AGGAGGATGGGTCTGAACGA-3'	Human
	reverse	5'-GGGCCAAGGTTGATTTGCTG-3'	
SOX9	forward	5'-AGCGAACGCACATCAAGAC-3'	Human
	reverse	5'-CTGTAGGCGATCTGTTGGGG-3'	
STIM1	forward	5'-AAGAAGGCATTACTGGCGCT-3'	Human
	reverse	5'-GATGGTGTGTCTGGGTCTGG-3'	

Table 2.6: List of antibodies used in the project.

Target	Lot No.	Source	Dilution	Supplier
Purified anti-GAPDH antibody	2118S	Rabbit	1:1000	Cell Signaling Technology, Danvers, USA
Purified anti-ORAI1 antibody	13130-1-AP	Rabbit	1:1000	Proteintech, Rosemont, USA
Purified anti-STIM1 antibody	4916S	Rabbit	1:1000	Cell Signaling Technology, Danvers, USA
Purified anti-rabbit	7074S		1:2500	Cell Signaling Technology,

horseradish peroxidase (HRP)-conjugated antibody				Danvers, USA

2.1.4 Solutions and buffers

Table 2.7 List of solutions and buffers used in the study.

Solutions or buffers	Composition	
Tris-buffered saline (TBS) (pH 7.6, 10x)	Tris-base	500 mM
	NaCl	1.5 M
Tris buffered saline, with tween-20 (TBST)	1xTBS	
	Tween-20	0.1%
Blocking buffer/Antibody dilution buffer	1xTBS	
	Tween-20	0.1%
	Non-fat milk powder/BSA	5% w/v
Transfer buffer	Tris-base	25 mM
	Glycine	200 mM
	Methanol	20%
Electrophoresis buffer (10x)	Tris-base	250 mM
	Glycine	2.5 M
	SDS	1% w/v
Standard HEPES solution (pH 7.4)	NaCl	125 mM
	KCl	5 mM
	$MgSO_4$	1.2 mM
	$CaCl_2$	1 mM
	Na_2HPO_4	2 mM
	HEPES	32 mM
	D-(+)-glucose	5 mM
Ca^{2+}-free HEPES solution (pH 7.4)	NaCl	125 mM
	KCl	5 mM
	$MgSO_4$	1.2 mM

	Na_2HPO_4	2 mM
	HEPES	32 mM
	EGTA	0.5 mM
	D-(+)-glucose	5 mM

2.1.5 Consumables and instruments

Table 2.8: List of consumables and instruments used.

Name	Manufacturer
Amersham Hyperfilm™ ECL	GE Healthcare, Munich, Germany
Axiovert 100 microscope	Carl Zeiss, Oberkochen, Germany
BioPhotometer	Eppendorf, Hamburg, Germany
BioTek™ PowerWave™ Microplate Spectrophotometer	BioTek, Bad Friedrichshall, Germany
Borosilicate glass pipettes	Harvard Apparatus, UK
Cell culture plates 6, 12, 24, 48 well	Corning incorporated, München, Germay
Centrifuge	Andreas Hettich GmbH, Tuttlingen, Germany
CFX96 Connect™ real-time System	Bio-Rad, München, Germany
Corning® Costar® Stripette® serological pipettes 5, 10, 25 mL	Corning incorporated, München, Germay
Cuvettes, Uvette	Eppendorf, Hamburg, Germany
Electrophoresis and blotting system	Bio-Rad, Munich, Germany
Eppendorf 5331 MasterCycler gradient thermal cycler	Eppendorf, Hamburg, Germany
Eppendorf 5417R refrigerated centrifuge	Eppendorf, Hamburg, Germany
Eppendorf tube 0.5, 1.5, 2.0 mL	Eppendorf, Hamburg, Germany
Heraeus cell culture hood	Hera Safe, Osterode, Germany
Heraeus cell culture incubator	Thermo Fisher Scientific, USA
Inverted optical microscope	Nikon, Dusseldorf

pH meter	SI Analytics, Mainz, Germany
qPCR 96-well plates	VWR, Leuven, Belgium
Sterile tips 10, 100, 200, 1000 µL	Biozyme, USA
Sterile tubes 15, 50 mL	Greiner bio-one, Frickenhausen, Germany
Tissue Culture Flask 25, 75 mL	SARSTEDT, Nübrecht, Germany
Vortex-Genie2	Scientific Industries, New York, USA
Water baths	Janke & Kunkel, Staufen, Germany

2.1.6 Software

Table 2.9: List of software used.

Software	Supplier
Endnote	Version X9, Clarivate Analytics, USA
GraphPad Prism	Version 8.0.2, San Diego, California, USA
ImageJ	Version 1.52, National Institutes of Health, Bethesda, MD, USA
Metafluor	Version 7.5, Universal Imaging, Downingtown, PA, USA
SPSS	Version 26.0, SPSS Inc., Chicago, IL, USA
Word/Excel/PowerPoint	Version 2016 pro, Microsoft, USA

2.2 Methods

2.2.1 Cell culture

HAoSMCs were cultured in Medium 231 supplemented with 10% FBS and antibiotic-antimycotic (1x) at 37°C in a humidified atmosphere containing 5% CO_2. The culture medium was replaced every 2 or 3 days. HAoSMCs between passages 4 and 10 were utilized in all experiments upon reaching 70-80% confluence.

2.2.2 Drug preparation and *in vitro* treatment

The indicated concentrations of BGP were prepared in serum- and antibiotic-free Medium 231, which is frequently employed instead of phosphate to promote calcification (Moe and Chen, 2004).

Unless specified otherwise, HAoSMCs were treated with BGP for 24 hours before quantitative PCR, western blotting, and calcium measurements. Cells were exposed to the same concentration of BGP for 7 days before the TNSALP activity assay.

All pharmacological inhibitors (2-APB, MRS1845, GSK650394, and TG) were prepared in DMSO (1:1000 final concentration in the cell medium), and all relevant control groups were treated with the same amount of DMSO.

HAoSMCs were treated with 10 mM BGP for 14 days to quantify the extracellular calcium content, and alizarin red S staining was used to visualize calcified deposits.

2.2.3 Quantitative PCR

2.2.3.1 RNA extraction from HAoSMCs

RNA was extracted from those cell samples using TriFast reagent (1 mL/10 cm^2), and the cell lysate was passed through a pipette multiple times before an incubation at room temperature for 5 minutes.

After the dissociation of cells at room temperature, 0.2 mL of chloroform per 1 mL of TriFast was added, followed by vigorous vibration for 15 seconds. The

samples were mixed well and incubated at room temperature for 2-3 minutes before centrifugation at 12000 x g for 20 minutes at 4°C. Following centrifugation, the aqueous phase was transferred to a clean RNase-free centrifuge tube. RNA was precipitated by adding 0.5 mL of isopropanol per 1 mL of TriFast to the tube. After mixing well, the mixture was incubated on ice for 10-15 minutes before being centrifuged at 12000 x g for 10 minutes at 4°C.

After the supernatant was carefully removed, the RNA pellet was washed twice with 75% prechilled ethanol and centrifuged at 12000 x g for 10 minutes at 4°C.

The RNA pellet was then air-dried at room temperature for approximately 10-15 minutes after the removal of the supernatant and then dissolved in RNase-free H_2O for 10-15 minutes at 65°C. The concentrations of the RNA samples were determined using the BioPhotometer (Eppendorf) at 260 nm and 280 nm after dilution at a 1:69 ratio in RNase-free H_2O (Sukkar, 2020).

2.2.3.2 cDNA synthesis

Reverse transcription of total RNA was conducted with the GoScript™ Reverse Transcription System (Promega) according to the manufacturer's protocol. Following DNase digestion, 1 µL of oligo$(dT)_{15}$ primers, 1 µL of random primers and nuclease-free H_2O were added to a volume containing 2 µg of RNA to a total volume of 5 µL. Each tube was heated to 70°C in the thermocycler (Eppendorf) with a hot lid for 5 minutes and was then immediately cooled to 4°C for 5 minutes.

A mixture containing 4.0 µL of 5x GoScript™ reaction buffer, 2.0 µL of $MgCl_2$, 1.0 µL of PCR Nucleotide Mix, 1.0 µL of GoScript™ reverse transcriptase and 0.5 µL of recombinant RNasin® ribonuclease inhibitor was prepared, and a total volume of 15 µL was reached by adding nuclease-free H_2O.

Each 5 µL mixture of RNA and primers was added to 15 µL of the reverse transcription reaction mixture. The final reaction volume per tube was 20 µL. The

samples were placed in the thermocycler and incubated at 25°C for 5 minutes, 42°C for 60 minutes, and 70°C for 15 minutes.

2.2.3.3 Quantitative PCR

The transcript levels of target genes were determined using quantitative PCR. Samples were processed on ice. The total volume of the reaction mixture (15 µL) contained 100 µg of cDNAs, 2x GoTaq® qPCR Master Mix (Promega), 500 nM forward and reverse primers (Thermo Fischer Scientific), and nuclease-free H_2O.

Quantitative PCR was conducted using a CFX96 Real-Time System (Bio–Rad). The cycling program consisted of the following steps: predenaturation at 95°C for 3 minutes, followed by 40 cycles of 95°C for 15 seconds, 59°C for 30 seconds, and 72°C for 30 seconds. The primers used for amplification are shown in Table 2.5.

All experiments were performed in duplicate. A melting curve analysis was performed to determine the specificity of the PCR products. The relative mRNA expression was calculated using the $2^{-\Delta\Delta Ct}$ method and normalized to the control group, with GAPDH serving as an internal reference.

2.2.4 Silencing of ORAI1

HAoSMCs were transfected with 10 nM validated ORAI1 siRNA (siORAI1; Dharmacon & Santa Cruz Biotech) or negative control siRNA (Dharmacon & Santa Cruz Biotech) using Lipofectamine™ transfection reagent (Invitrogen) to silence ORAI1.

A total of 3.75 µL of Lipofectamine™ transfection reagent in 125 µL of serum- and antibiotic-free Medium 231 was added to HAoSMCs cultured in each well. Then, 125 µL of the same medium were mixed with 10 nM siORAI1 (prepared with RNase-free H_2O) or negative control siRNA. Each tube of diluted siORAI1 or negative control siRNA was added to a tube of diluted Lipofectamine™ transfection reagent (1:1 ratio) and incubated for 10-15 minutes at room temperature. Finally, the cells were treated with the combination of siRNA and

lipid and incubated at 37°C for 2-4 days. Quantitative PCR and immunoblotting were used to assess the silencing efficiency.

2.2.5 Protein extraction and western blotting

2.2.5.1 Protein extraction

HAoSMC samples were washed twice with 4°C precooled D-PBS. After adding an appropriate volume of ice-cold RIPA lysis buffer (Cell Signaling Technology) containing 1 mM PMSF, the cell lysate was harvested by scraping with a cell scraper. The supernatant was collected after an incubation on ice for 30 minutes, followed by centrifugation at 12000 x g for 10 minutes at 4°C.

2.2.5.2 Determination of the protein concentration

The Bradford assay (Bio–Rad) was used to determine the protein content. An appropriate volume of protein lysate (obtained using the abovementioned protein extraction process, usually 2 µL) was combined with 1 mL of diluted Bradford buffer (diluted 1:5 with dH_2O), and the protein concentration was determined by measuring the absorbance at 595 nm using the BioPhotometer (Eppendorf). Roti®-Load 1 was then added to the protein samples and heated for 5 minutes at 95°C.

2.2.5.3 Preparation of resolving and stacking sodium dodecyl sulfate (SDS)–polyacrylamide gels

Table 2.10: Recipes for the resolving and stacking gels.

Gel	Component	Volume
Resolving gel (10%)/ 15 mL	dH_2O	6.03 mL
	30% acrylamid/bis-acrylamid	5 mL
	1.5 M Tris (pH 8.8)	3.75 mL
	10% SDS	150 µL
	10% APS	75 µL
	TEMED	7.5µL
Stacking gel (4%)/ 5 mL	dH_2O	3 mL
	30% acrylamid/bis-acrylamid	0.66 mL

	1.0 M Tris (pH 6.8)	1.26 mL
	10% SDS	50 μL
	10% APS	25 μL
	TEMED	5 μL

Gels were prepared in the format described in the table shown above, followed by pouring into a special glass plate device for electrophoresis.

2.2.5.4 SDS–polyacrylamide gel electrophoresis (PAGE)

After the protein concentration was calibrated, each well was loaded with 30 μg of protein from the samples. Electrophoretic separation was started at 80 V for 30 minutes and then increased to 100 V for one and a half hours (Sukkar, 2020). A protein marker (Thermo Fisher Scientific) was used to estimate the size of the proteins.

2.2.5.5 Transfer of proteins to membranes

Protein transfer to a polyvinylidene fluoride (PVDF) membrane was conducted in an ice bath at 100 V (the current was approximately 0.3 A) for approximately 1 hour.

After the transfer was complete, Ponceau S was used to determine whether the proteins had been transferred to the membrane, which was then washed with distilled H_2O until decolorized.

2.2.5.6 Antibody incubation and protein detection

Nonspecific binding sites were blocked for 1 hour at room temperature with blocking buffer, and the membrane was incubated overnight at 4°C with primary antibodies against ORAI1, STIM1, and GAPDH. The detailed information on the antibodies is provided in Table 2.6. The next day, the membrane was washed three times for 10 minutes each with TBST and then incubated with a secondary antibody for one hour, both at room temperature. Following three additional washes with TBST, an ECL working solution was prepared (A:B=1:1) and incubated with the membrane in the dark for 1-5 minutes. Western blot images were digitized and analyzed using ImageJ software (NIH, USA) for protein

quantification.

2.2.6 Ca^{2+} measurements

$[Ca^{2+}]_i$ was measured using fura-2 AM fluorescence (Bird et al., 2008, Schmid et al., 2012), and the cells were treated accordingly and loaded onto chambered glass coverslips.

HAoSMCs were treated with fura-2 AM for 30-45 minutes at 37°C in the dark. Variations in $[Ca^{2+}]_i$ were measured using the technique outlined below. Cells were initially incubated with a standard HEPES solution for 3 minutes and then with a Ca^{2+}-free HEPES solution for 3 minutes, followed by 7 minutes of a Ca^{2+}-free HEPES solution together with TG (1 μM) and an incubation with a standard HEPES solution for 7 minutes. During this procedure, cells were excited alternately at 340 nm and 380 nm, the intensity was measured at 505 nm through an oil objective (Fluor 40×/1.30) of an inverted phase contrast microscope (Axiovert 100, Zeiss), and data acquisition (10 second intervals) was performed using MetaFluor software (Ma et al., 2019, Ma et al., 2020).

The extent of SOCE activity was quantified as the peak (delta ratio) and slope (delta ratio/s) increase following the readdition of Ca^{2+} (standard HEPES). The solutions are described in Table 2.7.

2.2.7 TNSALP activity assay

An ALP colorimetric assay kit (Abcam) was used to measure TNSALP activity in HAoSMCs according to the manufacturer's procedure (Abcam, 2021). The kit contained a p-nitrophenyl phosphate (pNPP) solution, an aliquot of ALP enzyme, Assay Buffer and Stop Solution. The ALP enzyme converts an equivalent quantity of pNPP substrate to colored p-nitrophenol (pNP), and the absorbance is measured at 405 nm. A standard curve of pNPP was prepared in advance (Abcam, 2021). HAoSMCs lysate was prepared in Assay Buffer, and the protein content was determined using the Bradford assay as described above. The pNPP solution was then added to each sample well, and ALP enzyme

solution was added to each pNPP standard well, followed by an incubation at 25°C for 60 minutes in the dark. Stop Solution was used to stop the reaction in all wells. The plate was gently shaken, and the absorbance was measured at 405 nm using a microplate reader (BioTek).

2.2.8 Alizarin red S staining

A 1% alizarin red S solution was prepared in dH_2O (pH 4.5). Cells were fixed with 4% paraformaldehyde (PFA) for 30-45 minutes at 4°C and then washed twice with dH_2O. The cells were then stained with the indicated alizarin red S solution for one hour at room temperature and washed three times with dH_2O. Finally, images of stained cells were acquired using an inverted phase contrast microscope (Nikon).

2.2.9 Calcium content assay

For this experiment**,** 0.6 M HCl was used to decalcify HAoSMCs for 24 hours at 4°C. The calcium content was determined using the QuantiChrom™ Calcium Assay Kit (BioAssay Systems). Next, 0.1 M NaOH/0.1% SDS was used to lyse cells. The calcium content was reported in units per mg of protein (U/mg protein) (Bio–Rad).

2.2.10 Statistical analysis

Data are presented as the mean ± SD values. GraphPad Prism (version 8.0.2) and SPSS (version 26.0) software were used to analyze the data. The statistical tests included both paired and unpaired Student's t tests and one-way analysis of variance (ANOVA) with the Bonferroni post hoc test. A p value ≤ 0.05 was considered statistically significant for all tests.

3. Results

3.1 BGP sensitivity of osteogenic markers in HAoSMCs

Cells were treated with different concentrations of BGP for 24 hours to determine the optimal phosphate concentration required to induce the expression of osteogenic markers in HAoSMCs predicted in previous VCm studies (Voelkl et al., 2013, Leibrock et al., 2015, Alesutan et al., 2016, Leibrock et al., 2016). The quantitative PCR results showed that treatment with 2 mM BGP substantially increased *CBFA1, MSX2, SOX9*, and *ALPL* transcript levels in HAoSMCs (Figure 5).

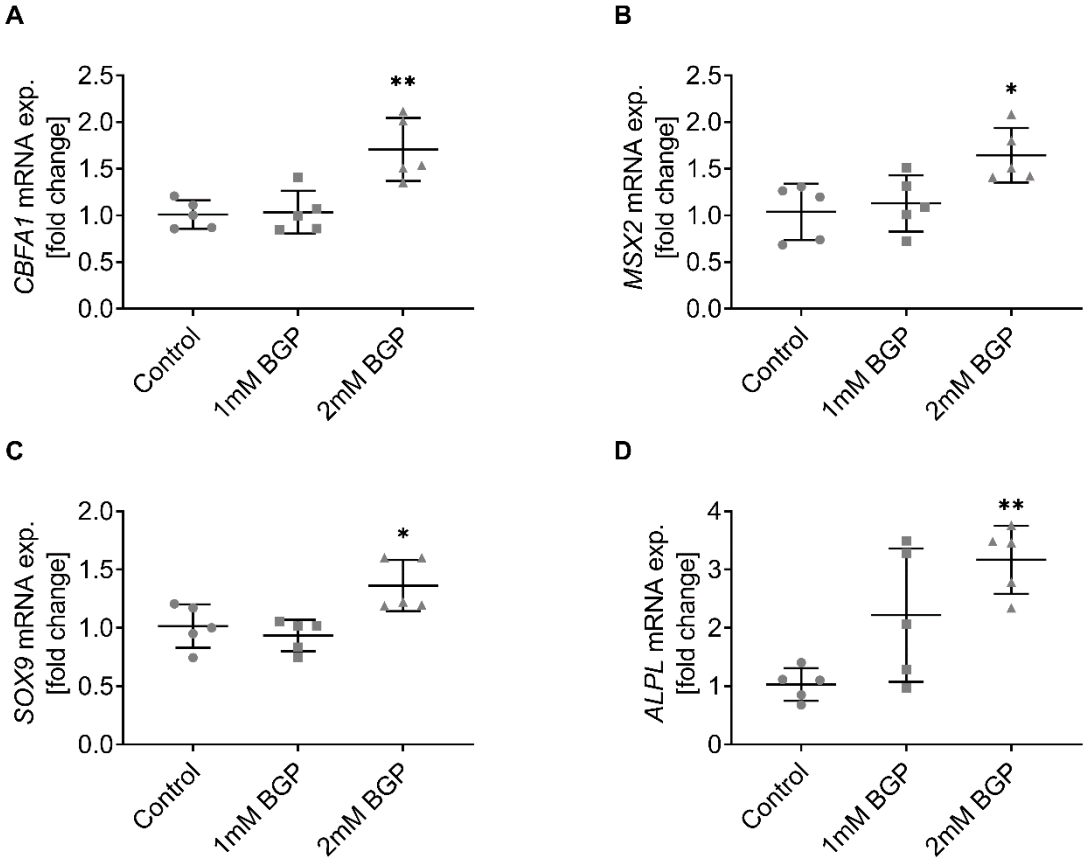

Figure 5 Treatment with 2 mM BGP stimulated osteogenic marker expression in HAoSMCs

A-D. Single values and arithmetic means ± SDs (n = 5) of (**A**) *CBFA1*, (**B**) *MSX2*, (**C**)

SOX9 and (**D**) *ALPL* transcript levels in HAoSMCs without (Control) and with 24 hours of exposure to the indicated concentrations of BGP.
*p<0.05 and **p<0.01 indicate statistically significant differences in HAoSMCs from the Control group (ANOVA).

3.2 Phosphate stimulated ORAI1 and STIM1 mRNA and protein expression in HAoSMCs

HAoSMCs were analyzed using quantitative PCR and immunoblotting at the same time point to investigate whether the expression levels of ORAI1 and STIM1 were affected by 2 mM BGP, which was indicated to be effective at inducing the expression of osteogenic markers. As a result, 2 mM BGP significantly stimulated ORAI1 and STIM1 expression at both the mRNA and protein levels (Figure 6) (Ma et al., 2019).

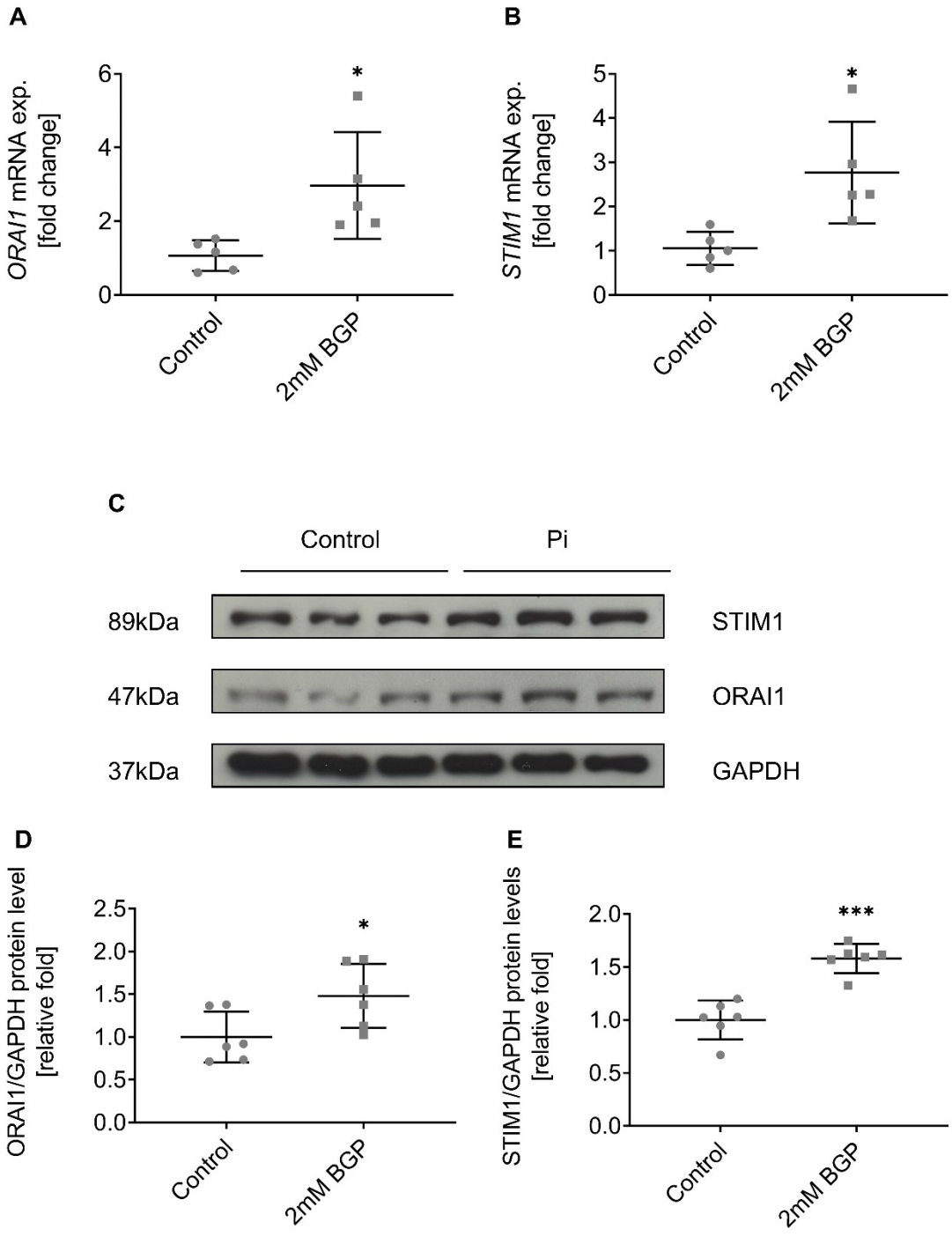

Figure 6 Phosphate stimulated ORAI1 and STIM1 mRNA and protein expression in HAoSMCs

A, B. Single values and arithmetic means ± SDs (n = 5) of (**A**) *ORAI1* and (**B**) *STIM1* transcript levels in HAoSMCs without (Control) and with 24 hours of exposure to 2 mM BGP.

C. Representative immunoblot showing the abundance of the ORAI1, STIM1 and

GAPDH proteins in HAoSMCs without (Control) and with 24 hours of exposure to 2 mM BGP.
D, E. Single values and arithmetic means ± SDs (n = 6) of (**D**) ORAI1 and (**E**) STIM1 protein levels in HAoSMCs without (Control) and with 24 hours exposure to 2 mM BGP. GAPDH was used as an internal control.
*p<0.05 and ***p<0.001 indicate statistically significant differences compared to the Control group (Student's t test). Adapted from (Ma et al., 2019).

3.3 Phosphate stimulated SOCE in HAoSMCs

$[Ca^{2+}]_i$ was measured by detecting fura-2 AM fluorescence to explore whether phosphate-induced upregulation of ORAI1 and STIM1 expression is associated with alterations in Ca^{2+} signaling. As previously described, HAoSMCs were pretreated either with or without (Control) 2 mM BGP for 24 hours. We assessed SOCE by first treating HAoSMCs with a Ca^{2+}-free HEPES solution and then exposing them to the SERCA inhibitor TG in Ca^{2+}-free HEPES solution to deplete ER Ca^{2+} stores. SOCE was assessed by again supplementing the cells with extracellular Ca^{2+} in the continued presence of TG. After the readdition of extracellular Ca^{2+}, fura-2 AM fluorescence rapidly increased, and SOCE was then assessed as the peak (delta ratio) and slope (delta ratio/s) increase. These results showed that BGP did not affect Ca^{2+} release from the ER significantly but considerably increased the slope and peak value of SOCE (Figure 7) (Ma et al., 2019). Together with the aforementioned quantitative PCR and immunoblotting findings, elevated phosphate levels increased the expression of ORAI1 and STIM1 mRNAs and proteins in HAoSMCs, with a subsequent increase in SOCE.

In addition, HAoSMCs were treated with BGP for only 30 minutes to investigate whether phosphate can directly act on SOCE, as shown in Figure 8. Short-term exposure to BGP did not significantly alter SOCE, indicating that the effect of BGP on SOCE was time-dependent (Ma et al., 2019).

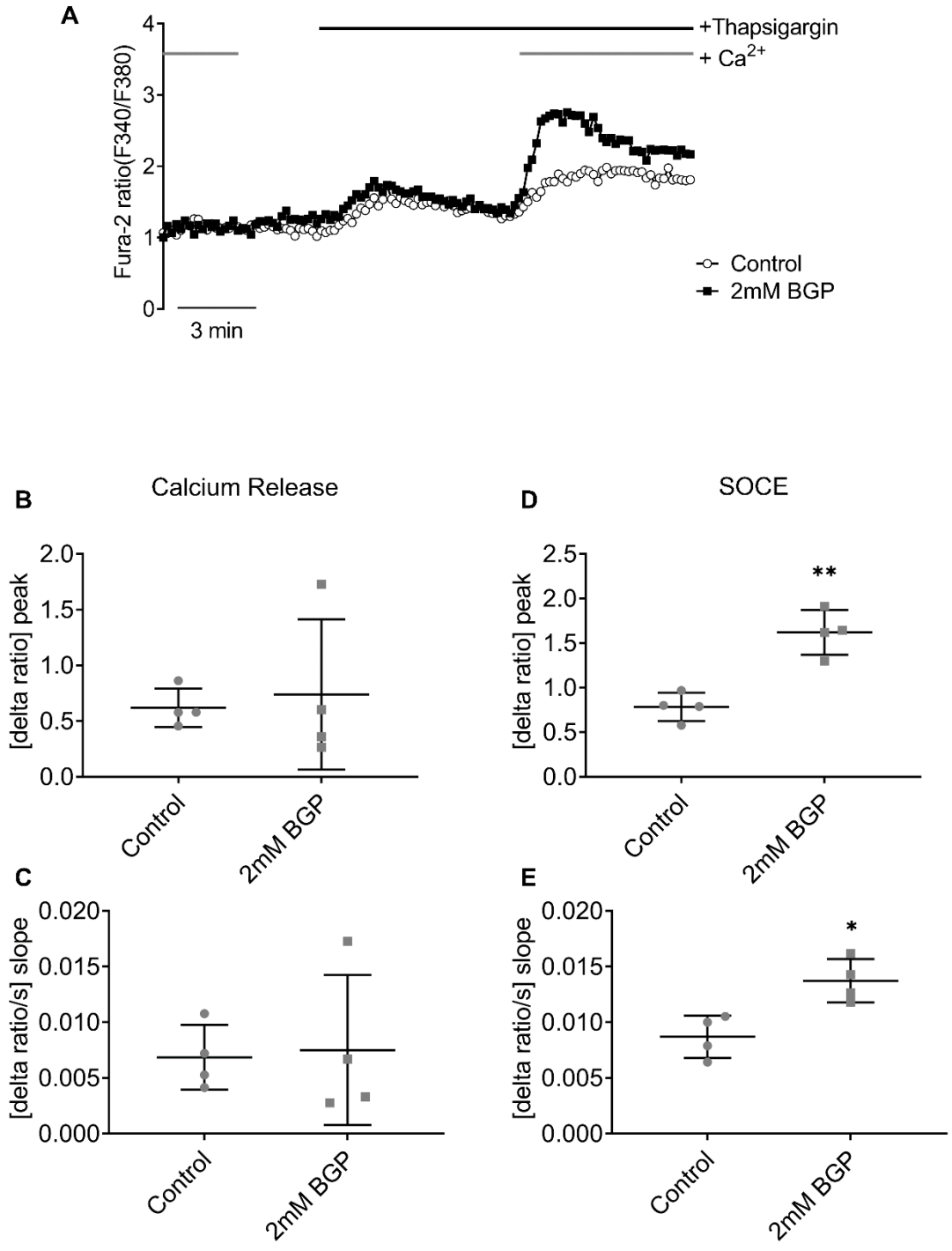

Figure 7 Phosphate stimulated SOCE in HAoSMCs

A. Representative tracings of the fura-2 AM fluorescence ratio in the presence of physiological Ca^{2+} concentrations and in the absence of extracellular Ca^{2+} following the addition of TG (1 µM) and the readdition of extracellular Ca^{2+} in HAoSMCs without (Control) and with 24 hours of prior exposure to 2 mM BGP.

B, C. Single values and arithmetic means ± SDs (n = 28-35 cells from 4 different batches)

of the (**B**) peak and (**C**) slope increase in the fura-2 AM fluorescence ratio after the addition of TG (1 µM) in HAoSMCs without (Control) and with 24 hours of prior exposure to 2 mM BGP.
D, E. Single values and arithmetic means ± SDs (n = 28-35 cells from 4 different batches) of the (**B**) peak and (**C**) slope increase in fura-2 AM fluorescence ratio after the readdition of extracellular Ca^{2+} to HAoSMCs without (Control) and with 24 hours of prior exposure to 2 mM BGP.
*p<0.05 and **p<0.01 indicate a statistically significant difference compared to the Control group (Student's t test). Figure adapted from (Ma et al., 2019).

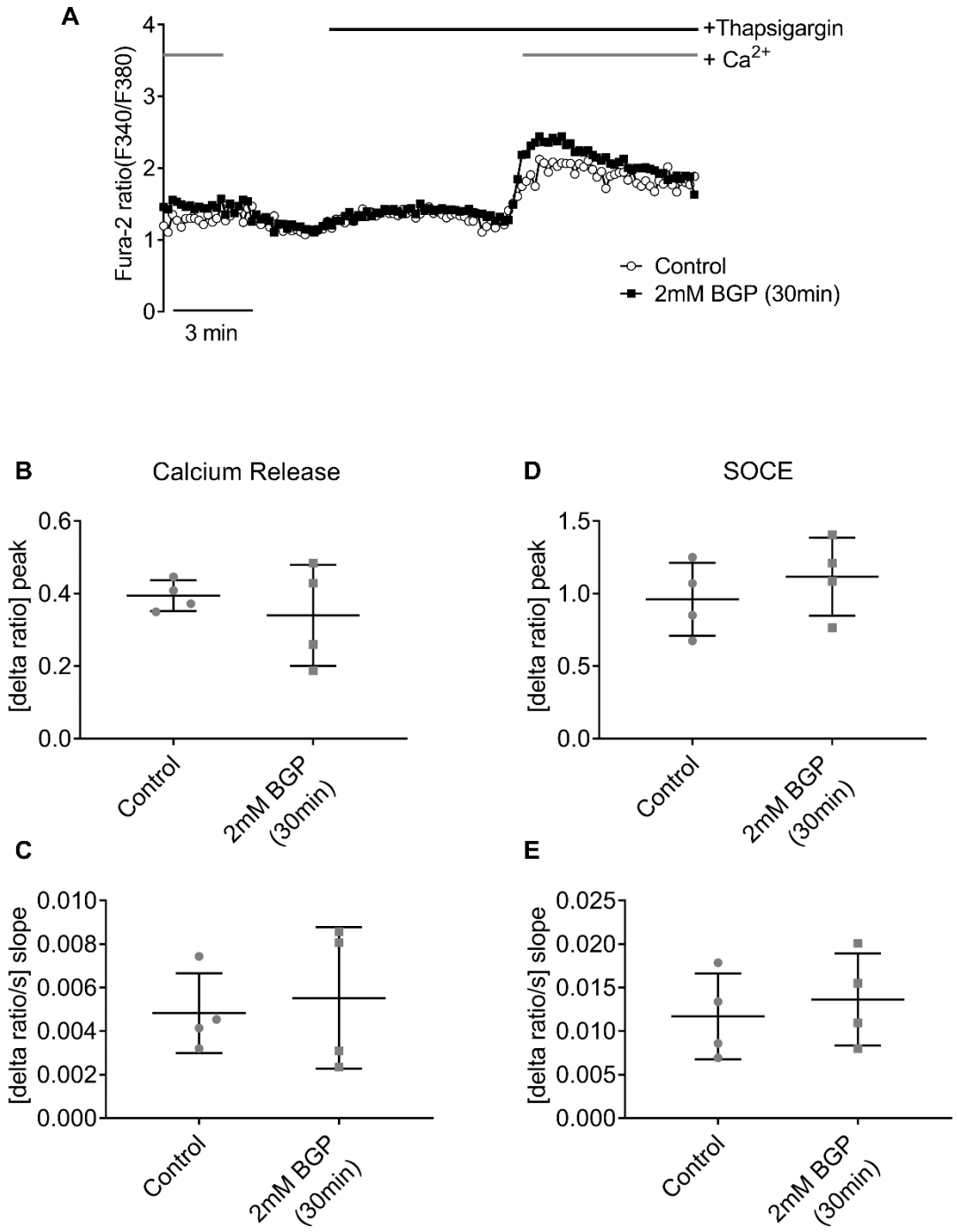

Figure 8 Thirty minutes of phosphate treatment did not affect intracellular Ca^{2+} release or SOCE in HAoSMCs

A. Representative tracings of the fura-2 AM fluorescence ratio in the presence of physiological Ca^{2+} concentrations, in the absence of extracellular Ca^{2+} following the addition of TG (1 μM), and after the addition of extracellular Ca^{2+} in HAoSMCs without (Control) and with 30 minutes of prior exposure to 2 mM BGP.

B, C. Single values and arithmetic means ± SDs (n = 25-36 cells from 4 different batches) of the (**B**) peak and (**C**) slope increase in the fura-2 AM fluorescence ratio after the addition of TG (1 µM) to HAoSMCs without (Control) and with 30 minutes of prior exposure to 2 mM BGP.
D, E. Single values and arithmetic means ± SDs (n = 25-36 cells from 4 different batches) of the (**B**) peak and (**C**) slope increase in the fura-2 AM fluorescence ratio after the readdition of extracellular Ca^{2+} to HAoSMCs without (Control) and with 30 minutes of prior exposure to 2 mM BGP.
Figure adapted from (Ma et al., 2019).

3.4 ORAI1 antagonists inhibited phosphate-stimulated SOCE

HAoSMCs were treated with or without the ORAI1 antagonists MRS1845 (10 µM) (Salker et al., 2018, Abdelazeem et al., 2019, Zhu et al., 2021) or 2-APB (50 µM) (Prakriya and Lewis, 2001, Zhang et al., 2016, Pelzl et al., 2017, Salker et al., 2018) for 24 hours in the absence or presence of 2 mM BGP to investigate the role of ORAI1 in phosphate-stimulated SOCE. The results from our preliminary experiments suggested that the effective concentration of MRS1845 that inhibited SOCE in HAoSMCs was 10 µM (Figure 9). At this concentration, MRS1845 significantly reduced both the slope and peak increase in SOCE in the presence of BGP (Figure 10) (Ma et al., 2019). Similarly, the effect of BGP on SOCE was abolished by 2-APB (Figure 11). In conclusion, these findings suggest that ORAI1 mediates phosphate-stimulated SOCE in HAoSMCs.

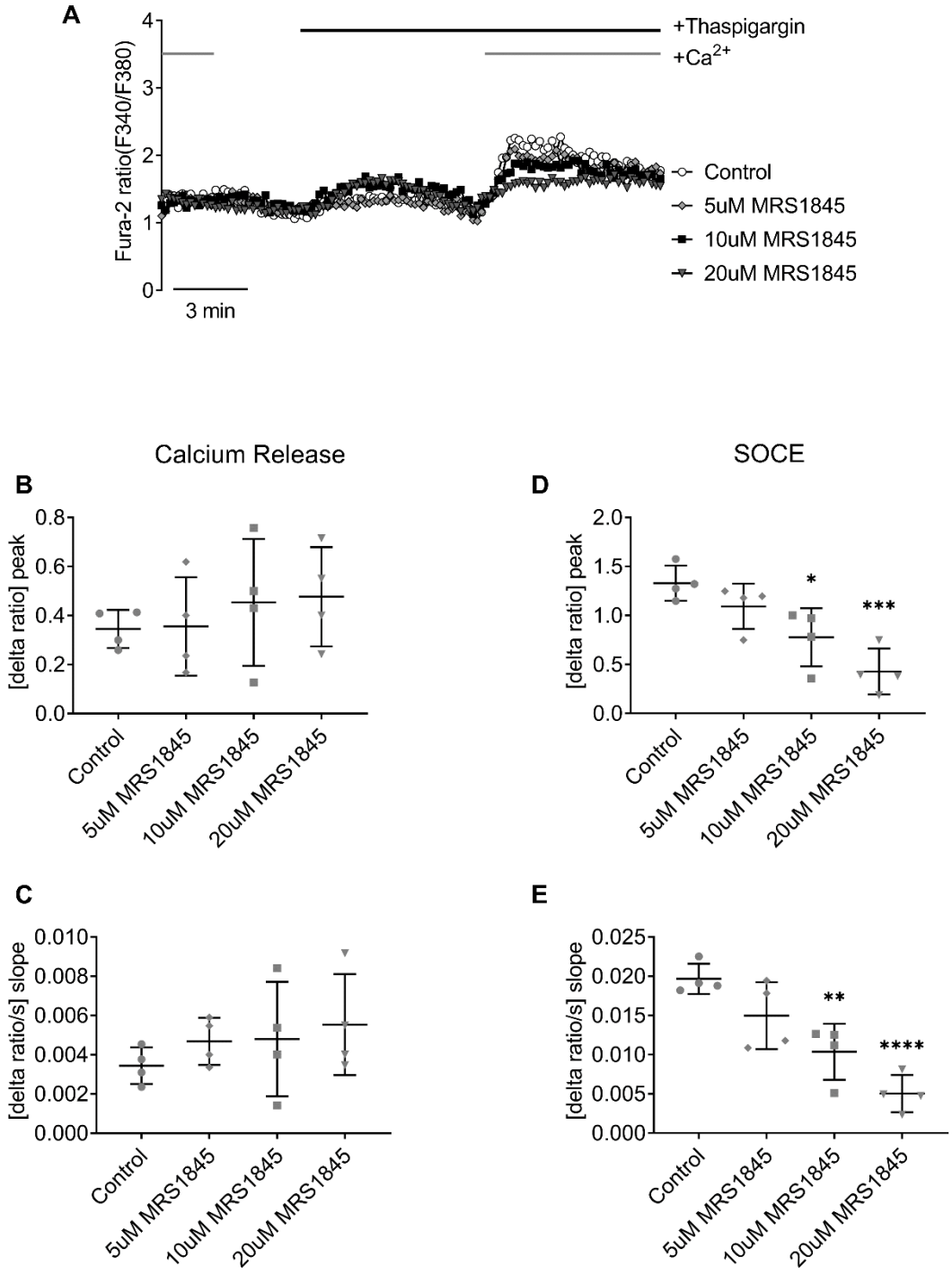

Figure 9 Inhibition of SOCE by MRS1845 at different concentrations

A. Representative tracings of the fura-2 AM fluorescence ratio in the presence of physiological Ca^{2+} concentrations, in the absence of extracellular Ca^{2+} following the addition of TG (1 μM) and after the readdition of extracellular Ca^{2+} to HAoSMCs without (Control) and with 24 hours of prior exposure to different concentrations of MRS1845 (5 μM, 10 μM, or 20 μM).

B, C. Single values and arithmetic means ± SDs (n = 35-42 cells from 4 different batches) of the (**B**) peak and (**C**) slope increase in the fura-2 AM fluorescence ratio after the addition of TG (1 µM) to HAoSMCs without (Control) and with 24 hours of previous exposure to different concentrations of MRS1845 (5 µM, 10 µM, or 20 µM).
D, E. Single values and arithmetic means ± SDs (n = 35-42 cells from 4 different batches) of the (**B**) peak and (**C**) slope increase in the fura-2 AM fluorescence ratio after the readdition of extracellular Ca^{2+} to HAoSMCs without (Control) and with 24 hours of prior exposure to different concentrations of MRS1845 (5 µM, 10 µM, or 20 µM).
*p<0.05, **p<0.01, ***p<0.001, and ****p<0.0001 indicate a statistically significant difference compared to the Control group (ANOVA).

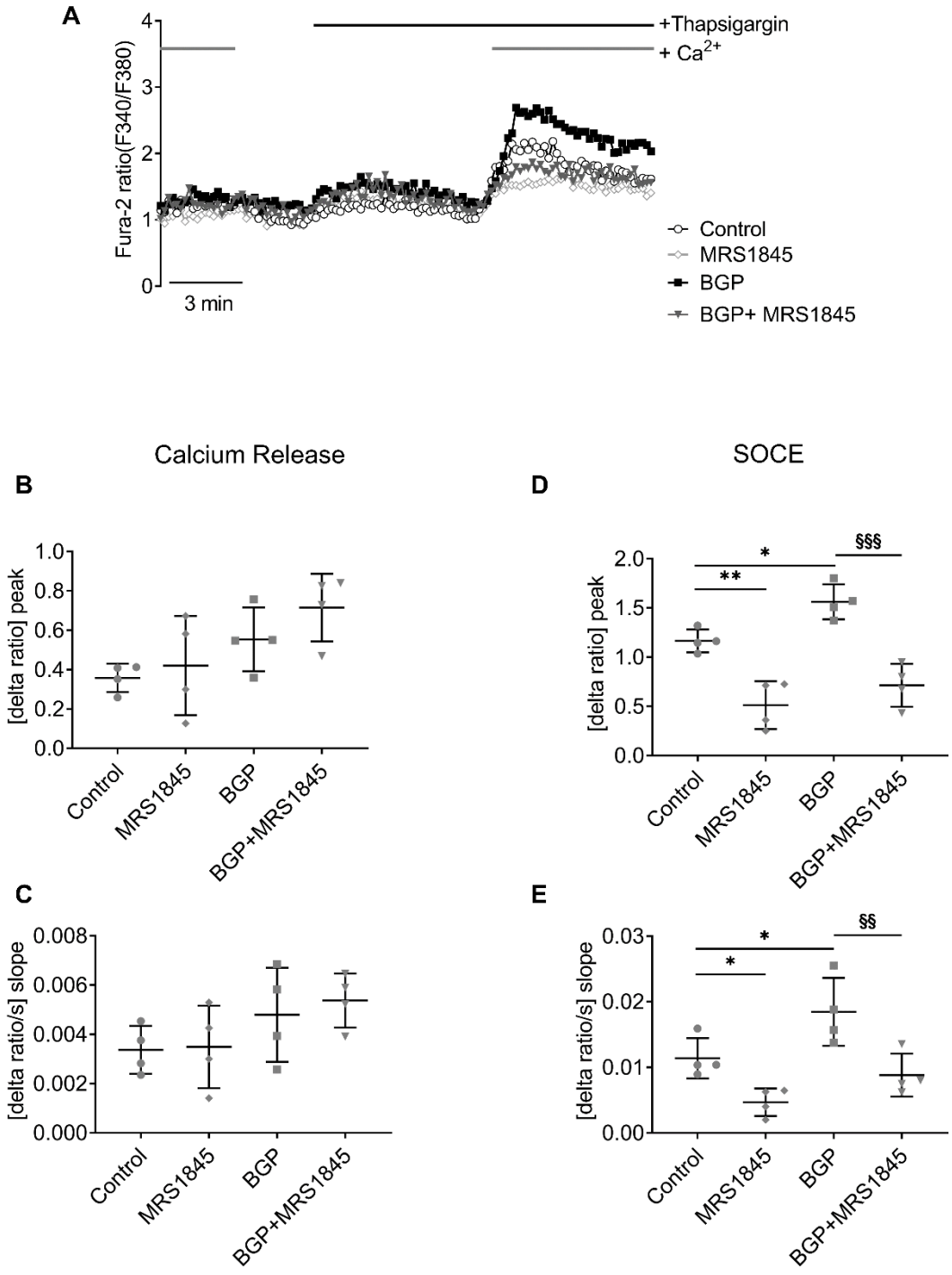

Figure 10 MRS1845 inhibited phosphate-stimulated SOCE in HAoSMCs

A. Representative tracings of the fura-2 AM fluorescence ratio in the presence of physiological Ca^{2+} concentrations, in the absence of extracellular Ca^{2+} following the addition of TG (1 μM), and after the addition of extracellular Ca^{2+} in HAoSMCs without (Control) and with 24 hours of prior exposure to MRS1845 (10 μM) in the absence and presence of 2 mM BGP (BGP+MRS1845).

B, C. Single values and arithmetic means ± SDs (n = 30-42 cells from 4 different batches) of the (**B**) peak and (**C**) slope increase in the fura-2 AM fluorescence ratio after the addition of TG (1 µM) in HAoSMCs without (Control) and with 24 hours of prior exposure to MRS1845 (10 µM) in the absence and presence of 2 mM BGP (BGP+MRS1845).
D, E. Single values and arithmetic means ± SDs (n = 30-42 cells from 4 different batches) of the (**B**) peak and (**C**) slope increase in the fura-2 AM fluorescence ratio after readdition of extracellular Ca^{2+} in HAoSMCs without (Control) and with 24 hours of prior to exposure to MRS1845 (10 µM) in the absence and presence of 2 mM BGP (BGP+MRS1845).
*p<0.05 and **p<0.01 indicate statistically significant differences compared to the Control group, and §§p<0.01 and §§§p<0.001 indicate statistically significant differences compared to the respective values from the group treated with BGP treatment (ANOVA). Figure adapted from (Ma et al., 2019).

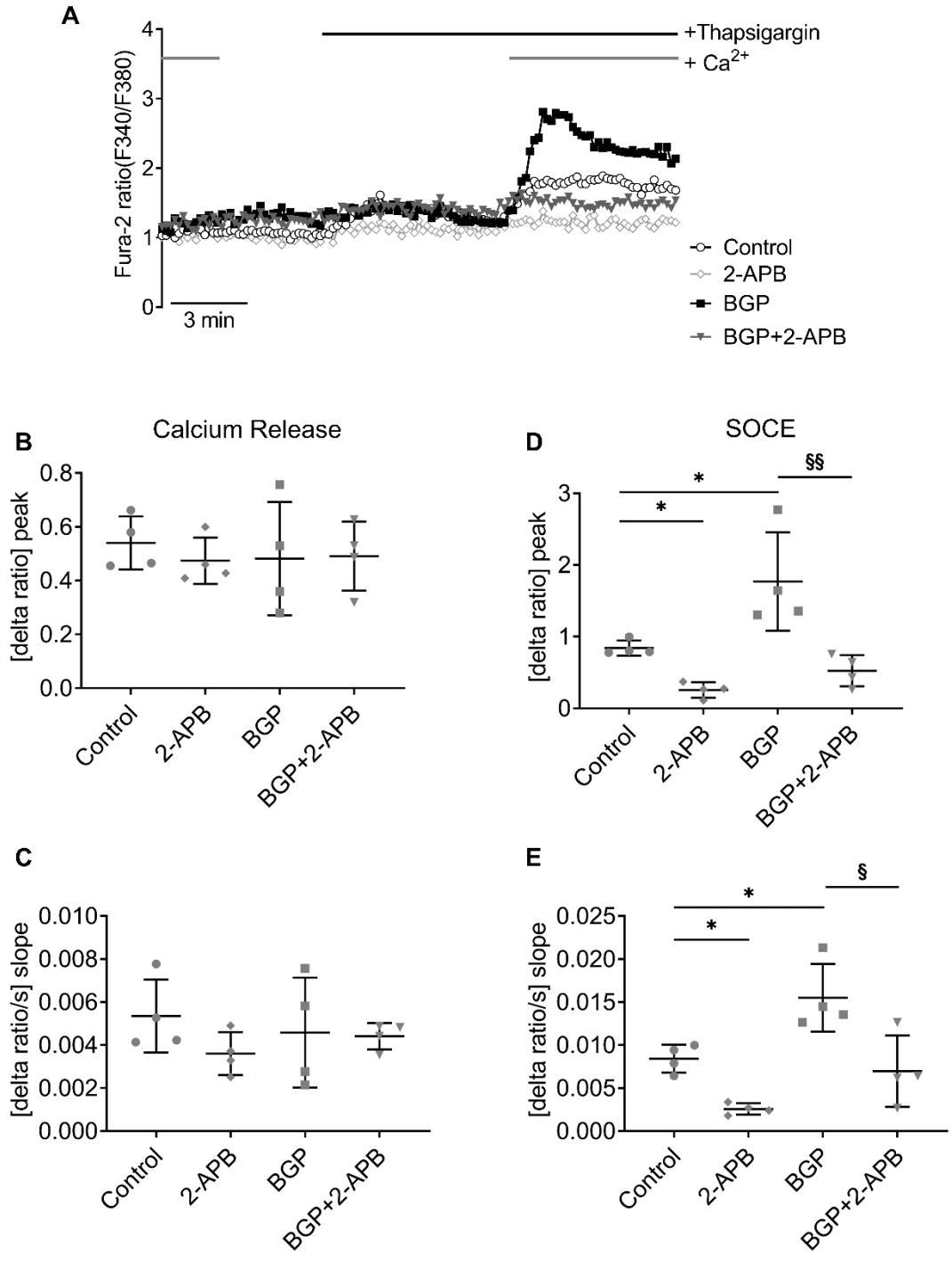

Figure 11 2-APB inhibited phosphate-stimulated SOCE in HAoSMCs

A. Representative tracings of the fura-2 AM fluorescence ratio in the presence of physiological Ca^{2+} concentrations, in the absence of extracellular Ca^{2+} following the addition of TG (1 μM) and after the addition of extracellular Ca^{2+} to HAoSMCs without (Control) and with 24 hours of prior exposure to 2-APB (50 μM) in the absence and presence of 2 mM BGP (BGP+2-APB).

B, C. Single values and arithmetic means ± SDs (n = 28-38 cells from 4 different batches) of the (**B**) peak and (**C**) slope increase in the fura-2 AM fluorescence ratio after the addition of TG (1 μM) in HAoSMCs without (Control) and with 24 hours of prior exposure to 2-APB (50 μM) in the absence and presence of 2 mM BGP (BGP+2-APB).
D, E. Single values and arithmetic means ± SDs (n = 28-38 cells from 4 different batches) of the (**B**) peak and (**C**) slope increase in the fura-2 AM fluorescence ratio after readdition of extracellular Ca^{2+} to HAoSMCs without (Control) and with 24 hours of prior exposure to 2-APB (50 μM), in the absence and presence of 2 mM BGP (BGP+2-APB).
*$p<0.05$ indicates a statistically significant difference compared to the Control group, and $^{§}p<0.05$ and $^{§§}p<0.01$ indicate statistically significant differences compared to the respective values from the group treated with BGP alone (ANOVA).

3.5 The SGK1 antagonist GSK650394 inhibited phosphate-stimulated *ORAI1* and *STIM1* gene expression in HAoSMCs

We further explored the associations among the transcription of *SGK1*, *ORAI1,* and *STIM1* in HAoSMCs treated with phosphate. A well-recognized SGK1 pharmacological inhibitor, GSK650394 (10 μM) (Al-Maghout et al., 2017, Pelzl et al., 2017, Sahu et al., 2017, Hosseinzadeh et al., 2020), was added to cells together with the BGP treatment described above. As shown in Figure 12, *SGK1* transcription was upregulated following BGP treatment. In addition, GSK650394 had no significant effects on SGK1 expression levels, while it considerably inhibited phosphate-stimulated *ORAI1* and *STIM1* mRNA expression in HAoSMCs.

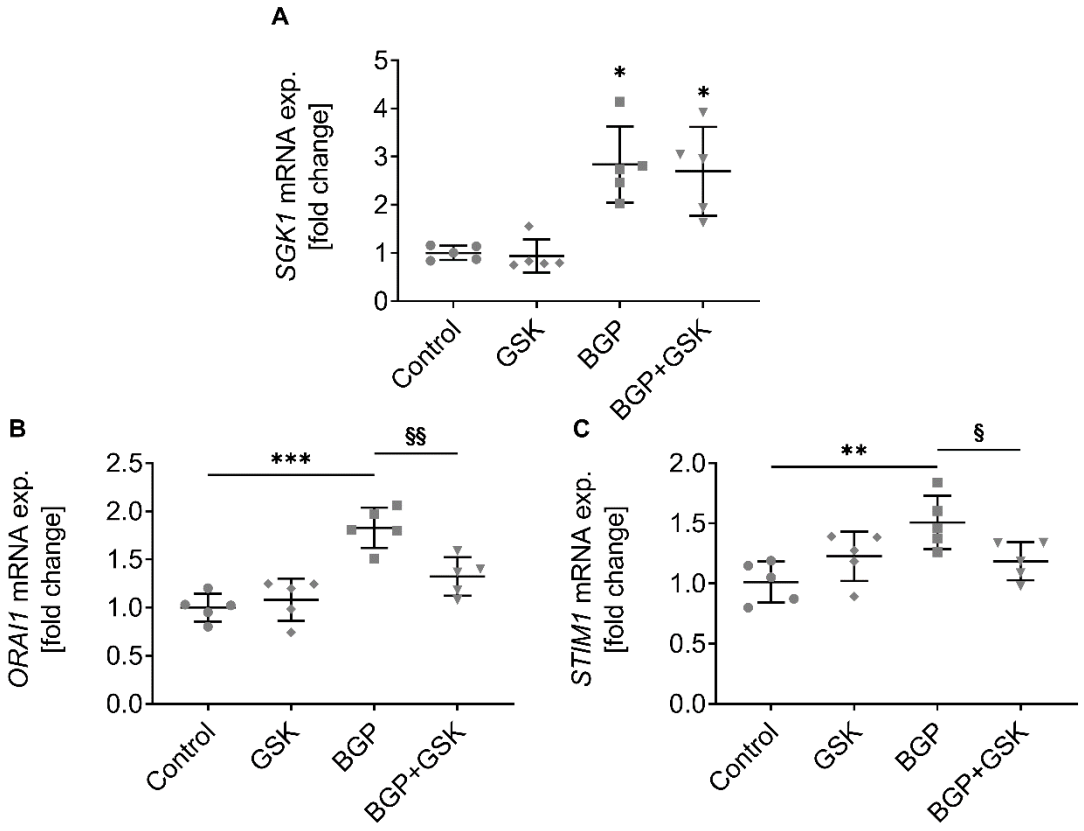

Figure 12 GSK650394 inhibited phosphate-stimulated *ORAI1* and *STIM1* mRNA expression in HAoSMCs

A-C. Single values and arithmetic means ± SDs (n = 5) of (**A**) *SGK1,* (**B**) *ORAI1* and (**C**) *STIM1* transcript levels in HAoSMCs without (Control) and with 24 hours of previous exposure to 2 mM BGP in the absence and presence of GSK650394 (GSK, 10 µM) (BGP+GSK).

*p<0.05, **p<0.01, and ***p<0.001 indicate statistically significant differences compared to the Control group, and §p<0.05 and §§p<0.01 indicate statistically significant differences compared to the respective values from the group treated with BGP alone (ANOVA).

3.6 The SGK1 antagonist GSK650394 inhibited phosphate-stimulated SOCE in HAoSMCs

GSK650394 (10 µM) was also added to HAoSMC samples under the same BGP treatment conditions described above to investigate whether the reduction in *ORAI1* and *STIM1* expression caused by SGK1 inhibition correlated with a decrease in SOCE. As illustrated in Figure 13, 10 µM GSK650394 significantly

inhibited the BGP-induced increase in SOCE (Ma et al., 2019). Thus, SGK1 is required for phosphate-induced SOCE activation in HAoSMCs. Taken together, these findings indicate that SGK1 participates in phosphate-stimulated ORAI1 and STIM1 expression and SOCE.

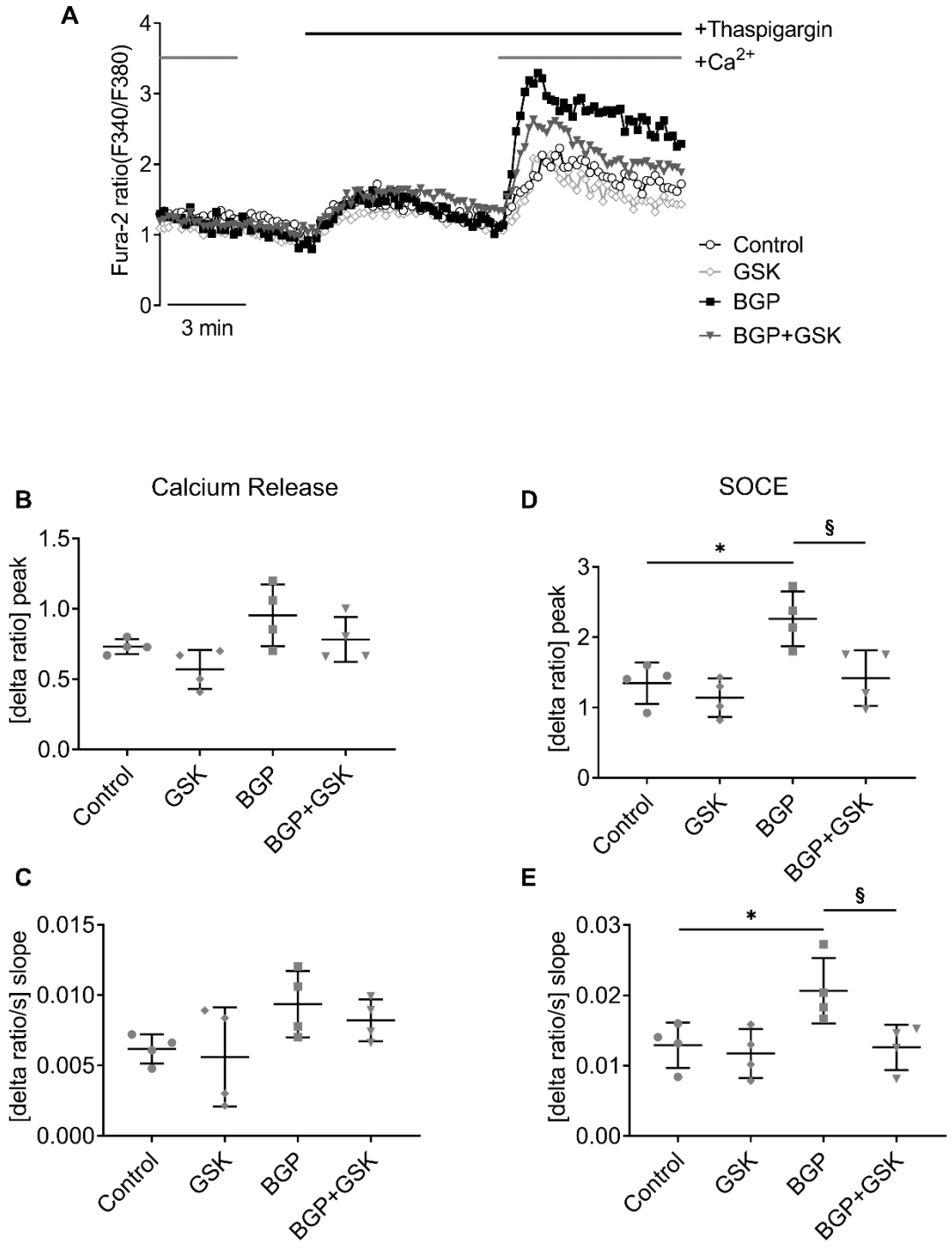

Figure 13 GSK650394 inhibited phosphate-stimulated SOCE

A. Representative tracings of the fura-2 AM fluorescence ratio in the presence of physiological Ca^{2+} concentrations, in the absence of extracellular Ca^{2+} following the addition of TG (1 μM), and after the addition of extracellular Ca^{2+} to HAoSMCs without (Control) and with 24 hours of exposure to 2 mM BGP in the absence and presence of GSK650394 (GSK, 10 μM) (BGP+GSK).

B, C. Single values and arithmetic means ± SDs (n = 22-35 cells from 4 different batches) of the (**B**) peak and (**C**) slope increase in the fura-2 AM fluorescence ratio after the addition of TG (1 μM) in HAoSMCs without (Control) and with 24 hours of prior exposure to 2 mM BGP in the absence and presence of GSK650394 (GSK, 10 μM) (BGP+GSK). **D, E.** Single values and arithmetic means ± SDs (n = 22-35 cells from 4 different batches) of the (**B**) peak and (**C**) slope increase in the fura-2 AM fluorescence ratio after readdition of extracellular Ca^{2+} to HAoSMCs without (Control) and with 24 hours of prior exposure to 2 mM BGP in the absence and presence of GSK650394 (GSK, 10 μM) (BGP+GSK). *$p<0.05$ denotes statistically significant differences compared to the Control group, and $^{§}p<0.05$ denotes statistically significant differences compared to the respective value obtained from the group treated with BGP alone (ANOVA). Figure updated from (Ma et al., 2019).

3.7 ORAI1 inhibition blocked phosphate-stimulated osteo/chondrogenic signaling and extracellular calcification in HAoSMCs

We next identified whether the observed phosphate-stimulated ORAI1 and STIM1 expression, along with SOCE, were associated with osteo/chondrogenic signaling in HAoSMCs by measuring previously examined osteogenic markers and TNSALP activity again in cells treated with BGP in the absence or presence of the ORAI1 antagonist MRS1845 (10 μM)/2-APB (50 μM). Quantitative PCR was employed to detect osteogenic markers at the same time points using the procedures described above. TNSALP activity in HAoSMCs was determined after 7 days of the indicated treatment. As a result, MRS1845 (10 μM) significantly inhibited both the phosphate-stimulated expression of osteogenic markers and TNSALP activity (Figure 14) (Ma et al., 2019). 2-APB treatment (50 μM) similarly diminished the phosphate-stimulated expression of osteogenic markers and TNSALP activity in HAoSMCs (Figure 15).

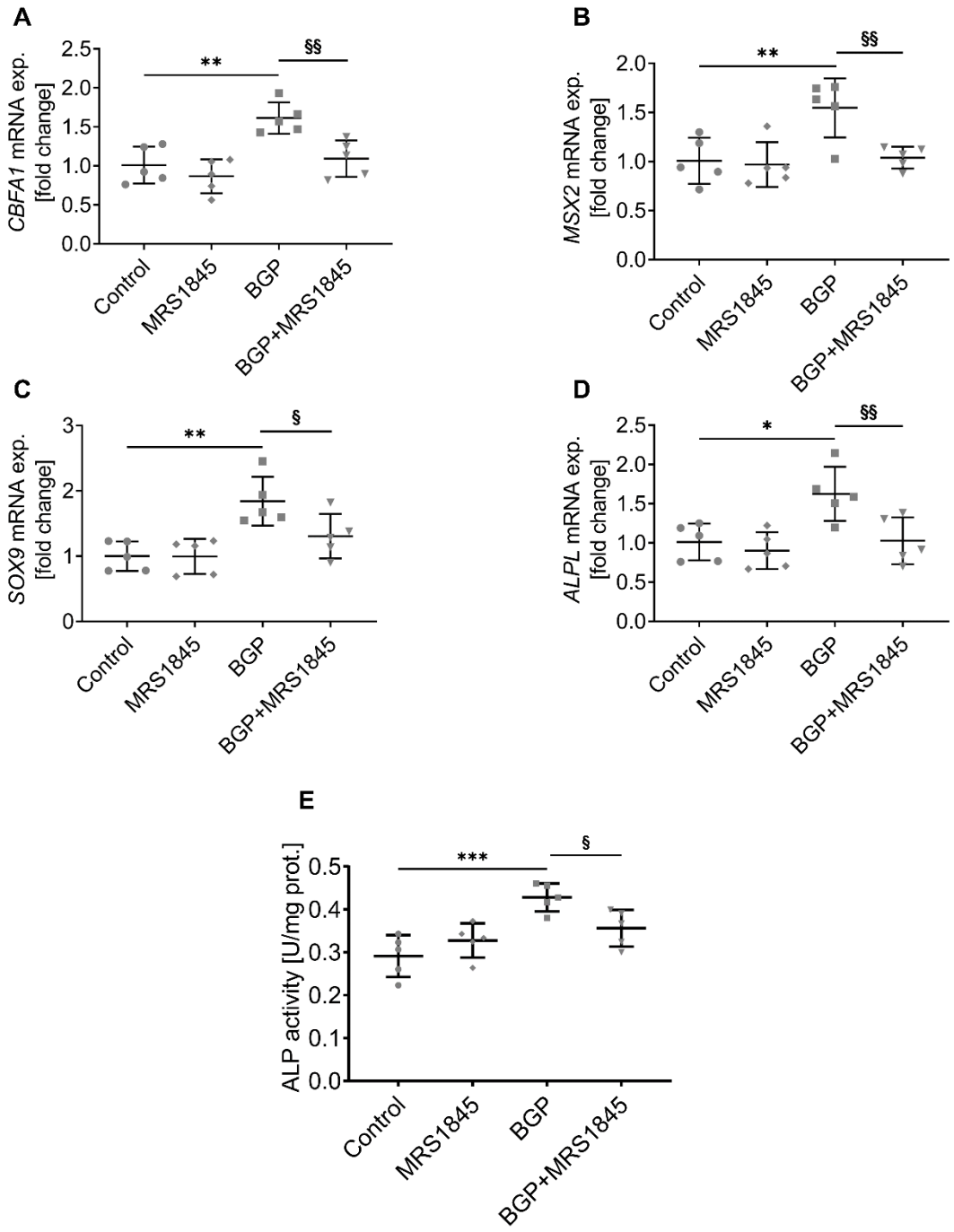

Figure 14 MRS1845 inhibited phosphate-stimulated osteo/chondrogenic signaling in HAoSMCs

A-D. Single values with arithmetic means ± SDs (n = 5) of (**A**) *CBFA1*, (**B**) *MSX2*, (**C**) *SOX9*, and (**D**) *ALPL* transcript levels and (**E**) ALP activity in HAoSMCs without (Control) and with 24 hours of prior exposure to 2 mM BGP in the absence and presence of MRS1845 (10 µM).

E. Single values with arithmetic means ± SDs (n = 5) of ALP activity in HAoSMCs without (Control) and with 7 days of previous exposure to 2 mM BGP in the absence and presence of MRS1845 (10 μM).
*p<0.05, **p<0.01, and ***p<0.001 denote statistically significant differences compared to the Control group, and §p<0.05 and §§p<0.01 denote statistically significant differences from the respective value obtained from the group treated with BGP alone (ANOVA). Figure updated from (Ma et al., 2019).

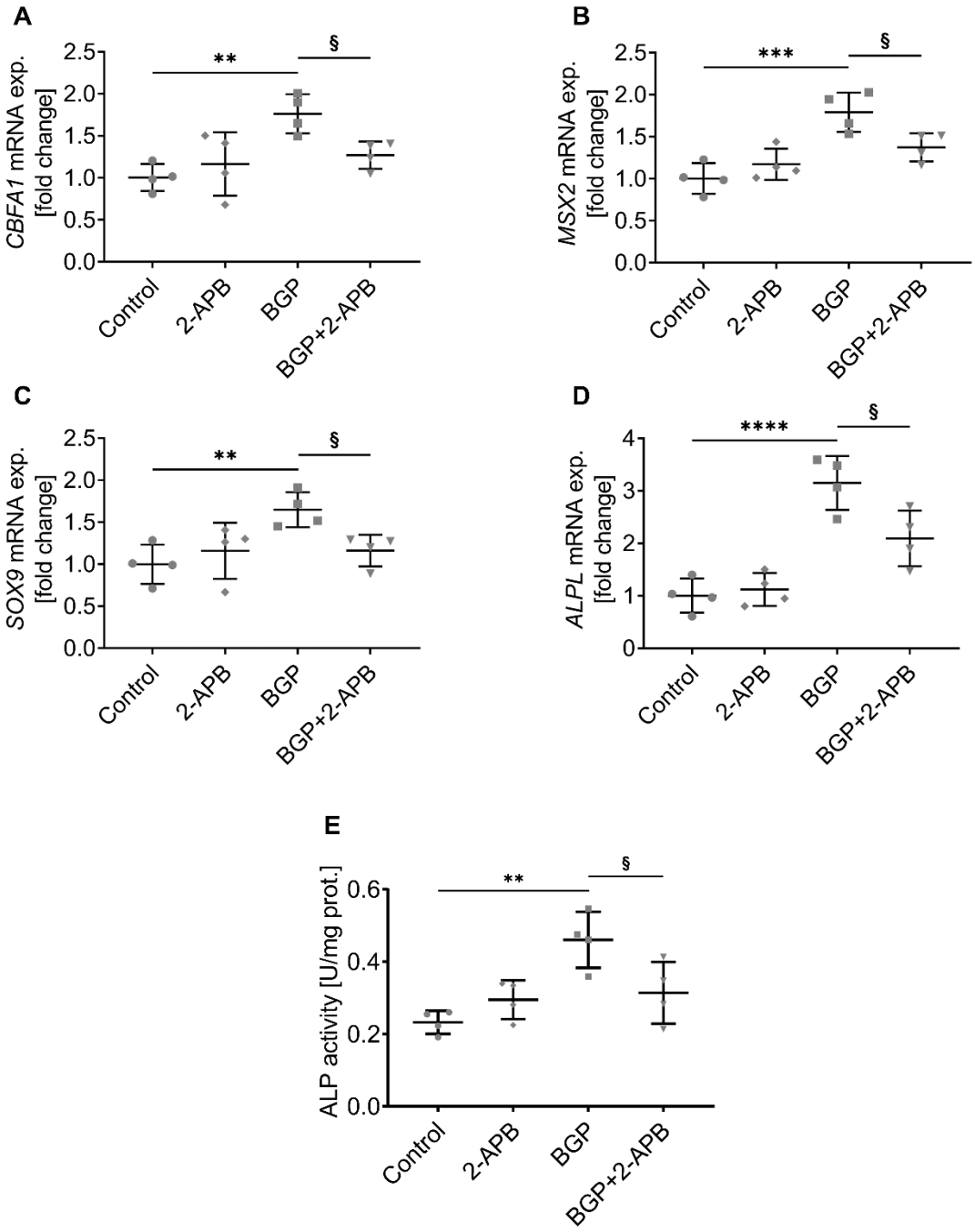

Figure 15 2-APB inhibited phosphate-stimulated osteo/chondrogenic signaling in HAoSMCs

A-D. Single values with arithmetic means ± SDs (n = 4) of (**A**) *CBFA1*, (**B**) *MSX2*, (**C**) *SOX9*, and (**D**) *ALPL* transcript levels and (**E**) ALP activity in HAoSMCs without (Control) and with 24 hours of prior exposure to 2 mM BGP in the absence and presence of 2-APB (50 µM).

E. Single values with arithmetic means ± SDs (n = 4) of ALP activity in HAoSMCs without (Control) and with 7 days of prior exposure to 2 mM BGP in the absence and presence of 2-APB (50 μM).
**p<0.01, ***p<0.001, and ****p<0.0001 indicated a statistically significant difference compared to the Control group, and §p<0.05 indicates a statistically significant difference compared to the respective value obtained from the group treated with BGP alone (ANOVA).

HAoSMCs were treated with 10 mM BGP in the absence or presence of the ORAI1 antagonist MRS1845 (5-20 μM) or 2-APB (50 μM) for 14 days and then subjected to alizarin red S staining to visualize extracellular calcium deposits. Cells were analyzed using a calcium content assay kit (BioAssay Systems) before staining to quantify calcium deposits. As indicated in Figure 16, calcium deposition was ameliorated by treatment with the ORAI1 antagonists MRS1845 (10 μM and 20 μM) (Ma et al., 2019) and 2-APB (50 μM).

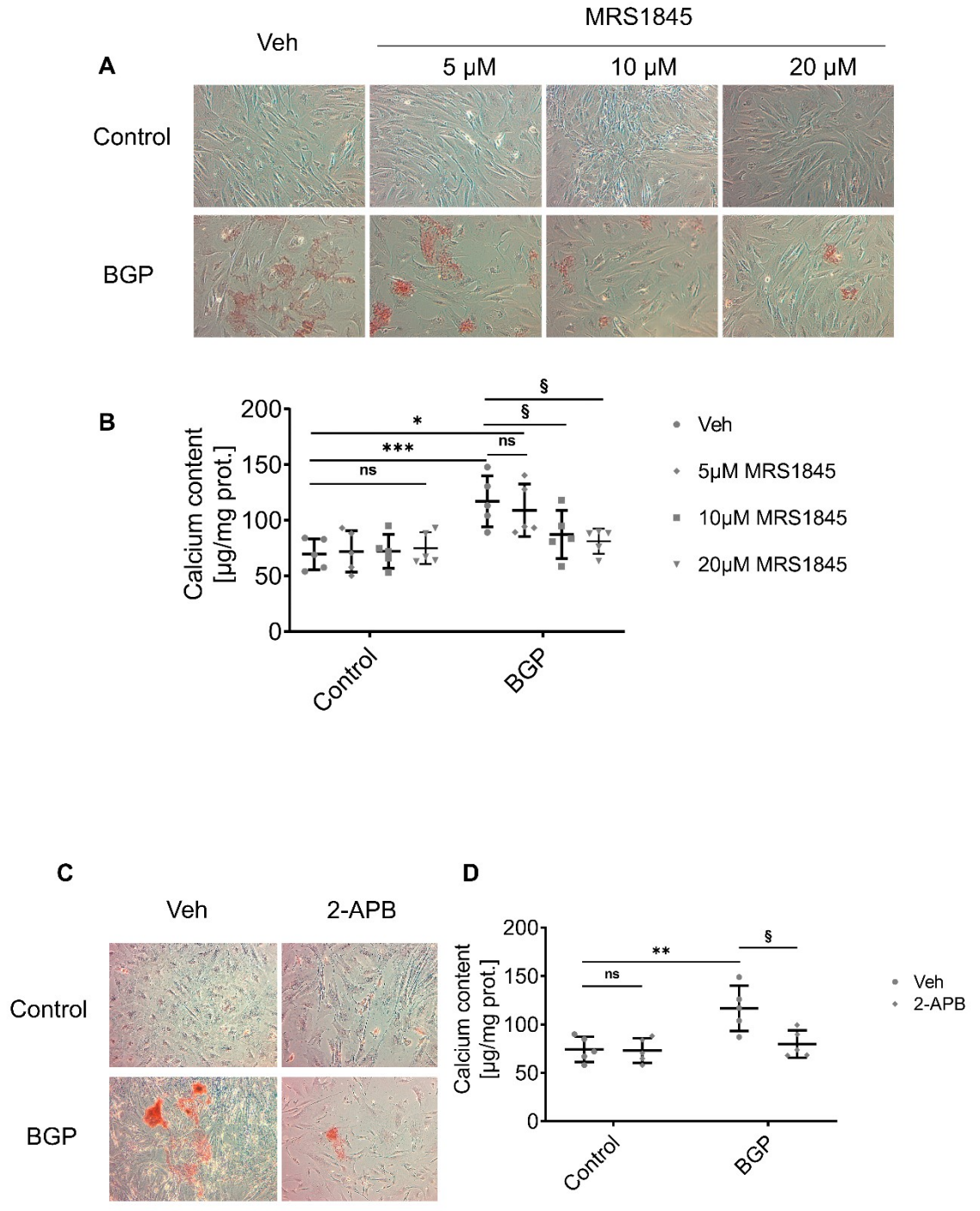

Figure 16 MRS1845 and 2-APB inhibited phosphate-stimulated extracellular calcification in HAoSMCs

A. Calcium deposits (100x) in HAoSMCs treated without (Control) and with BGP prior to 14 days of exposure to 10 mM BGP in the absence (Veh) and presence of different concentrations of MRS1845 (5-20 µM). (Ma et al., 2019)

B. Single values and arithmetic means ± SDs (n = 5) of calcium content in HAoSMCs

treated without (Control) and with BGP prior to 14 days of exposure to 10 mM BGP in the absence (Veh) and presence of different concentrations of MRS1845 (5-20 μM).
C. Calcium deposits (100x) in HAoSMCs treated without (Control) and with BGP prior to 14 days of exposure to 10 mM BGP in the absence (Veh) and presence of 2-APB (50 μM).
D. Single values and arithmetic means ± SDs (n = 5) of calcium content in HAoSMCs treated without (Control) and with BGP prior to 14 days of exposure to 10 mM BGP in the absence (Veh) and presence of 2-APB (50 μM).
*p<0.05, **p<0.01, and ***p<0.001 indicate a statistically significant difference compared to the Control group, and §p<0.05 indicates a statistically significant difference compared to the respective value from the group treated with BGP alone (ANOVA).

The levels of osteogenic markers were determined after ORAI1 silencing to further establish the involvement of ORAI1 in phosphate-induced osteogenic signaling in HAoSMCs. Cells were initially silenced with siORAI1 (Dharmacon & Santa Cruz Biotech) and were then treated with 2 mM BGP for 24 or 48 hours. Quantitative PCR and immunoblotting were adopted to assess the efficiency of siORAI1 silencing. Figure 17 shows that ORAI1 expression was effectively suppressed by siORAI1 at both the mRNA and protein levels in HAoSMCs (Ma et al., 2019). As shown in Figure 18, siORAI1 treatment significantly reduced the phosphate-stimulated expression of osteo/chondrogenic markers (Ma et al., 2019).

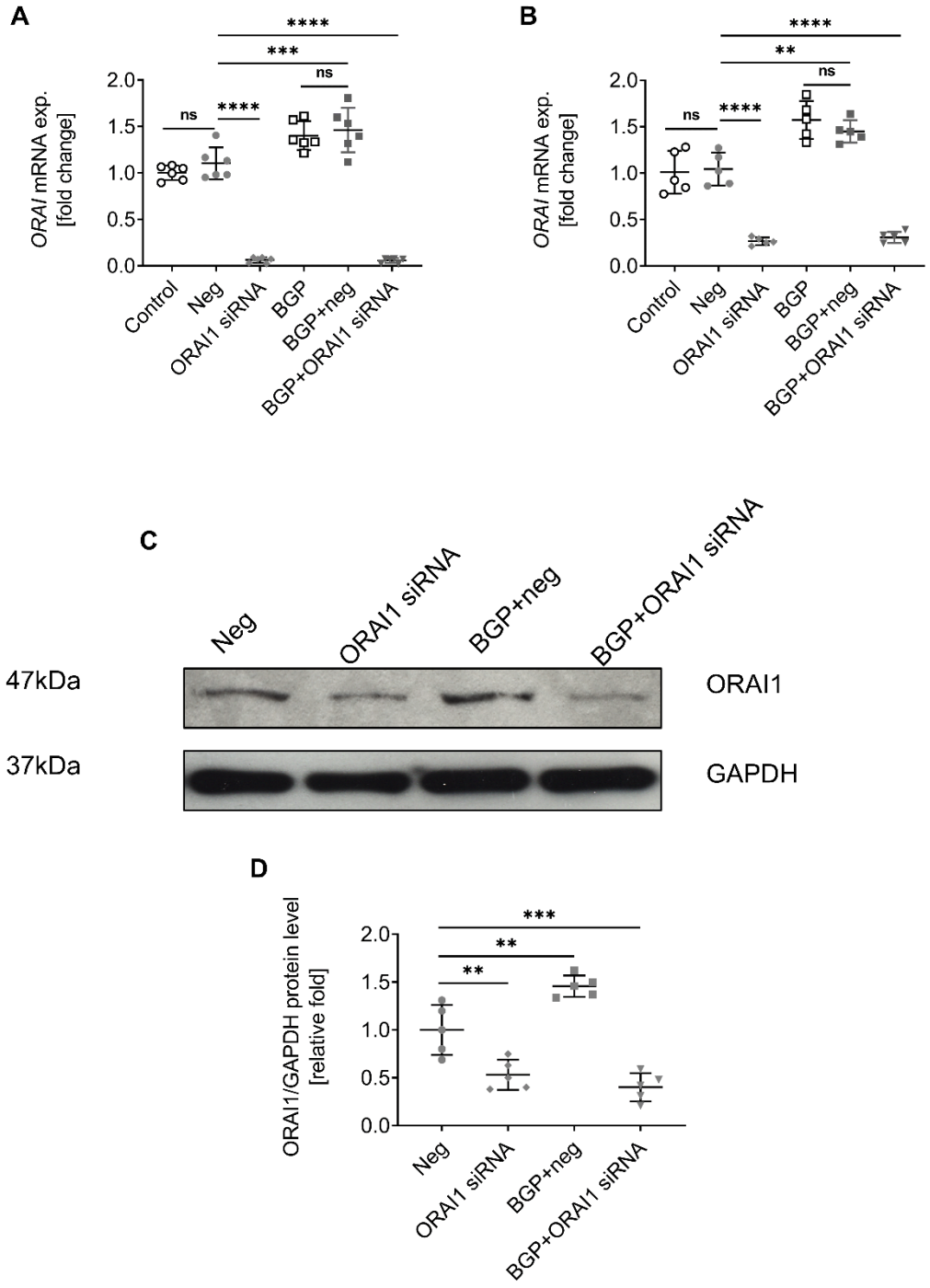

Figure 17 siORAI1 suppressed ORAI1 mRNA and protein expression in HAoSMCs

A. Single values and arithmetic means ± SDs (n = 6) of *ORAI1* transcript levels in HAoSMCs without (Control) or with nontargeting siRNA treatment (Neg) or with targeted ORAI1 silencing (siORAI1) in the absence and presence of exposure to 2 mM BGP (BGP) for 24 hours (Dharmacon). Figure updated from (Ma et al., 2019).

B. Single values and arithmetic means ± SDs (n = 5) of *ORAI1* transcript levels in

HAoSMCs without (Control) or with nontargeting siRNA treatment (Neg) or with targeted ORAI1 silencing (siORAI1) in the absence and presence of exposure to 2 mM BGP (BGP) for 24 hours (Santa Cruz Biotech).
C. Representative immunoblots of ORAI1 and GAPDH protein expression in HAoSMCs with nontargeting siRNA treatment (Neg) or with targeted ORAI1 silencing (siORAI1) in the absence and presence of 48 hours of exposure to 2 mM BGP (BGP). Figure updated from (Ma et al., 2019).
D. Single values and arithmetic means ± SDs (n = 5) of ORAI1 protein expression in HAoSMCs with nontargeting siRNA treatment (Neg) or with targeted ORAI1 silencing (siORAI1) in the absence and presence of exposure to 2 mM BGP (BGP) for 48 hours. **p<0.01, ***p<0.001, and ****p<0.0001 indicate statistically significant differences compared to the nontargeting siRNA treatment group (Neg).

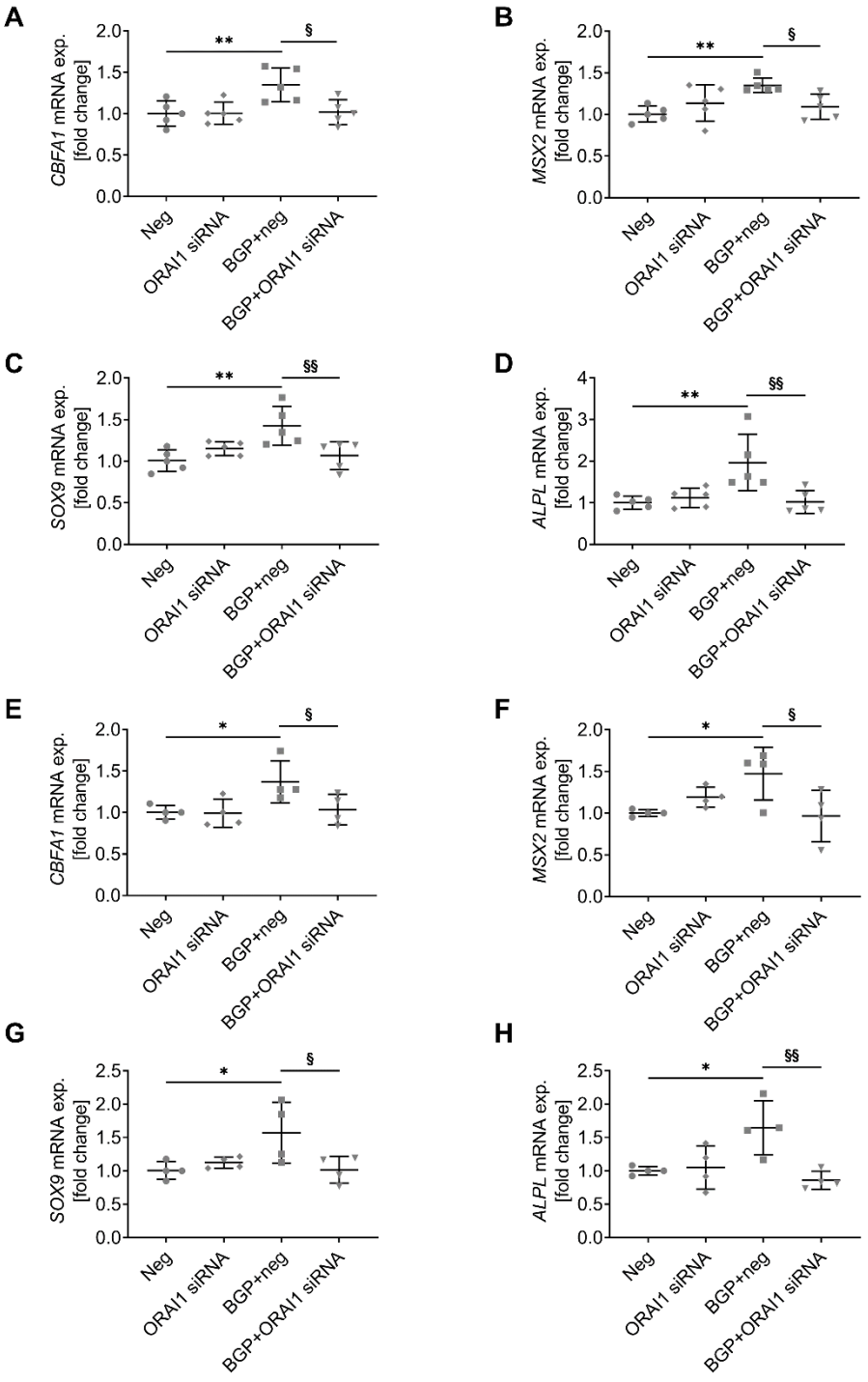

Figure 18 siORAI1 inhibited phosphate-stimulated expression of osteogenic markers in HAoSMCs

A-D. Single values and arithmetic means ± SDs (n = 5) of (**A**) *CBFA1*, (**B**) *MSX2*, (**C**) *SOX9*, and (**D**) *ALPL* transcript levels in HAoSMCs with nontargeting siRNA treatment (Neg) or with targeted ORAI1 silencing (siORAI1) in the absence and presence of exposure to 2 mM BGP (BGP) for 24 hours (Dharmacon).

E-H. Single values and arithmetic means ± SDs (n = 4) of (**E**) *CBFA1*, (**F**) *MSX2*, (**G**) *SOX9*, and (**H**) *ALPL* transcript levels in HAoSMCs with nontargeting siRNA treatment (Neg) or with targeted ORAI1 silencing (siORAI1) in the absence and presence of the exposure to 2 mM BGP(BGP) for 24 hours (Santa Cruz Biotech).
*p<0.05 and **p<0.01 indicate a statistically significant difference compared to the nontargeting siRNA treatment group (Neg), and §p<0.05 and §§p<0.01 indicate a statistically significant difference from the respective value for the group treated with both BGP and the nontargeting siRNA (BGP+Neg) (ANOVA). Figure updated from (Ma et al., 2019).

3.8 High K^+ concentrations stimulated osteogenic marker expression in HAoSMCs

HAoSMCs were treated with a physiological concentration (5 mM) or 60 mM extracellular K^+ for 24 hours to determine whether the expression levels of osteo/chondrogenic markers were affected by extracellular Ca^{2+} influx through Ca^{2+} channels other than CRACs, as an increase in the extracellular K^+ concentration activates VOCCs. As shown in Figure 19, an increase in the extracellular K^+ concentration tended to increase *CBFA1* transcript levels, however, this difference did not reach statistical significance, while the levels of the other three osteogenic markers were substantially increased in HAoSMCs (Ma et al., 2019).

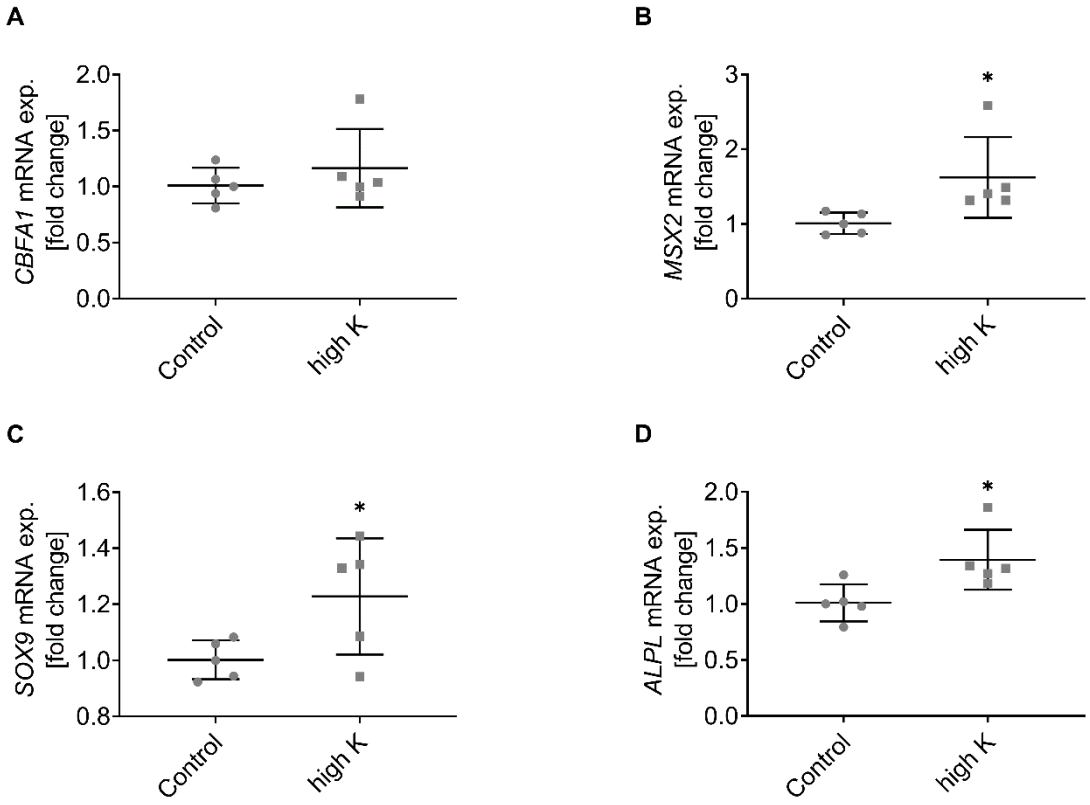

Figure 19 High K^+ concentrations stimulated osteogenic marker expression in HAoSMCs

A-D. Single values and arithmetic means ± SDs (n = 5) of (**A**) *CBFA1*, (**B**) *MSX2*, (**C**) *SOX9*, and (**D**) *ALPL* transcript levels in HAoSMCs with prior exposure to 5 mM extracellular K^+ (Control) or 60 mM extracellular K^+ (high K).

*$p<0.05$ indicates statistically significant differences compared to the Control group (Student's t test). Figure updated from (Ma et al., 2019).

4. Discussion

Here, we present a novel effect of phosphate on ORAI1 and STIM1 mRNA and protein expression levels, as well as the subsequent SOCE, in HAoSMCs. Under the influence of phosphate, pharmacological inhibition of ORAI1 leads to a commensurate reduction in SOCE. Both ORAI1 antagonists and siRNA-mediated ORAI1 silencing abolished phosphate-stimulated osteo/chondrogenic signaling in HAoSMCs, ORAI1 antagonists inhibited phosphate-stimulated extracellular calcification. Moreover, we further explored the role of SGK1 in this process and found that SGK1 at least partially participates in phosphate-stimulated SOCE, possibly through an interaction with ORAI1 and/or STIM1. This finding also supports earlier observations that SGK1 plays a decisive role in VCm via NF-κB activation (Voelkl et al., 2018a). Taken together, these findings suggest that ORAI1 participates in orchestrating the phosphate-stimulated osteo/chondrogenic phenotypic switching of VSMCs and VCm. A schematic diagram summarizing our findings is provided in Figure 20.

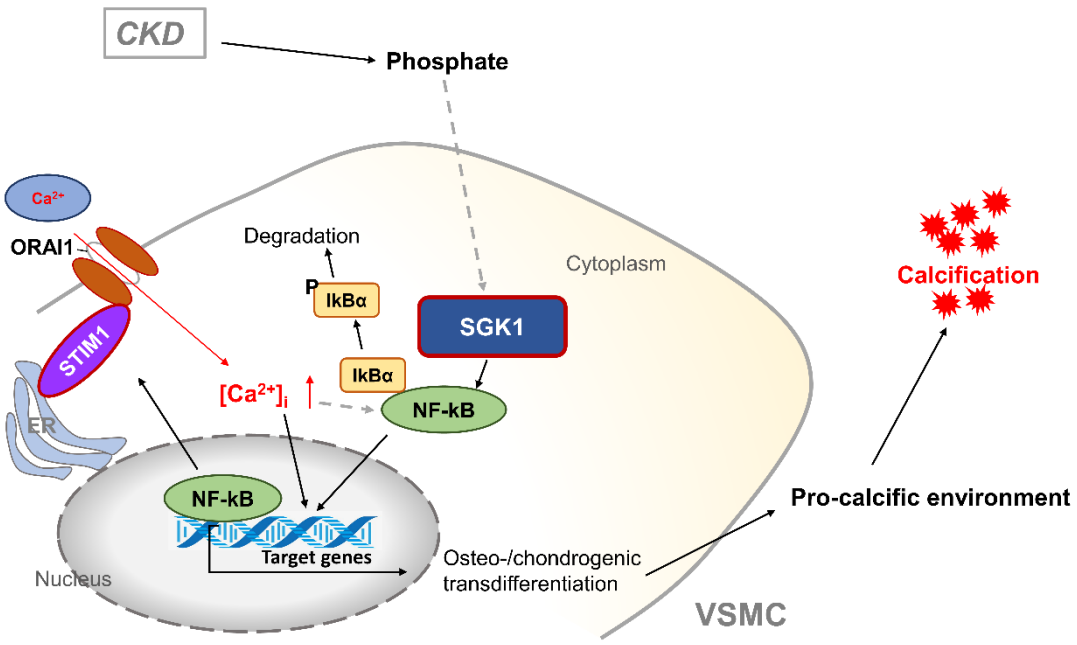

Figure 20 Schematic representation of the signaling cascade involved in

phosphate-stimulated osteo/chondrogenic transdifferentiation of VSMCs and VCm

In VSMCs, phosphate induces upregulation of SGK1, which results in the degradation of IκB followed by nuclear translocation and activation of NF-κB. This event results in increased ORAI1 and STIM1 expression, as well as increased SOCE, which increases $[Ca^{2+}]_i$ and ultimately orchestrates the osteo/chondrogenic transdifferentiation of VSMCs.

4.1 Research models for studying VCm

We employed an *in vitro* model that included primary HAoSMCs and 2 mM BGP as a calcification stimulator to investigate VCm. VSMCs are critical in VCm for two reasons: phenotypic switching and active cell signaling. Thus, VSMCs from various animal origins, including human, mouse, rat, and bovine VSMCs, have been extensively investigated as *in vitro* models for VCm (Shioi et al., 1995, Speer et al., 2010, Schuchardt et al., 2012, Alesutan et al., 2015, Luong et al., 2019). Most cells studied *in vitro* do not undergo spontaneous calcification but require external stimulation. VSMC culture medium is often supplemented with BGP (1.25-10 mM) (Shioi et al., 1995, Leibrock et al., 2015, Alesutan et al., 2016, Voelkl et al., 2018b) or extra inorganic phosphate (sodium phosphate, 1-5 mM) (Jono et al., 2000a, Beazley et al., 2012) to mimic hyperphosphatemia in the population with CKD, as both stimuli induce VCm in a time- and dose-dependent manner. *In vitro* cell culture experiments are beneficial for screening inducing or inhibiting substrates and elucidating the signaling pathways involved. However, as cultured VSMCs rapidly lose their contractile characteristics and the tissue structure of physiological blood vessel walls and the matrix are not preserved *in vitro* models, the potential interaction of VSMCs with the extracellular matrix cannot be studied under these conditions.

Many markers have been detected to assess VCm. *ALPL* is a phenotypic osteoblast gene and a sensitive marker of VSMC transdifferentiation into osteoblast-like cells. The *ALPL* gene encodes TNSALP, a protein that increases the inorganic phosphate concentration in the microenvironment by hydrolyzing

phosphate esters and provides adequate substrates for calcium phosphate production. TNSALP is also a prominent osteogenic enzyme that mediates the mineralization of vascular tissue (Johnson et al., 2006, Demer and Tintut, 2008, Voelkl et al., 2019). Additionally, alizarin red S staining was used to visualize extracellular calcification. Alizarin red S is an anthraquinone derivative that forms an orange–red complex upon binding to calcium salts. It is a sensitive indicator for qualitatively measuring the amount of calcification since it detects calcium salts at a low concentration. In this study, interference with the function of ORAI1 effectively inhibited the phosphate-stimulated expression of osteogenic markers, including *ALPL* transcript levels and TNSALP activity, in HAoSMCs; it also suppressed extracellular calcification, as determined by calcium content assays and alizarin red S staining. These data reveal the feasibility of our *in vitro* calcification model and further indicate the participation of ORAI1 in mediating the transcription of genes related to osteo/chondrogenic transdifferentiation, osteoblast-like function and phosphate-induced calcification.

4.2 Signaling pathways involved in VCm

An increased $[Ca^{2+}]_i$ contributes to the osteogenic differentiation of VSMCs and VCm (Aghagolzadeh et al., 2016, Nguyen et al., 2020). $[Ca^{2+}]_i$ increases with CKD progression in rat models, implying the importance of uremic toxins in the resting $[Ca^{2+}]_i$ of VSMCs. This increase is partially due to both an impaired Ca^{2+} extrusion system and enhanced SOCE (Rodenbeck et al., 2017). Our study indicates that enhanced SOCE mediates phosphate-induced VCm. In addition, changes in voltage-operated calcium entry (VOCE) occur during phenotypic switching of VSMCs. In VSMCs with the proliferative, synthetic phenotype, $[Ca^{2+}]_i$ increases consistently, SOCE is exceedingly dominant, and VOCE is residual at this stage (Munoz et al., 2013). This observation is generally consistent with our findings, although the role of VOCE requires further investigation. For this analysis, HAoSMCs were treated with a K^+-rich medium, resulting in membrane

depolarization via VOCE. The upregulation of osteogenic markers induced by the high K^+ concentration suggests that VOCCs are involved in phenotypic switching of HAoSMCs, implying that the effect of VOCCs on VCm cannot be excluded. As stated above, cell membrane depolarization caused by a high extracellular K^+ concentration leads to a prolonged increase in $[Ca^{2+}]_i$, which is related to VSMC-mediated vasoconstriction (Flemming et al., 2003). When VOCCs are blocked, however, depletion of ER Ca^{2+} stores still leads to a prolonged increase in $[Ca^{2+}]_i$ (Flemming et al., 2003). Thus, we deduced that SOCE may play a dominant role in the sustained increase in $[Ca^{2+}]_i$ during the osteo/chondrogenic phenotypic switching of VSMCs based on those findings. Additionally, Ca^{2+} store depletion was previously found to activate a biphasic inward current in freshly isolated mouse VSMCs (Wayman et al., 1996). One possible explanation is that initial Ca^{2+} release from the ER triggers the opening of Ca-dependent Cl channels (CaCCs), resulting in the first phase of the transient current, and activation of CaCCs may result in membrane depolarization that facilitates Ca^{2+} entry via VOCCs, forming the second phase. Interestingly, a recent study hypothesized that the coupling between SOCE, SERCAs, and IP_3 mediates Ca^{2+} signaling between spatially distant effectors (Courjaret and Machaca, 2014). Ca^{2+} entering via SOCE is sequestered into the ER by SERCAs and is then released again by IP_3Rs to activate remote CaCCs, leading to changes in the cell membrane potential via VOCCs. Currently, we speculate that hyperphosphatemia increases SOCE, thereby activating VOCCs; thus, the coupling between SOCE, SERCAs, and VOCE results in a continuous increase in $[Ca^{2+}]_i$ in VSMCs during CKD. Other mechanisms may also contribute to the involvement of VOCE, and SOCE itself suppresses VOCE. STIM1 modulates the C-terminus of L-type VOCCs via its Ca^{2+} release-activated Ca^{2+} activation domain, inhibiting gating and causing long-term internalization of L-type VOCCs (Park et al., 2010). Upregulation of STIM1 thus very likely impairs L-type VOCC activity. However, we must

emphasize that we did not measure VOCE or investigate the relationship between SOCE and VOCE in HAoSMCs treated with phosphate.

Furthermore, we showed that SGK1 is involved in the upregulation of SOCE in the presence of elevated phosphate concentrations. SGK1 is reported to perform a critical function in VCm (Voelkl et al., 2018a). Inhibition or genetic silencing of SGK1 abolishes the phosphate-stimulated osteo/chondrogenic transdifferentiation of VSMCs and VCm (Voelkl et al., 2018a), and this procalcific function of SGK1 is mediated partially by NF-κB activation (Voelkl et al., 2018a). Additionally, SGK1 affects the migration of VSMCs via transcriptional regulation of ORAI1 expression. This effect depends on the activation of NF-κB, which acts downstream of SGK1 (Walker-Allgaier et al., 2017). However, previous research has not examined the possibility that ORAI1/STIM1 and SOCE are involved in VCm. In other cell types, SGK1 phosphorylates the ubiquitin ligase NEDD4-2 (**n**eural precursor cell-**e**xpressed **d**evelopmentally **d**ownregulated 4-2), and phospho-NEDD4-2 then binds to the 14-3-3 protein (Liang et al., 2008), which abolishes the ubiquitination activity of NEDD4-2 toward ORAI1, thereby reversing the NEDD4-2-induced downregulation of SOCE (Eylenstein et al., 2011). SGK1 also promotes nuclear translocation and activation of NF-κB (BelAiba et al., 2006, Vallon et al., 2006, Tai et al., 2009). SGK1 phosphorylates IκB kinase β (IKKβ), leading to IκB phosphorylation and degradation(Zhang et al., 2005a), and SGK1 also phosphorylates IκB kinase α (IKKα), leading to the activation of IKKβ, which subsequently activates the IKK complex (Tai et al., 2009); both processes lead to the activation of the NF-κB pathway. Moreover, NF-κB was implicated in the regulation of ORAI1 and STIM1. NF-κB inhibition decreases ORAI1 and STIM1 mRNA expression, and NF-κB activation increases ORAI1 and STIM1 mRNA expression; these effects are paralleled by the associated changes in SOCE (Eylenstein et al., 2012).

The ORAI/STIM-mediated Ca^{2+} signaling pathway modulates various

functions of VSMCs. It is required for VSMC proliferation and migration and for neointima formation following injury (Potier et al., 2009, Bisaillon et al., 2010, Zhang et al., 2011, Walker-Allgaier et al., 2017). Moreover, this pathway is involved in the inflammatory response (Feske, 2009, Beech, 2012), and inflammation accelerates CKD progression and promotes associated complications (Benz et al., 2018, Mihai et al., 2018). Thus, we speculated that phosphate-stimulated ORAI1 and/or STIM1 expression and SOCE played a role in various pathophysiological alterations in the cardiovascular system during CKD.

4.3 Interference with functional ORAI1

We utilized 2-APB and MRS1845 as ORAI1 inhibitors in this study. 2-APB is a membrane-permeable compound that was initially reported to inhibit IP_3R (IC_{50} = 42 μM) (Maruyama et al., 1997); it stimulates SOCE at 1-5 μM while inhibiting it at 30-100 μM (Prakriya and Lewis, 2001, Singaravelu et al., 2006, Potier et al., 2009, Dellis et al., 2011). Although the effect of 2-APB on SOCE has been established in numerous cells, different cell-based experiments designed to inhibit IP_3R and hence decrease internal calcium concentrations have produced conflicting results. 2-APB inhibits the IP_3-induced release of Ca^{2+} in certain cells, including platelets, VSMCs and neurons. This inhibitory effect may be due to the binding of IP_3 to a certain site in IP_3R or to different sensitivities of IP_3R (Bootman et al., 2002). Subsequently, an IP_3R-deficient cell line was discovered to respond to calcium store depletion with normal SOCE, which was inhibited by 2-APB (Broad et al., 2001). Although 2-APB also inhibits other channels, including voltage-gated K^+ channels, capacity-regulated anion channels, and magnesium–nucleotide-regulated metal cation currents (MagNuMs) (Bootman et al., 2002, Wang et al., 2002, Lemonnier et al., 2004), it is relatively selective for CRACs (Maruyama et al., 1997, Luo et al., 2001). According to a recent study, 2-APB directly inhibits ORAI1 channels by blocking the interaction between ORAI1 and STIM1 (Wei et al., 2016). 2-APB inhibits CRACs in rabbit pial arteriole VSMCs at

75 mM (66% efficacy) (Flemming et al., 2003).

Another selective CRAC inhibitor is N-propargyl-nitrendipine, also called MRS1845. It inhibits CRACs but does not induce intracellular calcium release and calcium influx under some conditions, in contrast to most imidazoles (e.g., SKF96365 and miconazole) and tricyclics (e.g., trifluoperazine). Increased intracellular calcium levels caused by these agents appear to be associated with the generation of inositol phosphates, but MRS1845 did not generate significant amounts of inositol phosphates at the concentrations required to inhibit CRACs (in HL-60 cells: IC_{50} 1.7 ± 1.3 μM; max CRAC inhibition: 30 μM, 78 ± 12%) (Harper et al., 2003). However, the potency of MRS1845 against L-type VOCCs is diminished but not abolished (Harper et al., 2003). Despite this phenomenon, MRS1845 is frequently utilized as a relatively selective CRAC inhibitor in various cell types (Itagaki et al., 2005, McMeekin et al., 2006, Szikra et al., 2008, Salker et al., 2018, Abdelazeem et al., 2019).

In addition to the abovementioned ORAI1 inhibitors, we further confirmed that ORAI1 is required for phosphate-stimulated osteo/chondrogenic signaling in VSMCs and VCm using siORAI1.

4.4 Conclusions

In summary, we found that phosphate stimulates SGK1, ORAI1 and STIM1 expression in VSMCs, thereby augmenting SOCE. ORAI1 inhibition substantially compromises the phosphate-stimulated osteo/chondrogenic transdifferentiation of VSMCs. Therefore, ORAI1, STIM1 and SOCE collaborate to regulate VSMC osteo/chondrogenic transdifferentiation and VCm in response to hyperphosphatemia. However, our findings do not exclude the possibility that VOCCs affect osteogenic signaling. The lack of in-depth investigations of the link between SOCE and VOCE may limit our understanding of changes in the $[Ca^{2+}]_i$ during osteogenic signaling in VSMCs. In addition, the underlying relationship between ORAI1 and STIM1, as well as their associations with inflammation,

require more experimentation. The potential $[Ca^{2+}]_i$ coupling (SOCE, SERCA, and VOCE) and its association with inflammation in CKD will be examined in a future study.

5. Summary

Cardiovascular disease (CVD) is the primary complication associated with a significant increase in the death rate of individuals with CKD, and VCm is a major risk factor for CVD in patients with CKD. Hyperphosphatemia is a key component contributing to the development of VCm when renal function declines. Based on accumulating data, VCm is not a simple degenerative change but a highly controlled bone-like ossification process. Transdifferentiation of VSMCs into osteoblast-like cells is a critical event in this process. *In vitro* and *in vivo* experiments have shown that when VSMCs are stimulated with high phosphate concentrations, the expression of osteogenesis-related genes, such as *CBFA1*, *MSX2*, *SOX9*, and *ALPL*, increases, along with TNSALP activity.

Previous research has documented that when VSMCs undergo osteogenic transdifferentiation, their resting $[Ca^{2+}]_i$ increases. SGK1 is essential for VSMC transdifferentiation and VCm induced by high phosphate levels, which is accomplished partially by NF-κB signaling. In other cells, SGK1 positively modulates the expression of ORAI1, the protein that forms the CRAC mediating SOCE, as well as STIM1, thus enhancing SOCE activity; NF-κB exerts a similar effect. Increased SOCE activity results in a sustained increase in $[Ca^{2+}]_i$. The purpose of this study was to determine whether a high phosphate concentration upregulates ORAI1 and STIM1 and, accordingly, SOCE function, as well as whether the increase in $[Ca^{2+}]_i$ includes alternative calcium entry mechanisms.

For this purpose, the phosphate donor BGP was used as a calcification stimulator to treat HAoSMCs. Transcript levels were determined using quantitative PCR, protein expression levels were evaluated using immunoblotting, TNSALP activity was assessed using colorimetry, $[Ca^{2+}]_i$ was measured by detecting fura-2 AM fluorescence, and SOCE was calculated as the increase in $[Ca^{2+}]_i$ following the readdition of extracellular Ca^{2+} after TG-induced store depletion. Additionally, HAoSMCs were cultured in K^+-rich medium to activate

VOCCs via an increased extracellular K^+ concentration. Treatment with BGP increased the ORAI1 and STIM1 transcript and protein expression levels and enhanced SOCE in HAoSMCs. The ORAI1 inhibitors MRS1845 and 2-APB, as well as the SGK1 inhibitor GSK650394, effectively eliminated BGP-stimulated SOCE. ORAI1 antagonist treatment and ORAI1 silencing significantly inhibited BGP-induced expression of osteogenic markers in HAoSMCs and suppressed extracellular calcification. Additionally, activation of VOCCs influenced osteogenic signaling in HAoSMCs.

In conclusion, increased phosphate concentrations stimulate ORAI1 and STIM1 expression and enhance SOCE, which, together with VOCCs, play a role in orchestrating osteo/chondrogenic signaling in VSMCs.

Zusammenfassung

Herz-Kreislauf-Erkrankungen (HKE) sind primäre Komplikationen, die mit einer signifikanten Mortalität bei Menschen mit chronischer Nierenerkrankung (englisch "chronic kidney disease; CKD") verbunden sind, und Gefäßverkalkungen in der Media (englisch "medial vascular calcification; VCm") ist ein Hauptrisikofaktor für HKE bei Patienten mit CKD. Bei abnehmender Nierenfunktion ist Hyperphosphatämie eine Schlüsselkomponente bei der Entwicklung von VCm. Immer mehr Daten deuten darauf hin, dass VCm keine einfache degenerative Veränderung ist, sondern ein hochgradig kontrollierter Ossifikationsprozess. Die Transdifferenzierung von vaskulären glatten Muskelzellen (englisch "vascular smooth muscle cells; VSMCs") in osteoblastenähnliche Zellen ist ein wichtiger Bestandteil in diesem Prozess. *In vitro* und *in vivo* Experimente haben gezeigt, dass, wenn VSMCs mit hohen Phosphatkonzentrationen stimuliert werden, die Expression von Osteogenese-bezogenen Genen wie *CBFA1*, *MSX2*, *SOX9* und *ALPL* zunimmt, ebenso wie die Aktivität der Gewebe-unspezifischen alkalischen Phosphatase (englisch "tissue non-specific alkaline phosphatase; TNSALP").

Frühere Forschungen haben gezeigt, dass, wenn VSMCs einer osteogenen Transdifferenzierung unterzogen werden, ihre basale zytosolisches Ca^{2+} ($[Ca^{2+}]_i$) zunimmt. SGK1 ist essenziell für die VSMCs-Transdifferenzierung und VCm, die durch hohe Phosphatkonzentrationen induziert werden, was teilweise über NF-κB erreicht wird. In anderen Zellen wirkt sich SGK1 positiv auf ORAI1 aus. ORAI1 bildet den Kanal, der den speicher-gesteuerten Ca^{2+}-Eintritt (englisch "store-operated calcium entry; SOCE") vermittelt. Parallel wird STIM1 stimuliert, wodurch die SOCE-Aktivität erhöht wird. NF-κB hat eine ähnliche Wirkung. Eine erhöhte SOCE-Aktivität führt zu einem nachhaltigen Anstieg von $[Ca^{2+}]_i$. Ziel dieser Arbeit war es, zu bestimmen, ob ein hoher Phosphatgehalt ORAI1, STIM1

und dementsprechend die SOCE-Funktion hochreguliert und ob der Anstieg von $[Ca^{2+}]_i$ alternative Kalziumeintrittsmechanismen einschließt.

Zu diesem Zweck wurde der Phosphatdonator β-Glycerophosphat als Verkalkungsstimulator zur Behandlung von humanen glatten Muskelzellen der Aorta (englisch "human aorta smooth muscle cells; HAoSMCs") eingesetzt. Die Gentranskriptwerte wurden durch quantitative PCR bestimmt, die Proteinexpressionsniveaus wurden durch Immunoblotanalyse bewertet, die TNSALP-Aktivität wurde durch Kolorimetrie gemessen, $[Ca^{2+}]_i$ wurde durch Fura-2-Fluoreszenz gemessen und SOCE wurde als Anstieg von $[Ca^{2+}]_i$ nach Zugabe von extrazellulärem Ca^{2+} nach Thapsigargin-induzierter Speichererschöpfung berechnet. Zusätzlich wurden HAoSMCs in K^+-reichem Medium kultiviert, um spannungsgesteuerte Ca^{2+}-Kanäle (englisch "voltage operated calcium channels; VOCCs") über eine erhöhte extrazelluläre K^+-Konzentration zu aktivieren. Die Behandlung mit β-Glycerophosphat verbesserte die Transkript- und Proteinexpressionsniveaus von ORAI1 und STIM1 und erhöhte SOCE in HAoSMCs. Eine zusätzliche Behandlung mit den ORAI1-Inhibitoren MRS1845 und 2-APB sowie dem SGK1-Inhibitor GSK650394 beseitigte effektiv die Wirkungen von β-Glycerophosphat auf SOCE. Die Behandlung mit ORAI1-Antagonisten und die ORAI1-Stummschaltung hemmten signifikant die β-Glycerophosphat-induzierte Expression osteogener Marker in HAoSMCs und unterdrückten die extrazelluläre Verkalkung. Darüber hinaus beeinflusste die Aktivierung von VOCCs die osteogene Signalgebung in HAoSMCs.

Zusammenfassend lässt sich sagen, dass erhöhte Phosphatspiegel die ORAI1- und STIM1-Expression hochregulieren und SOCE verstärken, die zusammen mit VOCCs eine Rolle bei der Orchestrierung der osteo/ chondogenen Signalgebung in VSMCs spielen.

6. References

ABCAM. 2021. *ab83369 Alkaline Phosphatase Assay Kit (Colorimetric)* [Online]. Available: https://www.abcam.com/ps/products/83/ab83369/documents/alkaline-phosphatase-assay-kit-protocol-book-v13b-ab83369%20(website).pdf [Accessed 19 October 2021].

ABDELAZEEM, K. N. M., DROPPOVA, B., SUKKAR, B., AL-MAGHOUT, T., PELZL, L., ZACHAROPOULOU, N., ALI HASSAN, N. H., ABDEL-FATTAH, K. I., STOURNARAS, C. & LANG, F. 2019. Upregulation of Orai1 and STIM1 expression as well as store-operated Ca(2+) entry in ovary carcinoma cells by placental growth factor. *Biochem Biophys Res Commun,* 512**,** 467-472.

ADENEY, K. L., SISCOVICK, D. S., IX, J. H., SELIGER, S. L., SHLIPAK, M. G., JENNY, N. S. & KESTENBAUM, B. R. 2009. Association of serum phosphate with vascular and valvular calcification in moderate CKD. *J Am Soc Nephrol,* 20**,** 381-7.

AGHAGOLZADEH, P., BACHTLER, M., BIJARNIA, R., JACKSON, C., SMITH, E. R., ODERMATT, A., RADPOUR, R. & PASCH, A. 2016. Calcification of vascular smooth muscle cells is induced by secondary calciprotein particles and enhanced by tumor necrosis factor-alpha. *Atherosclerosis,* 251**,** 404-414.

AL-MAGHOUT, T., PELZL, L., SAHU, I., SUKKAR, B., HOSSEINZADEH, Z., GUTTI, R., LAUFER, S., VOELKL, J., PIESKE, B., GAWAZ, M. & LANG, F. 2017. P38 Kinase, SGK1 and NF-kappaB Dependent Up-Regulation of Na+/Ca2+ Exchanger Expression and Activity Following TGFss1 Treatment of Megakaryocytes. *Cell Physiol Biochem,* 42**,** 2169-2181.

ALESUTAN, I., FEGER, M., TUFFAHA, R., CASTOR, T., MUSCULUS, K., BUEHLING, S. S., HEINE, C. L., KURO, O. M., PIESKE, B., SCHMIDT, K., TOMASCHITZ, A., MAERZ, W., PILZ, S., MEINITZER, A., VOELKL, J. & LANG, F. 2016. Augmentation of phosphate-induced osteo-/chondrogenic transformation of vascular smooth muscle cells by homoarginine. *Cardiovasc Res,* 110**,** 408-18.

ALESUTAN, I., MUSCULUS, K., CASTOR, T., ALZOUBI, K., VOELKL, J. & LANG, F. 2015. Inhibition of Phosphate-Induced Vascular Smooth Muscle Cell Osteo-/Chondrogenic Signaling and Calcification by Bafilomycin A1 and Methylamine. *Kidney Blood Press Res,* 40**,** 490-9.

AMANN, K. 2008. Media calcification and intima calcification are distinct entities in chronic kidney disease. *Clin J Am Soc Nephrol,* 3**,** 1599-605.

BEAZLEY, K. E., DEASEY, S., LIMA, F. & NURMINSKAYA, M. V. 2012. Transglutaminase 2-mediated activation of beta-catenin signaling has a critical role in warfarin-induced vascular calcification. *Arterioscler Thromb*

Vasc Biol, 32**,** 123-30.
BEECH, D. J. 2012. Orai1 calcium channels in the vasculature. *Pflugers Arch,* 463**,** 635-47.
BELAIBA, R. S., DJORDJEVIC, T., BONELLO, S., ARTUNC, F., LANG, F., HESS, J. & GORLACH, A. 2006. The serum- and glucocorticoid-inducible kinase Sgk-1 is involved in pulmonary vascular remodeling: role in redox-sensitive regulation of tissue factor by thrombin. *Circ Res,* 98**,** 828-36.
BELLASI, A., KOOIENGA, L., BLOCK, G. A., VELEDAR, E., SPIEGEL, D. M. & RAGGI, P. 2009. How long is the warranty period for nil or low coronary artery calcium in patients new to hemodialysis? *J Nephrol,* 22**,** 255-62.
BENZ, K., HILGERS, K. F., DANIEL, C. & AMANN, K. 2018. Vascular Calcification in Chronic Kidney Disease: The Role of Inflammation. *Int J Nephrol,* 2018**,** 4310379.
BERRA-ROMANI, R., MAZZOCCO-SPEZZIA, A., PULINA, M. V. & GOLOVINA, V. A. 2008. Ca2+ handling is altered when arterial myocytes progress from a contractile to a proliferative phenotype in culture. *Am J Physiol Cell Physiol,* 295**,** C779-90.
BERRIDGE, M. J. 1997. Elementary and global aspects of calcium signalling. *J Physiol,* 499 (Pt 2)**,** 291-306.
BERRIDGE, M. J. 2012. Calcium signalling remodelling and disease. *Biochem Soc Trans,* 40**,** 297-309.
BERRIDGE, M. J., BOOTMAN, M. D. & RODERICK, H. L. 2003. Calcium signalling: dynamics, homeostasis and remodelling. *Nat Rev Mol Cell Biol,* 4**,** 517-29.
BI, W., DENG, J. M., ZHANG, Z., BEHRINGER, R. R. & DE CROMBRUGGHE, B. 1999. Sox9 is required for cartilage formation. *Nat Genet,* 22**,** 85-9.
BIRD, G. S., DEHAVEN, W. I., SMYTH, J. T. & PUTNEY, J. W., JR. 2008. Methods for studying store-operated calcium entry. *Methods,* 46**,** 204-12.
BISAILLON, J. M., MOTIANI, R. K., GONZALEZ-COBOS, J. C., POTIER, M., HALLIGAN, K. E., ALZAWAHRA, W. F., BARROSO, M., SINGER, H. A., JOURD'HEUIL, D. & TREBAK, M. 2010. Essential role for STIM1/Orai1-mediated calcium influx in PDGF-induced smooth muscle migration. *Am J Physiol Cell Physiol,* 298**,** C993-1005.
BLOCK, G. A., KLASSEN, P. S., LAZARUS, J. M., OFSTHUN, N., LOWRIE, E. G. & CHERTOW, G. M. 2004. Mineral metabolism, mortality, and morbidity in maintenance hemodialysis. *J Am Soc Nephrol,* 15**,** 2208-18.
BOOTMAN, M. D., COLLINS, T. J., MACKENZIE, L., RODERICK, H. L., BERRIDGE, M. J. & PEPPIATT, C. M. 2002. 2-aminoethoxydiphenyl borate (2-APB) is a reliable blocker of store-operated Ca2+ entry but an inconsistent inhibitor of InsP3-induced Ca2+ release. *FASEB J,* 16**,** 1145-50.

BRANDMAN, O., LIOU, J., PARK, W. S. & MEYER, T. 2007. STIM2 is a feedback regulator that stabilizes basal cytosolic and endoplasmic reticulum Ca2+ levels. *Cell,* 131**,** 1327-39.

BRINI, M. & CARAFOLI, E. 2009. Calcium pumps in health and disease. *Physiol Rev,* 89**,** 1341-78.

BROAD, L. M., BRAUN, F. J., LIEVREMONT, J. P., BIRD, G. S., KUROSAKI, T. & PUTNEY, J. W., JR. 2001. Role of the phospholipase C-inositol 1,4,5-trisphosphate pathway in calcium release-activated calcium current and capacitative calcium entry. *J Biol Chem,* 276**,** 15945-52.

BURTIS, C. A., ASHWOOD, E. R. & BRUNS, D. E. 2012. *Tietz textbook of clinical chemistry and molecular diagnostics-e-book*, Elsevier Health Sciences.

CAHALAN, M. D. 2009. STIMulating store-operated Ca(2+) entry. *Nat Cell Biol,* 11**,** 669-77.

CARAFOLI, E. 2002. Calcium signaling: a tale for all seasons. *Proc Natl Acad Sci U S A,* 99**,** 1115-22.

CHEN, N. X., DUAN, D., O'NEILL, K. D., WOLISI, G. O., KOCZMAN, J. J., LACLAIR, R. & MOE, S. M. 2006. The mechanisms of uremic serum-induced expression of bone matrix proteins in bovine vascular smooth muscle cells. *Kidney Int,* 70**,** 1046-53.

CHEN, N. X., O'NEILL, K. D., DUAN, D. & MOE, S. M. 2002. Phosphorus and uremic serum up-regulate osteopontin expression in vascular smooth muscle cells. *Kidney Int,* 62**,** 1724-31.

CLAPHAM, D. E. 1995. Calcium signaling. *Cell,* 80**,** 259-68.

CLAPHAM, D. E. 2007. Calcium signaling. *Cell,* 131**,** 1047-58.

COLLINS, S. R. & MEYER, T. 2011. Evolutionary origins of STIM1 and STIM2 within ancient Ca2+ signaling systems. *Trends Cell Biol,* 21**,** 202-11.

COURJARET, R. & MACHACA, K. 2014. Mid-range Ca2+ signalling mediated by functional coupling between store-operated Ca2+ entry and IP3-dependent Ca2+ release. *Nat Commun,* 5**,** 3916.

CRAVER, L., MARCO, M. P., MARTINEZ, I., RUE, M., BORRAS, M., MARTIN, M. L., SARRO, F., VALDIVIELSO, J. M. & FERNANDEZ, E. 2007. Mineral metabolism parameters throughout chronic kidney disease stages 1-5--achievement of K/DOQI target ranges. *Nephrol Dial Transplant,* 22**,** 1171-6.

DELLIS, O., MERCIER, P. & CHOMIENNE, C. 2011. The boron-oxygen core of borinate esters is responsible for the store-operated calcium entry potentiation ability. *BMC Pharmacol,* 11**,** 1.

DEMER, L. L. & TINTUT, Y. 2008. Vascular calcification: pathobiology of a multifaceted disease. *Circulation,* 117**,** 2938-48.

DOLMETSCH, R. E., XU, K. & LEWIS, R. S. 1998. Calcium oscillations increase the efficiency and specificity of gene expression. *Nature,* 392**,**

933-6.
EDDINGTON, H., HOEFIELD, R., SINHA, S., CHRYSOCHOU, C., LANE, B., FOLEY, R. N., HEGARTY, J., NEW, J., O'DONOGHUE, D. J., MIDDLETON, R. J. & KALRA, P. A. 2010. Serum phosphate and mortality in patients with chronic kidney disease. *Clin J Am Soc Nephrol,* 5**,** 2251-7.
EYLENSTEIN, A., GEHRING, E. M., HEISE, N., SHUMILINA, E., SCHMIDT, S., SZTEYN, K., MUNZER, P., NURBAEVA, M. K., EICHENMULLER, M., TYAN, L., REGEL, I., FOLLER, M., KUHL, D., SOBOLOFF, J., PENNER, R. & LANG, F. 2011. Stimulation of Ca2+-channel Orai1/STIM1 by serum- and glucocorticoid-inducible kinase 1 (SGK1). *FASEB J,* 25**,** 2012-21.
EYLENSTEIN, A., SCHMIDT, S., GU, S., YANG, W., SCHMID, E., SCHMIDT, E. M., ALESUTAN, I., SZTEYN, K., REGEL, I., SHUMILINA, E. & LANG, F. 2012. Transcription factor NF-kappaB regulates expression of pore-forming Ca2+ channel unit, Orai1, and its activator, STIM1, to control Ca2+ entry and affect cellular functions. *J Biol Chem,* 287**,** 2719-30.
FEDDE, K. N., BLAIR, L., SILVERSTEIN, J., COBURN, S. P., RYAN, L. M., WEINSTEIN, R. S., WAYMIRE, K., NARISAWA, S., MILLAN, J. L., MACGREGOR, G. R. & WHYTE, M. P. 1999. Alkaline phosphatase knock-out mice recapitulate the metabolic and skeletal defects of infantile hypophosphatasia. *J Bone Miner Res,* 14**,** 2015-26.
FERRè, S., NEYRA, J. A. & MOE, O. W. 2020. Chapter 41 - Calcium, Phosphate, and Magnesium Metabolism in Chronic Kidney Disease. *In:* KIMMEL, P. L. & ROSENBERG, M. E. (eds.) *Chronic Renal Disease (Second Edition).* Academic Press.
FESKE, S. 2009. ORAI1 and STIM1 deficiency in human and mice: roles of store-operated Ca2+ entry in the immune system and beyond. *Immunol Rev,* 231**,** 189-209.
FESKE, S., GWACK, Y., PRAKRIYA, M., SRIKANTH, S., PUPPEL, S. H., TANASA, B., HOGAN, P. G., LEWIS, R. S., DALY, M. & RAO, A. 2006. A mutation in Orai1 causes immune deficiency by abrogating CRAC channel function. *Nature,* 441**,** 179-85.
FLEMMING, R., XU, S. Z. & BEECH, D. J. 2003. Pharmacological profile of store-operated channels in cerebral arteriolar smooth muscle cells. *Br J Pharmacol,* 139**,** 955-65.
FOLEY, R. N. 2009. Phosphate levels and cardiovascular disease in the general population. *Clinical Journal of the American Society of Nephrology,* 4**,** 1136-1139.
FOLEY, R. N. & PARFREY, P. S. 1998. Cardiovascular disease and mortality in ESRD. *J Nephrol,* 11**,** 239-45.
FUSTER, V., STEIN, B., AMBROSE, J. A., BADIMON, L., BADIMON, J. J. &

CHESEBRO, J. H. 1990. Atherosclerotic plaque rupture and thrombosis. Evolving concepts. *Circulation,* 82**,** II47-59.
GO, A. S., CHERTOW, G. M., FAN, D., MCCULLOCH, C. E. & HSU, C. Y. 2004. Chronic kidney disease and the risks of death, cardiovascular events, and hospitalization. *N Engl J Med,* 351**,** 1296-305.
GOLDSMITH, D., RITZ, E. & COVIC, A. 2004. Vascular calcification: a stiff challenge for the nephrologist: does preventing bone disease cause arterial disease? *Kidney Int,* 66**,** 1315-33.
GOODMAN, W. G., GOLDIN, J., KUIZON, B. D., YOON, C., GALES, B., SIDER, D., WANG, Y., CHUNG, J., EMERICK, A., GREASER, L., ELASHOFF, R. M. & SALUSKY, I. B. 2000. Coronary-artery calcification in young adults with end-stage renal disease who are undergoing dialysis. *N Engl J Med,* 342**,** 1478-83.
GUERIN, A. P., PANNIER, B., METIVIER, F., MARCHAIS, S. J. & LONDON, G. M. 2008. Assessment and significance of arterial stiffness in patients with chronic kidney disease. *Curr Opin Nephrol Hypertens,* 17**,** 635-41.
GWACK, Y., SRIKANTH, S., FESKE, S., CRUZ-GUILLOTY, F., OH-HORA, M., NEEMS, D. S., HOGAN, P. G. & RAO, A. 2007. Biochemical and functional characterization of Orai proteins. *J Biol Chem,* 282**,** 16232-43.
HARPER, J. L., CAMERINI-OTERO, C. S., LI, A. H., KIM, S. A., JACOBSON, K. A. & DALY, J. W. 2003. Dihydropyridines as inhibitors of capacitative calcium entry in leukemic HL-60 cells. *Biochem Pharmacol,* 65**,** 329-38.
HEBERT, S. C. & BROWN, E. M. 1996. The scent of an ion: calcium-sensing and its roles in health and disease. *Curr Opin Nephrol Hypertens,* 5**,** 45-53.
HILGEMANN, D. W., YARADANAKUL, A., WANG, Y. & FUSTER, D. 2006. Molecular control of cardiac sodium homeostasis in health and disease. *J Cardiovasc Electrophysiol,* 17 Suppl 1**,** S47-S56.
HOSSEINZADEH, Z., HAUSER, S., SINGH, Y., PELZL, L., SCHUSTER, S., SHARMA, Y., HOFLINGER, P., ZACHAROPOULOU, N., STOURNARAS, C., RATHBUN, D. L., ZRENNER, E., SCHOLS, L. & LANG, F. 2020. Decreased Na(+)/K(+) ATPase Expression and Depolarized Cell Membrane in Neurons Differentiated from Chorea-Acanthocytosis Patients. *Sci Rep,* 10**,** 8391.
HOTH, M. & PENNER, R. 1992. Depletion of intracellular calcium stores activates a calcium current in mast cells. *Nature,* 355**,** 353-6.
HOUSE, S. J., POTIER, M., BISAILLON, J., SINGER, H. A. & TREBAK, M. 2008. The non-excitable smooth muscle: calcium signaling and phenotypic switching during vascular disease. *Pflugers Arch,* 456**,** 769-85.
ISAKOVA, T., WAHL, P., VARGAS, G. S., GUTIERREZ, O. M., SCIALLA, J., XIE, H., APPLEBY, D., NESSEL, L., BELLOVICH, K., CHEN, J., HAMM,

L., GADEGBEKU, C., HORWITZ, E., TOWNSEND, R. R., ANDERSON, C. A., LASH, J. P., HSU, C. Y., LEONARD, M. B. & WOLF, M. 2011. Fibroblast growth factor 23 is elevated before parathyroid hormone and phosphate in chronic kidney disease. *Kidney Int,* 79**,** 1370-8.

ITAGAKI, K., KANNAN, K. B. & HAUSER, C. J. 2005. Lysophosphatidic acid triggers calcium entry through a non-store-operated pathway in human neutrophils. *J Leukoc Biol,* 77**,** 181-9.

IYEMERE, V., PROUDFOOT, D., WEISSBERG, P. & SHANAHAN, C. 2006. Vascular smooth muscle cell phenotypic plasticity and the regulation of vascular calcification. *Journal of internal medicine,* 260**,** 192-210.

JOHNSON, R. C., LEOPOLD, J. A. & LOSCALZO, J. 2006. Vascular calcification: pathobiological mechanisms and clinical implications. *Circ Res,* 99**,** 1044-59.

JONO, S., MCKEE, M. D., MURRY, C. E., SHIOI, A., NISHIZAWA, Y., MORI, K., MORII, H. & GIACHELLI, C. M. 2000a. Phosphate regulation of vascular smooth muscle cell calcification. *Circ Res,* 87**,** E10-7.

JONO, S., PEINADO, C. & GIACHELLI, C. M. 2000b. Phosphorylation of osteopontin is required for inhibition of vascular smooth muscle cell calcification. *J Biol Chem,* 275**,** 20197-203.

KENDRICK, J. & CHONCHOL, M. B. 2008. Nontraditional risk factors for cardiovascular disease in patients with chronic kidney disease. *Nature clinical practice Nephrology,* 4**,** 672-681.

KESTENBAUM, B. R., ADENEY, K. L., DE BOER, I. H., IX, J. H., SHLIPAK, M. G. & SISCOVICK, D. S. 2009. Incidence and progression of coronary calcification in chronic kidney disease: the Multi-Ethnic Study of Atherosclerosis. *Kidney Int,* 76**,** 991-8.

KHANANSHVILI, D. 2014. Sodium-calcium exchangers (NCX): molecular hallmarks underlying the tissue-specific and systemic functions. *Pflugers Arch,* 466**,** 43-60.

KOH, N., FUJIMORI, T., NISHIGUCHI, S., TAMORI, A., SHIOMI, S., NAKATANI, T., SUGIMURA, K., KISHIMOTO, T., KINOSHITA, S., KUROKI, T. & NABESHIMA, Y. 2001. Severely reduced production of klotho in human chronic renal failure kidney. *Biochem Biophys Res Commun,* 280**,** 1015-20.

KOMORI, T., YAGI, H., NOMURA, S., YAMAGUCHI, A., SASAKI, K., DEGUCHI, K., SHIMIZU, Y., BRONSON, R. T., GAO, Y. H., INADA, M., SATO, M., OKAMOTO, R., KITAMURA, Y., YOSHIKI, S. & KISHIMOTO, T. 1997. Targeted disruption of Cbfa1 results in a complete lack of bone formation owing to maturational arrest of osteoblasts. *Cell,* 89**,** 755-64.

KOSK-KOSICKA, D. 2005. Measurement of Ca(2)+-ATPase activity (in PMCA and SERCA1). *Methods Mol Biol,* 312**,** 343-54.

KUNICHIKA, N., YU, Y., REMILLARD, C. V., PLATOSHYN, O., ZHANG, S. &

YUAN, J. X. 2004. Overexpression of TRPC1 enhances pulmonary vasoconstriction induced by capacitative Ca2+ entry. *Am J Physiol Lung Cell Mol Physiol,* 287**,** L962-9.

LANG, F., HENKE, G., EMBARK, H. M., WALDEGGER, S., PALMADA, M., BOHMER, C. & VALLON, V. 2003. Regulation of channels by the serum and glucocorticoid-inducible kinase - implications for transport, excitability and cell proliferation. *Cell Physiol Biochem,* 13**,** 41-50.

LANZER, P., BOEHM, M., SORRIBAS, V., THIRIET, M., JANZEN, J., ZELLER, T., ST HILAIRE, C. & SHANAHAN, C. 2014. Medial vascular calcification revisited: review and perspectives. *Eur Heart J,* 35**,** 1515-25.

LEE, H. L., WOO, K. M., RYOO, H. M. & BAEK, J. H. 2010. Tumor necrosis factor-alpha increases alkaline phosphatase expression in vascular smooth muscle cells via MSX2 induction. *Biochem Biophys Res Commun,* 391**,** 1087-92.

LEIBROCK, C. B., ALESUTAN, I., VOELKL, J., MICHAEL, D., CASTOR, T., KOHLHOFER, U., QUINTANILLA-MARTINEZ, L., KUBLER, L., MANNHEIM, J. G., PICHLER, B. J., ROSENBLATT, K. P., KURO-O, M. & LANG, F. 2016. Acetazolamide sensitive tissue calcification and aging of klotho-hypomorphic mice. *J Mol Med (Berl),* 94**,** 95-106.

LEIBROCK, C. B., ALESUTAN, I., VOELKL, J., PAKLADOK, T., MICHAEL, D., SCHLEICHER, E., KAMYABI-MOGHADDAM, Z., QUINTANILLA-MARTINEZ, L., KURO-O, M. & LANG, F. 2015. NH4Cl Treatment Prevents Tissue Calcification in Klotho Deficiency. *J Am Soc Nephrol,* 26**,** 2423-33.

LEMONNIER, L., PREVARSKAYA, N., MAZURIER, J., SHUBA, Y. & SKRYMA, R. 2004. 2-APB inhibits volume-regulated anion channels independently from intracellular calcium signaling modulation. *FEBS Lett,* 556**,** 121-6.

LEOPOLD, J. A. 2015. Vascular calcification: Mechanisms of vascular smooth muscle cell calcification. *Trends Cardiovasc Med,* 25**,** 267-74.

LEUNG, F. P., YUNG, L. M., YAO, X., LAHER, I. & HUANG, Y. 2008. Store-operated calcium entry in vascular smooth muscle. *Br J Pharmacol,* 153**,** 846-57.

LEVIN, A., BAKRIS, G. L., MOLITCH, M., SMULDERS, M., TIAN, J., WILLIAMS, L. A. & ANDRESS, D. L. 2007. Prevalence of abnormal serum vitamin D, PTH, calcium, and phosphorus in patients with chronic kidney disease: results of the study to evaluate early kidney disease. *Kidney Int,* 71**,** 31-8.

LEWIS, R. S. 2007. The molecular choreography of a store-operated calcium channel. *Nature,* 446**,** 284-7.

LI, X., YANG, H. Y. & GIACHELLI, C. M. 2008. BMP-2 promotes phosphate uptake, phenotypic modulation, and calcification of human vascular smooth muscle cells. *Atherosclerosis,* 199**,** 271-7.

LIANG, X., BUTTERWORTH, M. B., PETERS, K. W., WALKER, W. H. & FRIZZELL, R. A. 2008. An obligatory heterodimer of 14-3-3beta and 14-3-3epsilon is required for aldosterone regulation of the epithelial sodium channel. *J Biol Chem,* 283**,** 27418-27425.

LIS, A., PEINELT, C., BECK, A., PARVEZ, S., MONTEILH-ZOLLER, M., FLEIG, A. & PENNER, R. 2007. CRACM1, CRACM2, and CRACM3 are store-operated Ca2+ channels with distinct functional properties. *Curr Biol,* 17**,** 794-800.

LOMASHVILI, K. A., COBBS, S., HENNIGAR, R. A., HARDCASTLE, K. I. & O'NEILL, W. C. 2004. Phosphate-induced vascular calcification: role of pyrophosphate and osteopontin. *J Am Soc Nephrol,* 15**,** 1392-401.

LONDON, G. M. 2011. Arterial calcification: cardiovascular function and clinical outcome. *Nefrologia,* 31**,** 644-7.

LONDON, G. M., MARCHAIS, S. J., GUERIN, A. P. & METIVIER, F. 2005. Arteriosclerosis, vascular calcifications and cardiovascular disease in uremia. *Curr Opin Nephrol Hypertens,* 14**,** 525-31.

LUO, D., BROAD, L. M., BIRD, G. S. & PUTNEY, J. W., JR. 2001. Signaling pathways underlying muscarinic receptor-induced [Ca2+]i oscillations in HEK293 cells. *J Biol Chem,* 276**,** 5613-21.

LUONG, T. T. D., ESTEPA, M., BOEHME, B., PIESKE, B., LANG, F., ECKARDT, K. U., VOELKL, J. & ALESUTAN, I. 2019. Inhibition of vascular smooth muscle cell calcification by vasorin through interference with TGFbeta1 signaling. *Cell Signal,* 64**,** 109414.

MA, K., LIU, P., AL-MAGHOUT, T., SUKKAR, B., CAO, H., VOELKL, J., ALESUTAN, I., PIESKE, B. & LANG, F. 2019. Phosphate-induced ORAI1 expression and store-operated Ca(2+) entry in aortic smooth muscle cells. *J Mol Med (Berl),* 97**,** 1465-1475.

MA, K., SUKKAR, B., ZHU, X., ZHOU, K., CAO, H., VOELKL, J., ALESUTAN, I., NüRNBERG, B. & LANG, F. 2020. Stimulation of ORAI1 expression, store-operated Ca(2+) entry, and osteogenic signaling by high glucose exposure of human aortic smooth muscle cells. *Pflugers Arch,* 472**,** 1093-1102.

MARUYAMA, T., KANAJI, T., NAKADE, S., KANNO, T. & MIKOSHIBA, K. 1997. 2APB, 2-aminoethoxydiphenyl borate, a membrane-penetrable modulator of Ins(1,4,5)P3-induced Ca2+ release. *J Biochem,* 122**,** 498-505.

MATHEW, S., LUND, R. J., STREBECK, F., TUSTISON, K. S., GEURS, T. & HRUSKA, K. A. 2007. Reversal of the adynamic bone disorder and decreased vascular calcification in chronic kidney disease by sevelamer carbonate therapy. *J Am Soc Nephrol,* 18**,** 122-30.

MATHEW, S., TUSTISON, K. S., SUGATANI, T., CHAUDHARY, L. R., RIFAS, L. & HRUSKA, K. A. 2008. The mechanism of phosphorus as a

cardiovascular risk factor in CKD. *J Am Soc Nephrol,* 19**,** 1092-105.
MCMEEKIN, S. R., DRANSFIELD, I., ROSSI, A. G., HASLETT, C. & WALKER, T. R. 2006. E-selectin permits communication between PAF receptors and TRPC channels in human neutrophils. *Blood,* 107**,** 4938-45.
MERCER, J. C., DEHAVEN, W. I., SMYTH, J. T., WEDEL, B., BOYLES, R. R., BIRD, G. S. & PUTNEY, J. W., JR. 2006. Large store-operated calcium selective currents due to co-expression of Orai1 or Orai2 with the intracellular calcium sensor, Stim1. *J Biol Chem,* 281**,** 24979-90.
MIHAI, S., CODRICI, E., POPESCU, I. D., ENCIU, A. M., ALBULESCU, L., NECULA, L. G., MAMBET, C., ANTON, G. & TANASE, C. 2018. Inflammation-Related Mechanisms in Chronic Kidney Disease Prediction, Progression, and Outcome. *J Immunol Res,* 2018**,** 2180373.
MINKE, B. 2006. TRP channels and Ca2+ signaling. *Cell Calcium,* 40**,** 261-75.
MITSNEFES, M. M. 2012. Cardiovascular disease in children with chronic kidney disease. *J Am Soc Nephrol,* 23**,** 578-85.
MIZOBUCHI, M., TOWLER, D. & SLATOPOLSKY, E. 2009. Vascular calcification: the killer of patients with chronic kidney disease. *J Am Soc Nephrol,* 20**,** 1453-64.
MOE, S. M. & CHEN, N. X. 2004. Pathophysiology of vascular calcification in chronic kidney disease. *Circ Res,* 95**,** 560-7.
MOE, S. M. & CHEN, N. X. 2008. Mechanisms of vascular calcification in chronic kidney disease. *J Am Soc Nephrol,* 19**,** 213-6.
MUNOZ, E., HERNANDEZ-MORALES, M., SOBRADILLO, D., ROCHER, A., NUNEZ, L. & VILLALOBOS, C. 2013. Intracellular Ca(2+) remodeling during the phenotypic journey of human coronary smooth muscle cells. *Cell Calcium,* 54**,** 375-85.
NGUYEN, N. T., NGUYEN, T. T., DA LY, D., XIA, J. B., QI, X. F., LEE, I. K., CHA, S. K. & PARK, K. S. 2020. Oxidative stress by Ca(2+) overload is critical for phosphate-induced vascular calcification. *Am J Physiol Heart Circ Physiol,* 319**,** H1302-H1312.
NISHIO, Y., DONG, Y., PARIS, M., O'KEEFE, R. J., SCHWARZ, E. M. & DRISSI, H. 2006. Runx2-mediated regulation of the zinc finger Osterix/Sp7 gene. *Gene,* 372**,** 62-70.
NOORDZIJ, M., KOREVAAR, J. C., BOS, W. J., BOESCHOTEN, E. W., DEKKER, F. W., BOSSUYT, P. M. & KREDIET, R. T. 2006. Mineral metabolism and cardiovascular morbidity and mortality risk: peritoneal dialysis patients compared with haemodialysis patients. *Nephrol Dial Transplant,* 21**,** 2513-20.
PAREKH, A. B. & PUTNEY, J. W., JR. 2005. Store-operated calcium channels. *Physiol Rev,* 85**,** 757-810.
PARK, C. Y., SHCHEGLOVITOV, A. & DOLMETSCH, R. 2010. The CRAC channel activator STIM1 binds and inhibits L-type voltage-gated calcium

channels. *Science,* 330**,** 101-5.
PELZL, L., HAUSER, S., ELSIR, B., SUKKAR, B., SAHU, I., SINGH, Y., HOFLINGER, P., BISSINGER, R., JEMAA, M., STOURNARAS, C., SCHOLS, L. & LANG, F. 2017. Lithium Sensitive ORAI1 Expression, Store Operated Ca(2+) Entry and Suicidal Death of Neurons in Chorea-Acanthocytosis. *Sci Rep,* 7**,** 6457.
PERWAD, F., ZHANG, M. Y., TENENHOUSE, H. S. & PORTALE, A. A. 2007. Fibroblast growth factor 23 impairs phosphorus and vitamin D metabolism in vivo and suppresses 25-hydroxyvitamin D-1alpha-hydroxylase expression in vitro. *Am J Physiol Renal Physiol,* 293**,** F1577-83.
POTIER, M., GONZALEZ, J. C., MOTIANI, R. K., ABDULLAEV, I. F., BISAILLON, J. M., SINGER, H. A. & TREBAK, M. 2009. Evidence for STIM1- and Orai1-dependent store-operated calcium influx through ICRAC in vascular smooth muscle cells: role in proliferation and migration. *FASEB J,* 23**,** 2425-37.
PRAKRIYA, M., FESKE, S., GWACK, Y., SRIKANTH, S., RAO, A. & HOGAN, P. G. 2006. Orai1 is an essential pore subunit of the CRAC channel. *Nature,* 443**,** 230-3.
PRAKRIYA, M. & LEWIS, R. S. 2001. Potentiation and inhibition of Ca(2+) release-activated Ca(2+) channels by 2-aminoethyldiphenyl borate (2-APB) occurs independently of IP(3) receptors. *J Physiol,* 536**,** 3-19.
PUTNEY, J. W., JR. 1986. A model for receptor-regulated calcium entry. *Cell Calcium,* 7**,** 1-12.
PUTNEY, J. W., JR. 1990. Capacitative calcium entry revisited. *Cell Calcium,* 11**,** 611-24.
PUTNEY, J. W., JR. 1999. TRP, inositol 1,4,5-trisphosphate receptors, and capacitative calcium entry. *Proc Natl Acad Sci U S A,* 96**,** 14669-71.
PUTNEY, J. W., JR. & MCKAY, R. R. 1999. Capacitative calcium entry channels. *Bioessays,* 21**,** 38-46.
ROBERTS-THOMSON, S. J., PETERS, A. A., GRICE, D. M. & MONTEITH, G. R. 2010. ORAI-mediated calcium entry: mechanism and roles, diseases and pharmacology. *Pharmacol Ther,* 127**,** 121-30.
RODENBECK, S. D., ZARSE, C. A., MCKENNEY-DRAKE, M. L., BRUNING, R. S., STUREK, M., CHEN, N. X. & MOE, S. M. 2017. Intracellular calcium increases in vascular smooth muscle cells with progression of chronic kidney disease in a rat model. *Nephrol Dial Transplant,* 32**,** 450-458.
ROOS, J., DIGREGORIO, P. J., YEROMIN, A. V., OHLSEN, K., LIOUDYNO, M., ZHANG, S., SAFRINA, O., KOZAK, J. A., WAGNER, S. L., CAHALAN, M. D., VELICELEBI, G. & STAUDERMAN, K. A. 2005. STIM1, an essential and conserved component of store-operated Ca2+ channel function. *J Cell Biol,* 169**,** 435-45.

SAGE, A. P., TINTUT, Y. & DEMER, L. L. 2010. Regulatory mechanisms in vascular calcification. *Nat Rev Cardiol,* 7**,** 528-36.

SAHU, I., PELZL, L., SUKKAR, B., FAKHRI, H., AL-MAGHOUT, T., CAO, H., HAUSER, S., GUTTI, R., GAWAZ, M. & LANG, F. 2017. NFAT5-sensitive Orai1 expression and store-operated Ca(2+) entry in megakaryocytes. *FASEB J,* 31**,** 3439-3448.

SALKER, M. S., SINGH, Y., DURAIRAJ, R. R. P., YAN, J., ALAUDDIN, M., ZENG, N., STEEL, J. H., ZHANG, S., NAUTIYAL, J., WEBSTER, Z., BRUCKER, S. Y., WALLWIENER, D., ANNE CROY, B., BROSENS, J. J. & LANG, F. 2018. LEFTY2 inhibits endometrial receptivity by downregulating Orai1 expression and store-operated Ca(2+) entry. *J Mol Med (Berl),* 96**,** 173-182.

SATOKATA, I., MA, L., OHSHIMA, H., BEI, M., WOO, I., NISHIZAWA, K., MAEDA, T., TAKANO, Y., UCHIYAMA, M., HEANEY, S., PETERS, H., TANG, Z., MAXSON, R. & MAAS, R. 2000. Msx2 deficiency in mice causes pleiotropic defects in bone growth and ectodermal organ formation. *Nat Genet,* 24**,** 391-5.

SCHINDL, R., MUIK, M., FAHRNER, M., DERLER, I., FRITSCH, R., BERGSMANN, J. & ROMANIN, C. 2009. Recent progress on STIM1 domains controlling Orai activation. *Cell Calcium,* 46**,** 227-32.

SCHLIEPER, G., SCHURGERS, L., BRANDENBURG, V., REUTELINGSPERGER, C. & FLOEGE, J. 2016. Vascular calcification in chronic kidney disease: an update. *Nephrol Dial Transplant,* 31**,** 31-9.

SCHMID, E., BHANDARU, M., NURBAEVA, M. K., YANG, W., SZTEYN, K., RUSSO, A., LEIBROCK, C., TYAN, L., PEARCE, D., SHUMILINA, E. & LANG, F. 2012. SGK3 regulates Ca(2+) entry and migration of dendritic cells. *Cell Physiol Biochem,* 30**,** 1423-35.

SCHUCHARDT, M., TOLLE, M., PRUFER, J., PRUFER, N., HUANG, T., JANKOWSKI, V., JANKOWSKI, J., ZIDEK, W. & VAN DER GIET, M. 2012. Uridine adenosine tetraphosphate activation of the purinergic receptor P2Y enhances in vitro vascular calcification. *Kidney Int,* 81**,** 256-65.

SHANAHAN, C. M. 2007. Inflammation ushers in calcification: a cycle of damage and protection? *Circulation,* 116**,** 2782-5.

SHANAHAN, C. M., CARY, N. R., SALISBURY, J. R., PROUDFOOT, D., WEISSBERG, P. L. & EDMONDS, M. E. 1999. Medial localization of mineralization-regulating proteins in association with Monckeberg's sclerosis: evidence for smooth muscle cell-mediated vascular calcification. *Circulation,* 100**,** 2168-76.

SHANAHAN, C. M., CROUTHAMEL, M. H., KAPUSTIN, A. & GIACHELLI, C. M. 2011. Arterial calcification in chronic kidney disease: key roles for calcium and phosphate. *Circ Res,* 109**,** 697-711.

SHIMADA, T., HASEGAWA, H., YAMAZAKI, Y., MUTO, T., HINO, R., TAKEUCHI, Y., FUJITA, T., NAKAHARA, K., FUKUMOTO, S. & YAMASHITA, T. 2004. FGF-23 is a potent regulator of vitamin D metabolism and phosphate homeostasis. *J Bone Miner Res,* 19**,** 429-35.
SHIOI, A., NISHIZAWA, Y., JONO, S., KOYAMA, H., HOSOI, M. & MORII, H. 1995. Beta-glycerophosphate accelerates calcification in cultured bovine vascular smooth muscle cells. *Arterioscler Thromb Vasc Biol,* 15**,** 2003-9.
SHROFF, R. C., MCNAIR, R., FIGG, N., SKEPPER, J. N., SCHURGERS, L., GUPTA, A., HIORNS, M., DONALD, A. E., DEANFIELD, J., REES, L. & SHANAHAN, C. M. 2008. Dialysis accelerates medial vascular calcification in part by triggering smooth muscle cell apoptosis. *Circulation,* 118**,** 1748-57.
SINGARAVELU, K., LOHR, C. & DEITMER, J. W. 2006. Regulation of store-operated calcium entry by calcium-independent phospholipase A2 in rat cerebellar astrocytes. *J Neurosci,* 26**,** 9579-92.
SLATOPOLSKY, E., ROBSON, A. M., ELKAN, I. & BRICKER, N. S. 1968. Control of phosphate excretion in uremic man. *J Clin Invest,* 47**,** 1865-74.
SMYTH, J. T., HWANG, S. Y., TOMITA, T., DEHAVEN, W. I., MERCER, J. C. & PUTNEY, J. W. 2010. Activation and regulation of store-operated calcium entry. *J Cell Mol Med,* 14**,** 2337-49.
SNETKOV, V. A., AARONSON, P. I., WARD, J. P., KNOCK, G. A. & ROBERTSON, T. P. 2003. Capacitative calcium entry as a pulmonary specific vasoconstrictor mechanism in small muscular arteries of the rat. *Br J Pharmacol,* 140**,** 97-106.
SPEER, M. Y., LI, X., HIREMATH, P. G. & GIACHELLI, C. M. 2010. Runx2/Cbfa1, but not loss of myocardin, is required for smooth muscle cell lineage reprogramming toward osteochondrogenesis. *J Cell Biochem,* 110**,** 935-47.
STATHOPULOS, P. B., ZHENG, L. & IKURA, M. 2009. Stromal interaction molecule (STIM) 1 and STIM2 calcium sensing regions exhibit distinct unfolding and oligomerization kinetics. *J Biol Chem,* 284**,** 728-32.
STATHOPULOS, P. B., ZHENG, L., LI, G. Y., PLEVIN, M. J. & IKURA, M. 2008. Structural and mechanistic insights into STIM1-mediated initiation of store-operated calcium entry. *Cell,* 135**,** 110-22.
STEITZ, S. A., SPEER, M. Y., CURINGA, G., YANG, H. Y., HAYNES, P., AEBERSOLD, R., SCHINKE, T., KARSENTY, G. & GIACHELLI, C. M. 2001. Smooth muscle cell phenotypic transition associated with calcification: upregulation of Cbfa1 and downregulation of smooth muscle lineage markers. *Circ Res,* 89**,** 1147-54.
SUKKAR, B. 2020. *Effect of Lithium treatment on SOCE components in Chorea Acanthocytosis.* Universität Tübingen.
SUN, Y., BYON, C. H., YUAN, K., CHEN, J., MAO, X., HEATH, J. M., JAVED,

A., ZHANG, K., ANDERSON, P. G. & CHEN, Y. 2012. Smooth muscle cell-specific runx2 deficiency inhibits vascular calcification. *Circ Res,* 111**,** 543-52.

SZIKRA, T., CUSATO, K., THORESON, W. B., BARABAS, P., BARTOLETTI, T. M. & KRIZAJ, D. 2008. Depletion of calcium stores regulates calcium influx and signal transmission in rod photoreceptors. *J Physiol,* 586**,** 4859-75.

TAI, D. J., SU, C. C., MA, Y. L. & LEE, E. H. 2009. SGK1 phosphorylation of IkappaB Kinase alpha and p300 Up-regulates NF-kappaB activity and increases N-Methyl-D-aspartate receptor NR2A and NR2B expression. *J Biol Chem,* 284**,** 4073-89.

TANAKA, T., SATO, H., DOI, H., YOSHIDA, C. A., SHIMIZU, T., MATSUI, H., YAMAZAKI, M., AKIYAMA, H., KAWAI-KOWASE, K., ISO, T., KOMORI, T., ARAI, M. & KURABAYASHI, M. 2008. Runx2 represses myocardin-mediated differentiation and facilitates osteogenic conversion of vascular smooth muscle cells. *Mol Cell Biol,* 28**,** 1147-60.

TENTORI, F., BLAYNEY, M. J., ALBERT, J. M., GILLESPIE, B. W., KERR, P. G., BOMMER, J., YOUNG, E. W., AKIZAWA, T., AKIBA, T., PISONI, R. L., ROBINSON, B. M. & PORT, F. K. 2008. Mortality risk for dialysis patients with different levels of serum calcium, phosphorus, and PTH: the Dialysis Outcomes and Practice Patterns Study (DOPPS). *Am J Kidney Dis,* 52**,** 519-30.

TONELLI, M., CURHAN, G., PFEFFER, M., SACKS, F., THADHANI, R., MELAMED, M. L., WIEBE, N. & MUNTNER, P. 2009. Relation between alkaline phosphatase, serum phosphate, and all-cause or cardiovascular mortality. *Circulation,* 120**,** 1784-92.

TONELLI, M., SACKS, F., PFEFFER, M., GAO, Z., CURHAN, G., CHOLESTEROL & RECURRENT EVENTS TRIAL, I. 2005. Relation between serum phosphate level and cardiovascular event rate in people with coronary disease. *Circulation,* 112**,** 2627-33.

TUFFAHA, R., VOELKL, J., PIESKE, B., LANG, F. & ALESUTAN, I. 2018. Role of PKB/SGK-dependent phosphorylation of GSK-3alpha/beta in vascular calcification during cholecalciferol overload in mice. *Biochem Biophys Res Commun,* 503**,** 2068-2074.

TYSON, K. L., REYNOLDS, J. L., MCNAIR, R., ZHANG, Q., WEISSBERG, P. L. & SHANAHAN, C. M. 2003. Osteo/chondrocytic transcription factors and their target genes exhibit distinct patterns of expression in human arterial calcification. *Arterioscler Thromb Vasc Biol,* 23**,** 489-94.

VAETH, M., YANG, J., YAMASHITA, M., ZEE, I., ECKSTEIN, M., KNOSP, C., KAUFMANN, U., KAROLY JANI, P., LACRUZ, R. S., FLOCKERZI, V., KACSKOVICS, I., PRAKRIYA, M. & FESKE, S. 2017. ORAI2 modulates store-operated calcium entry and T cell-mediated immunity. *Nat*

Commun, 8**,** 14714.
VALLON, V., WYATT, A. W., KLINGEL, K., HUANG, D. Y., HUSSAIN, A., BERCHTOLD, S., FRIEDRICH, B., GRAHAMMER, F., BELAIBA, R. S., GORLACH, A., WULFF, P., DAUT, J., DALTON, N. D., ROSS, J., JR., FLOGEL, U., SCHRADER, J., OSSWALD, H., KANDOLF, R., KUHL, D. & LANG, F. 2006. SGK1-dependent cardiac CTGF formation and fibrosis following DOCA treatment. *J Mol Med (Berl),* 84**,** 396-404.
VARNAI, P., HUNYADY, L. & BALLA, T. 2009. STIM and Orai: the long-awaited constituents of store-operated calcium entry. *Trends Pharmacol Sci,* 30**,** 118-28.
VAZIRI, N. D. 2004. Oxidative stress in uremia: nature, mechanisms, and potential consequences. *Semin Nephrol,* 24**,** 469-73.
VIG, M., PEINELT, C., BECK, A., KOOMOA, D. L., RABAH, D., KOBLAN-HUBERSON, M., KRAFT, S., TURNER, H., FLEIG, A., PENNER, R. & KINET, J. P. 2006. CRACM1 is a plasma membrane protein essential for store-operated Ca2+ entry. *Science,* 312**,** 1220-3.
VOELKL, J., ALESUTAN, I., LEIBROCK, C. B., QUINTANILLA-MARTINEZ, L., KUHN, V., FEGER, M., MIA, S., AHMED, M. S., ROSENBLATT, K. P., KURO, O. M. & LANG, F. 2013. Spironolactone ameliorates PIT1-dependent vascular osteoinduction in klotho-hypomorphic mice. *J Clin Invest,* 123**,** 812-22.
VOELKL, J., LANG, F., ECKARDT, K.-U., AMANN, K., KURO-O, M., PASCH, A., PIESKE, B. & ALESUTAN, I. 2019. Signaling pathways involved in vascular smooth muscle cell calcification during hyperphosphatemia. *Cellular and Molecular Life Sciences,* 76**,** 2077-2091.
VOELKL, J., LUONG, T. T., TUFFAHA, R., MUSCULUS, K., AUER, T., LIAN, X., DANIEL, C., ZICKLER, D., BOEHME, B., SACHERER, M., METZLER, B., KUHL, D., GOLLASCH, M., AMANN, K., MULLER, D. N., PIESKE, B., LANG, F. & ALESUTAN, I. 2018a. SGK1 induces vascular smooth muscle cell calcification through NF-kappaB signaling. *J Clin Invest,* 128**,** 3024-3040.
VOELKL, J., TUFFAHA, R., LUONG, T. T. D., ZICKLER, D., MASYOUT, J., FEGER, M., VERHEYEN, N., BLASCHKE, F., KURO, O. M., TOMASCHITZ, A., PILZ, S., PASCH, A., ECKARDT, K. U., SCHERBERICH, J. E., LANG, F., PIESKE, B. & ALESUTAN, I. 2018b. Zinc Inhibits Phosphate-Induced Vascular Calcification through TNFAIP3-Mediated Suppression of NF-kappaB. *J Am Soc Nephrol,* 29**,** 1636-1648.
WALKER-ALLGAIER, B., SCHAUB, M., ALESUTAN, I., VOELKL, J., GEUE, S., MUNZER, P., RODRIGUEZ, J. M., KUHL, D., LANG, F., GAWAZ, M. & BORST, O. 2017. SGK1 up-regulates Orai1 expression and VSMC migration during neointima formation after arterial injury. *Thromb Haemost,* 117**,** 1002-1005.

WANG, X., WANG, Y., ZHOU, Y., HENDRON, E., MANCARELLA, S., ANDRAKE, M. D., ROTHBERG, B. S., SOBOLOFF, J. & GILL, D. L. 2014. Distinct Orai-coupling domains in STIM1 and STIM2 define the Orai-activating site. *Nat Commun,* 5**,** 3183.

WANG, Y., DENG, X., HEWAVITHARANA, T., SOBOLOFF, J. & GILL, D. L. 2008. Stim, ORAI and TRPC channels in the control of calcium entry signals in smooth muscle. *Clin Exp Pharmacol Physiol,* 35**,** 1127-33.

WANG, Y., DESHPANDE, M. & PAYNE, R. 2002. 2-Aminoethoxydiphenyl borate inhibits phototransduction and blocks voltage-gated potassium channels in Limulus ventral photoreceptors. *Cell Calcium,* 32**,** 209-16.

WAYMAN, C. P., MCFADZEAN, I., GIBSON, A. & TUCKER, J. F. 1996. Two distinct membrane currents activated by cyclopiazonic acid-induced calcium store depletion in single smooth muscle cells of the mouse anococcygeus. *Br J Pharmacol,* 117**,** 566-572.

WEI, M., ZHOU, Y., SUN, A., MA, G., HE, L., ZHOU, L., ZHANG, S., LIU, J., ZHANG, S. L., GILL, D. L. & WANG, Y. 2016. Molecular mechanisms underlying inhibition of STIM1-Orai1-mediated Ca(2+) entry induced by 2-aminoethoxydiphenyl borate. *Pflugers Arch,* 468**,** 2061-2074.

WILLIAMS, R. T., MANJI, S. S., PARKER, N. J., HANCOCK, M. S., VAN STEKELENBURG, L., EID, J. P., SENIOR, P. V., KAZENWADEL, J. S., SHANDALA, T., SAINT, R., SMITH, P. J. & DZIADEK, M. A. 2001. Identification and characterization of the STIM (stromal interaction molecule) gene family: coding for a novel class of transmembrane proteins. *Biochem J,* 357**,** 673-85.

XUAN, Y. T., WANG, O. L. & WHORTON, A. R. 1992. Thapsigargin stimulates Ca2+ entry in vascular smooth muscle cells: nicardipine-sensitive and -insensitive pathways. *Am J Physiol,* 262**,** C1258-65.

YAMADA, S., TANIGUCHI, M., TOKUMOTO, M., TOYONAGA, J., FUJISAKI, K., SUEHIRO, T., NOGUCHI, H., IIDA, M., TSURUYA, K. & KITAZONO, T. 2012. The antioxidant tempol ameliorates arterial medial calcification in uremic rats: important role of oxidative stress in the pathogenesis of vascular calcification in chronic kidney disease. *J Bone Miner Res,* 27**,** 474-85.

YAMASHIRO, T., WANG, X. P., LI, Z., OYA, S., ABERG, T., FUKUNAGA, T., KAMIOKA, H., SPECK, N. A., TAKANO-YAMAMOTO, T. & THESLEFF, I. 2004. Possible roles of Runx1 and Sox9 in incipient intramembranous ossification. *J Bone Miner Res,* 19**,** 1671-7.

YEROMIN, A. V., ZHANG, S. L., JIANG, W., YU, Y., SAFRINA, O. & CAHALAN, M. D. 2006. Molecular identification of the CRAC channel by altered ion selectivity in a mutant of Orai. *Nature,* 443**,** 226-9.

YOSHIDA, T., YAMASHITA, M., HORIMAI, C. & HAYASHI, M. 2017. Smooth Muscle-Selective Nuclear Factor-kappaB Inhibition Reduces Phosphate-

Induced Arterial Medial Calcification in Mice With Chronic Kidney Disease. *J Am Heart Assoc,* 6.

YOUNG, E. W., ALBERT, J. M., SATAYATHUM, S., GOODKIN, D. A., PISONI, R. L., AKIBA, T., AKIZAWA, T., KUROKAWA, K., BOMMER, J., PIERA, L. & PORT, F. K. 2005. Predictors and consequences of altered mineral metabolism: the Dialysis Outcomes and Practice Patterns Study. *Kidney Int,* 67**,** 1179-87.

ZHANG, B., YAN, J., UMBACH, A. T., FAKHRI, H., FAJOL, A., SCHMIDT, S., SALKER, M. S., CHEN, H., ALEXANDER, D., SPICHTIG, D., DARYADEL, A., WAGNER, C. A., FOLLER, M. & LANG, F. 2016. NFkappaB-sensitive Orai1 expression in the regulation of FGF23 release. *J Mol Med (Berl),* 94**,** 557-66.

ZHANG, D., BI, X., LIU, Y., HUANG, Y., XIONG, J., XU, X., XIAO, T., YU, Y., JIANG, W., HUANG, Y., ZHANG, J., ZHANG, B. & ZHAO, J. 2017. High Phosphate-Induced Calcification of Vascular Smooth Muscle Cells is Associated with the TLR4/NF-kappab Signaling Pathway. *Kidney Blood Press Res,* 42**,** 1205-1215.

ZHANG, L., CUI, R., CHENG, X. & DU, J. 2005a. Antiapoptotic effect of serum and glucocorticoid-inducible protein kinase is mediated by novel mechanism activating I{kappa}B kinase. *Cancer Res,* 65**,** 457-64.

ZHANG, S. L., YU, Y., ROOS, J., KOZAK, J. A., DEERINCK, T. J., ELLISMAN, M. H., STAUDERMAN, K. A. & CAHALAN, M. D. 2005b. STIM1 is a Ca2+ sensor that activates CRAC channels and migrates from the Ca2+ store to the plasma membrane. *Nature,* 437**,** 902-5.

ZHANG, W., HALLIGAN, K. E., ZHANG, X., BISAILLON, J. M., GONZALEZ-COBOS, J. C., MOTIANI, R. K., HU, G., VINCENT, P. A., ZHOU, J., BARROSO, M., SINGER, H. A., MATROUGUI, K. & TREBAK, M. 2011. Orai1-mediated I (CRAC) is essential for neointima formation after vascular injury. *Circ Res,* 109**,** 534-42.

ZHANG, X., XIN, P., YOAST, R. E., EMRICH, S. M., JOHNSON, M. T., PATHAK, T., BENSON, J. C., AZIMI, I., GILL, D. L., MONTEITH, G. R. & TREBAK, M. 2020. Distinct pharmacological profiles of ORAI1, ORAI2, and ORAI3 channels. *Cell Calcium,* 91**,** 102281.

ZHAO, G., XU, M. J., ZHAO, M. M., DAI, X. Y., KONG, W., WILSON, G. M., GUAN, Y., WANG, C. Y. & WANG, X. 2012. Activation of nuclear factor-kappa B accelerates vascular calcification by inhibiting ankylosis protein homolog expression. *Kidney Int,* 82**,** 34-44.

ZHOU, G., ZHENG, Q., ENGIN, F., MUNIVEZ, E., CHEN, Y., SEBALD, E., KRAKOW, D. & LEE, B. 2006. Dominance of SOX9 function over RUNX2 during skeletogenesis. *Proc Natl Acad Sci U S A,* 103**,** 19004-9.

ZHU, X., MA, K., ZHOU, K., LIU, J., NURNBERG, B. & LANG, F. 2021. Vasopressin-stimulated ORAI1 expression and store-operated Ca(2+)

entry in aortic smooth muscle cells. *J Mol Med (Berl),* 99**,** 373-382.

7. Declaration of Contributions

My dissertation is the result of independent research conducted under the supervision of my supervisor. This dissertation contains no previously published or authored works or findings by other individuals or collectives. The sources are appropriately cited.

I worked out all the technical details, conducted experiments, collected and analysed data, as well as drafted the dissertation and designed the figures.

Prof. Dr. Florian Lang developed the theoretical framework, contributed to the implementation of the research, and took the lead in paper writing and revision.

Prof. Dr. Bernd Nürnberg guided experiment design, verified the analytical methods, and aided in paper and dissertation revision.

Ping Liu and Tamer Al-Maghout guided technique details in Ca^{2+} measurements.

Basma Sukkar aided in technique details of western blotting and quantitative PCR.

Xuexue Zhu and Kuo Zhou assisted with sample preparation and technique details.

8. Publications

1. **Ma, K.**, Sukkar, B., Zhu, X., Zhou, K., Cao, H., Voelkl, J., Alesutan, I., Nürnberg, B., & Lang, F. (2020). Stimulation of ORAI1 expression, store-operated Ca^{2+} entry, and osteogenic signaling by high glucose exposure of human aortic smooth muscle cells. Pflugers Archiv : European journal of physiology, 472(8), 1093–1102. https://doi.org/10.1007/s00424-020-02405-1

2. **Ma, K.**, Liu, P., Al-Maghout, T., Sukkar, B., Cao, H., Voelkl, J., Alesutan, I., Pieske, B., & Lang, F. (2019). Phosphate-induced ORAI1 expression and store-operated Ca^{2+} entry in aortic smooth muscle cells. Journal of molecular medicine (Berlin, Germany), 97(10), 1465–1475. https://doi.org/10.1007/s00109-019-01824-7

3. Zhu, X., **Ma, K.**, Zhou, K., Pan, X., Liu, J., Nürnberg, B., Alesutan, I., Völkl, J., & Lang, F. (2022). Requirement of Na+/H+ exchanger NHE1 for vasopressin-induced osteogenic signaling and calcification in human aortic smooth muscle cells. Kidney & blood pressure research, 10.1159/000524050. Advance online publication. https://doi.org/10.1159/000524050

4. Zhu, X., **Ma, K**., Zhou, K., Liu, J., Nürnberg, B., & Lang, F. (2021). Vasopressin-stimulated ORAI1 expression and store-operated Ca^{2+} entry in aortic smooth muscle cells. Journal of molecular medicine (Berlin, Germany), 99(3), 373–382. https://doi.org/10.1007/s00109-020-02016-4

5. Zhu, X., **Ma, K.**, Zhou, K., Voelkl, J., Alesutan, I., Leibrock, C., Nürnberg, B., & Lang, F. (2020). Reversal of phosphate-induced ORAI1 expression, store-operated Ca^{2+} entry and osteogenic signaling by $MgCl_2$ in human aortic smooth muscle cells. Biochemical and biophysical research communications, 523(1), 18–24. https://doi.org/10.1016/j.bbrc.2019.11.005

6. Zhou, K., Zhu, X., **Ma, K.**, Liu, J., Nürnberg, B., Gawaz, M., & Lang, F. (2021). Effect of $MgCl_2$ and $GdCl_3$ on ORAI1 Expression and Store-Operated Ca^{2+} Entry in Megakaryocytes. International journal of molecular sciences, 22(7), 3292. https://doi.org/10.3390/ijms22073292

7. Pelzl, L., Sahu, I., **Ma, K.**, Heinzmann, D., Bhuyan, A., Al-Maghout, T., Sukkar, B., Sharma, Y., Marini, I., Rigoni, F., Artunc, F., Cao, H., Gutti, R., Voelkl, J., Pieske, B., Gawaz, M., Bakchoul, T., & Lang, F. (2020). Beta-Glycerophosphate-Induced ORAI1 Expression and Store Operated Ca^{2+} Entry in Megakaryocytes. Scientific reports, 10(1), 1728. https://doi.org/10.1038/s41598-020-58384-x

8. Liu, J., Bhuyan, A., **Ma, K.**, Zhang, S., Cheng, A., & Lang, F. (2020). Inhibition of suicidal erythrocyte death by pyrogallol. Molecular biology reports, 47(7), 5025–5032. https://doi.org/10.1007/s11033-020-05568-3

9. Lang, F., **Ma, K.**, Leibrock, C. B., Salker, M. S., & Singh, Y. (2020). The Putative Role of $1,25(OH)_2D_3$ in the Association of Milk Consumption and Parkinson's Disease. Neuro-Signals, 28(1), 14–24. https://doi.org/10.33594/000000321

10. Lang, F., Singh, Y., Salker, M. S., **Ma, K.**, Pandyra, A. A., Lang, P. A., & Lang, K. S. (2020). Glucose transport in lymphocytes. Pflugers Archiv : European journal of physiology, 472(9), 1401–1406. https://doi.org/10.1007/s00424-020-02416-y

11. Cao, H., Al Mamun Bhuyan, A., Umbach, A. T., **Ma, K.**, Borst, O., Gawaz, M., Zhang, S., Nürnberg, B., & Lang, F. (2019). Garcinol A Novel Inhibitor of Platelet Activation and Apoptosis. Toxins, 11(7), 382. https://doi.org/10.3390/toxins11070382

12. Lang, F., **Ma, K.**, & Leibrock, C. B. (2019). $1,25(OH)_2D_3$ in Brain Function and Neuropsychiatric Disease. Neuro-Signals, 27(1), 40–49. https://doi.org/10.33594/000000182

Acknowledgments

I would like to express sincere gratitude to my first supervisor, Prof. Dr. Florian Lang, for giving me this valuable opportunity to participate in internationally leading research and for his academic enlightenment, meticulous guidance, continuous resource and technical support on this project as well as spirit inspiration during my doctoral study.

I am deeply grateful to my second supervisor, Prof. Dr. Bernd Nürnberg, for his responsible and serious attitude towards the project and his valuable suggestions on the doctoral dissertation, and for providing us as much convenience as possible with the experiment instruments.

Special thanks to Lejla Subasic, for her warm-hearted help with reagents order, manuscripts preparation and submission.

Greatest gratitude to Basma Sukkar, Ping Liu, and Tamer Al-Maghout for their selfless help in the beginning of my doctoral study. Heartfelt thanks to Xuexue Zhu, Kuo Zhou, Hang Cao, Jibin Liu, and other colleagues for their support and encouragement during my period in the lab.

Endless thanks to my parents and my younger brother for their unconditional support, as well as for their blessing from heart, no matter what I pursue.

In particular, thanks to my man of love, Dr. Xie, for his silent dedication, from my master to doctor, from my stay in China to Germany.